MECHANISMS OF ION CHANNEL ACTIVATION IN PRIMARY CULTURED AND CLONAL CELL LINES.

Martin Gosling

Doctor of Philosophy.

THE UNIVERSITY OF ASTON IN BIRMINGHAM

September, 1995.

Mechanisms of ion channel activation in primary cultured and clonal cell lines.

Martin Gosling,
Ph.D. Thesis, 1995
The University of Aston in Birmingham.

Summary:

The effects of hypotonic shock upon membrane Cl^- permeability of ROS 17/2.8 osteoblast-like cells was investigated using the patch-clamp technique. Hypotonic shock produced cell swelling that was accompanied by large amplitude, outwardly rectifying, currents that were active across the entire physiological range of membrane potentials (-80 to +100 mV). At strong depolarisations (> +50 mV) the currents exhibited time-dependent inactivation that followed a monoexponential time course. The currents were anion selective and exhibited a selectivity sequence of $SCN^- > I^- > Br^- > Cl^- > F^- >$ gluconate$^-$. Current activation was unaffected by inhibitors of protein kinase A (H-89) and tyrosine kinase (tyrphostin A25), and could not be mimicked by elevation of intracellular Ca^{2+} or activation of protein kinase C. Similarly, disruption of actin filaments by dihydrocytochalsin B, or generation of membrane tension by dipyridamole failed to elicit significant increases in cell chloride permeability. The mechanism of current activation is as yet undetermined. The currents were effectively inhibited by the chloride channel inhibitors NPPB and DIDS but resistant to DPC. A Cl^- conductance with similar characteristics was found to be present in mouse primary cultured calvarial osteoblasts.

The volume-sensitive Cl^- current in ROS 17/2.8 cells was inhibited by arachidonic acid in two distinct phases. A rapid block that developed within 10 s, preceding a slower developing inhibitory phase that occurred approximately 90 s after onset of arachidonate superfusion. Arachidonic acid also induced kinetic modifications of the current which were evident as an acceleration of the time-dependent inactivation exhibited at depolarised potentials. Inhibitors of cyclo-oxygenases, lipoxygenases and cytochrome P-450 were ineffectual against arachidonic acid's effects suggesting that arachidonic acid may elicit it's effects directly.

Measurements of cell volume under hypotonic conditions showed that ROS 17/2.8 cells could effectively regulate their volume. However, effective inhibitors of the volume-sensitive Cl^- current drastically impaired this response suggesting that physiologically this current may have a vital role in cell volume regulation.

In L6 skeletal myocytes, vasopressin was found to rapidly hyperpolarise cells. This appears to occur as the result of activation of Ca^{2+}-sensitive K^+ channels in a process dependent upon the presence of extracellular Ca^{2+}.

Keywords:- osteoblasts, ion channels, vasopressin, arachidonic acid.

Acknowledgements:

This thesis is an account of original work carried out in the laboratories of the Pharmacology Research Group, Department of Pharmaceutical Sciences, Aston University. This investigation was funded by the BBSRC and the Wellcome Trust, to whom I am grateful.

Numerous people have made this work and manuscript possible, far too many to mention individually. I would however like to take this opportunity to express my sincere gratitude to my supervisors Dr. D.R. Poyner and Dr. J.W. Smith, for their advice, constructive criticism and above all encouragement and belief in the work I was performing. I would also like to thank Dr. S.J. Publicover and Dr. A. El Haj at Birmingham University for the kind gift of the ROS 17/2.8 cell line and some stimulating discussions.

I would also like to thank all my colleagues at Aston, staff and students alike, who have ensured that my stay at Aston was a distinct pleasure, especially Mr. Alan Richardson for his unique sense of humour and technical expertise. My thanks are also extended to my parents for their support, both financial and otherwise.

This thesis is dedicated to the memory of my grandfather, Frederick Arthur Gosling (1915 - 1992). A simple man whose attitude to life will forever be an example to me.

Contents:

List of Figures:

List of Tables:

List of Abbreviations:

ABC	ATP-binding cassette
9-AC	Anthracene-9-carboxylate
ADP	Adenosine 5'-diphosphate
Ap	Apamin
ATP	Adenosine 5'-triphosphate
BAPTA	1,2-bis(2-aminophenoxy)ethane-N,N,N',N'-tetraacetic acid
BK_{Ca}	High conductance Ca^{2+}-activated K^+ channel
BSA	Bovine serum albumin
C	Centigrade
cADPR	Cylcic ADP ribose
cDNA	Complimentary deoxyribonucleic acid
CF	Cystic fibrosis
CFTR	Cystic fibrosis transmembrane regulator
CGRP	Calcitonin gene-related peptide
CICR	Ca^{2+}-induced Ca^{2+} release
cm	Centimetre
Cyclic AMP	Adenosine 3',5'-cyclic monophosphate
DDFSK	Dideoxyforskolin
DHCB	Dihydrocytochalasin B
dH_2O	Distilled water
DIDS	4,4'-diisothiocyanatostilbene-2,2'-disulphonic

	acid
DMEM	Dulbecco's modified Eagle medium
DMSO	Dimethyl sulfoxide
DNDS	4,4'-dinitrostilbene-2,2'-disulfonic acid
DPC	Diphenylamine-2-carboxylic acid (N-phenylanthanilic acid)
DPM	Dipyridamole
E_{Cl}	Chloride equilibrium potential
EDTA	Ethylenediaminetetraacetic acid
EDHF	Endothelium-derived hyperpolarising factor
EGTA	Ethylene glycol-bis(β-aminoethylether) N,N,N',N'-tetraacetic acid
E_K	Potassium equilibrium potential
ER	Endoplasmic reticulum
E_{rev}	Reversal potential
fS	Femto-Siemens
γ	Single channel conductance
GTP	Guanosine 5'-triphosphate
H-89	N-[2-(p-bromocinnamylamino)ethyl]-5-isoquinolinesulfonamide dihydrochloride
HEPES	(N-[2-hydroxyethyl]piperazine-N'-[2'-ethanesulfonic acid])
hr	Hour
Hz	Hertz

IC_{50}	50% inhibitory concentration
$InsP_3$	Inositol 1,4,5-trisphosphate
$InsP_3R$	Inositol 1,4,5-trisphosphate receptor
$InsP_4$	Inositol 1,3,4,5-tetrakisphosphate
I-V	Current-voltage
K_{ATP}	ATP-sensitive K^+ channel
kHz	Kilohertz
l	Litre
M	Molar
MDR	Multidrug resistance
min	Minute
ml	Millilitre
mm	Millimetre
mM	Millimolar
mosmol	Milliosmole
mRNA	Messenger ribonucleic acid
ms	Millisecond
mV	Millivolt
MΩ	Megaohm
n	Number of observations
NDGA	Nordihydroguaretic acid
n_H	Hill coeffecient
nM	Nanomolar
NMDA	N-methyl-D-aspartate

NMDG	N-methyl-D-glucamine
NPPB	5-nitro-2-(3-phenylpropylamino)benzoic acid
nS	Nano-Siemen
ORCC	'Outwardly-rectifying' Cl^- channels
ORDIC	'Outwardly-rectifying,depolarisation-induced' Cl^- channels
p	Probability
pA	Pico-Amp
pBPB	4-bromophenacryl bromide
pF	Pico-farad
P-gp	P-glycoprotein
PKA	Protein kinase A (cyclic AMP-dependent protein kinase)
PKC	Protein kinase C
PLA_2	Phospholipase A_2
PLC	Phospholipase C
PLD	Phospholipase D
P_{open}	Open probability
pS	Pico-Siemen
PTH	Parathyroid hormone
ROCC	Receptor-operated Ca^{2+} channel
RVD	Regulatory volume decrease
RVI	Regulatory volume increase
RyR	Ryanodine receptor

s	Second
S.E.M.	Standard error of the mean
SITS	4-acetamido-4'-isothiocyanato-stilbene-2,2'-disulphonic acid
TCA	Trichloroacetic acid
TEA	Tetraethylammonium
TPA	12-O-tetradecanoylphorbol 13-acetate
U	Unit
µl	Microlitre
µM	Micromolar
µg	Microgram
µCi	Micro-Curie
V	Volt
V_h	Boltzmann factor
VIP	Vasoactive intestinal polypeptide
Vp	Vasopressin
v/v	Volume by volume
w/v	Weight by volume

Chapter 1.

GENERAL INTRODUCTION

1.1. What are ion channels ?

Ion channels are large protein macromolecules that exist in cell membranes forming discrete pores. These pores selectively allow ions to flow down their electrochemical gradients, both into and out of the cell cytoplasm at rates often exceeding 10^6 ions s^{-1} (Hille, 1992). The role of ions in the excitability of nervous and muscle tissue has long been under investigation by physiologists subsequent to the initial work of Ringer (1883) and Nernst (1888) with their speculation of an ionic origin of bioelectric potentials. As technology progressed throughout the early 20th century, a group of scientists, most notably Alan Hodgkin and Andrew Huxley, investigated the passive membrane properties and the propagated action potential of the squid giant axon. Their work transformed the proposed membrane ionic theory of excitation from hypothesis to established fact (Hodgkin & Huxley, 1952) and the science of membrane biophysics was born. Today, technology and techniques have become more advanced, culminating in the patch-clamp technique (Hamill, Marty, Neher, Sakmann & Sigworth, 1981) which allows the ions flowing through a single ion channel to be accurately and routinely measured. This has allowed ion channels to be characterised at a previously unmeasurable resolution and provided valuable information regarding their physiological function and regulation.

Naming of ion channels has not been as systematic as that utilised for cell receptors but in most cases relies upon channel kinetics, pharmacology and responses to ionic substitution. The central pore of the ion channel has the important property of selective permeability i.e. it allows a restricted class of small ions to flow passively down their

electrochemical gradient. Channels are routinely named after the type of ion they allow to flow, a trend that was pioneered by Hodgkin and Huxley (1952) when they found the currents in the squid giant axon consisted of three separate components which they called sodium, potassium and leakage. Other properties of the channel also contribute to their naming, particularly the stimulus that leads to their opening or closing (e.g. the ATP-sensitive K^+ channel K_{ATP}) and their kinetic characteristics (e.g. 'long lasting' L-type Ca^{2+} channel, high conductance Ca^{2+}-activated K^+ channel BK_{Ca}).

1.2. Mechanisms of ion channel activation:

As mentioned above ion channels have been shown that both open and close in response to a variety of stimuli, occurring both intra- and extracellularly. These stimuli fall into three broad categories.

Voltage-gated ion channels open in response to changes in membrane potential and are responsible for the conducted electrical signals in neurones and other excitable cells. Activation of this type of channel is thought to result from a voltage-driven conformational change in the channel protein such that the central transmembrane pore opens. Structural analysis has shown that membrane potential is detected by a 'voltage-sensing' region that contains the gating charges of the channel, normally these are charged amino acid residues located in the membrane-associated segments of the channel protein (reviewed by Catterall, 1993). Voltage-gated ion channels that conduct Na^+, K^+, Ca^{2+} and Cl^- have been shown to exist in most cell types.

Ligand-gated ion channels are channels that open in response to the binding of a transmitter molecule to the channel protein. This type of channel can be divided into two further subclasses; those that utilise an intrinsic sensor, and those that use a remote sensor. Normally, channels that have an intrinsic sensor are actually receptor/channel proteins. Thus the binding of the transmitter molecule to the channel protein itself produces the conformational changes that lead to channel activation directly. This type of channel is commonly found to mediate fast chemical synaptic transmission, as the receptor moiety of the channel complex is specific to a single neurotransmitter. The first and most widely studied channel of this type is the acetylcholine-activated cation channel present in vertebrate neuromuscular junctions (nicotinic acetylcholine receptor or endplate channel). These were the first type of channel whose unitary conductance was measured by the patch-clamp technique (Neher & Sakmann, 1976). Other examples of this type of channel are the $GABA_A$, glycine and glutamate receptors (Hille, 1992). Channels that use a remote sensor normally rely upon the binding of a transmitter molecule to a receptor protein that is physically distinct from the ion channel itself. The receptor (the remote sensor) communicates with the ion channel via generation of diffusible, intracellular second messenger molecules. In some cases the second messenger molecule can interact with the ion channel protein directly (e.g. by G-proteins directly in a membrane delimited pathway; reviewed by Brown & Birnbaumer, 1990) or invoke a cascade of cellular effects that eventually result in generation of a molecule that does interact with the channel (e.g. the second messenger molecule, inositol 1,4,5-trisphosphate ($InsP_3$), produces release of Ca^{2+} from intracellular stores which can then activate a variety of Ca^{2+}-sensitive ion channels). The time scale for channel activation by this second

mechanism is much slower compared to the intrinsic sensor and membrane delimited pathways mentioned above. This is due to the time required for the eventual signalling molecule to be generated. However, this mechanism does have some advantages. A single receptor can invoke the formation of multiple signalling molecules which then activate a large number of ion channels, a process called signal amplification. Another advantage is that the effects of the transmitter molecule can last much longer than that with the intrinsic sensor mechanism i.e. they can continue long after the transmitter molecule has dissociated from the receptor.

A much smaller class of ion channels are those that respond to cell deformation, and are thus called mechano-gated or stretch-activated ion channels. This area of biophysical research is relatively young as the existence of this type of channel, though expected, was not confirmed until 1984 by Guharay and Sachs. The mechanism by which cell stretch is transduced into ion channel activation is unknown. By definition the channel will respond to tension but it is unclear whether tension purely within the membrane bilayer produces channel activation (intrinsic) or tension is applied directly to the channel protein by extracellular or cytoskeletal elements (extrinsic; Hamill & McBride, 1994).

The view of ion channel activation given above is greatly simplified as stimuli can interact to affect channel activation and its properties once activated. For example, the open probability of the large conductance (BK) Ca^{2+}-sensitive channel changes in response to both intracellular Ca^{2+} and membrane voltage (Rudy, 1998). This type of

channel has also been shown to be activated by membrane stretch in G292 osteoblastic cells (Davidson, 1993).

1.3. Chloride channels:

In comparison with other types of ion channel, Cl^- channels seem to have been generally ignored by physiologists for a number of years. Even today there is not an entry for Cl^- channels in the 1995 Trends in Pharmacological Sciences (TiPS) receptor and ion channel nomenclature supplement though it does comprehensively cover Na^+, K^+ and Ca^{2+} channels. However, Cl^- channels have become a more fashionable area of biophysical research, especially in epithelial cells (reviewed by Gögelein, 1988). This has resulted from the discovery that the underlying mechanism for the human genetic disease, cystic fibrosis (CF), is a severely reduced Cl^- permeability in the epithelia lining the respiratory and intestinal tracts (Quinton, 1983). Plasma membrane Cl^- channels serve a variety of physiological functions, in excitable cells subject to wide variations in membrane potential, activation of Cl^- channels serves to stabilise the membrane as E_{Cl} normally lies close (within 20 mV) of the cell resting membrane potential (Hille, 1992). In common with other ion channels Cl^- channels can be classified according to the stimulus that opens them (reviewed by Pusch & Jentsch, 1994; Franciolini & Petris, 1990). Here only the major classes of Cl^- channels found in the periphery are considered.

1.3.1. Chloride channel blockers:

In comparison with other channel types there are relatively few effective Cl^- channel inhibitors (for review see Greger, 1990). These fall into two main chemical classes; sulphonic acid stilbene derivatives and carboxylate derivatives. Initial work with the carboxylate analogues, anthracene-9-carboxylate (9-AC) and diphenylamine-2-carboxylate (DPC; see fig. 1.1 for structure) showed them to be effective inhibitors of Cl^- channels in epithelia (Oberleitner, Ritter, Lang & Guggino, 1983; Di Stefano, Wittner, Schlatter, Lang, Englert & Greger, 1985). Extensive experiments assessing the structure activity relationship for modifications of DPC eventually led to the synthesis of the potent Cl^- channel blocker, 5-Nitro-2-[(3-phenylpropyl)amino]-benzoic acid (NPPB, see fig. 1.1 for structure; Wangemann, Wittner, Di Stefano, Englert, Lang, Schlatter & Greger, 1986). The mechanism by which NPPB blocks Cl^- channels is unclear. It is only effective when applied to the extracellular face of the channel suggesting its site of interaction is on the outside of the channel (Tilmann, Kunzelmann, Fröbe, Cabantchik, Lang, Englert & Greger, 1991). Experiments utilising incorporation of a Ca^{2+}-dependent airway epithelial Cl^- channel into planar phospholipid bilayers have suggested that NPPB acts to modulate channel gating rather than as a blocker (Alton & Williams, 1992).

The stilbene sulphonate derivative Cl^- channel blockers are typified by 4,4'-diisothiocyanto-stilbene-2,2'-disulphonic acid (DIDS; see fig. 1.1 for structure) and 4-acetamido-4'-isothiocyanato-stilbene-2,2'-disulphonic acid (SITS). These compounds have been shown to effectively inhibit Cl^- channels in a wide variety of cells including

epithelia (Tilmann *et al.* 1991). Notable time- and voltage-dependent block of Cl^- currents by these compounds has been observed in a variety of studies where the stilbene derivatives have been shown to be more effective at depolarised potentials (e.g. cyclic AMP-dependent Cl^- current in osteoblasts; Chesnoy-Marchais & Fritsch, 1989). It has been proposed that this effect occurs as a result of these compounds being negatively charged at physiological pH and thus reversibly blocking the channel, entering the pore more easily at positive potentials (Gray & Ritchie, 1986).

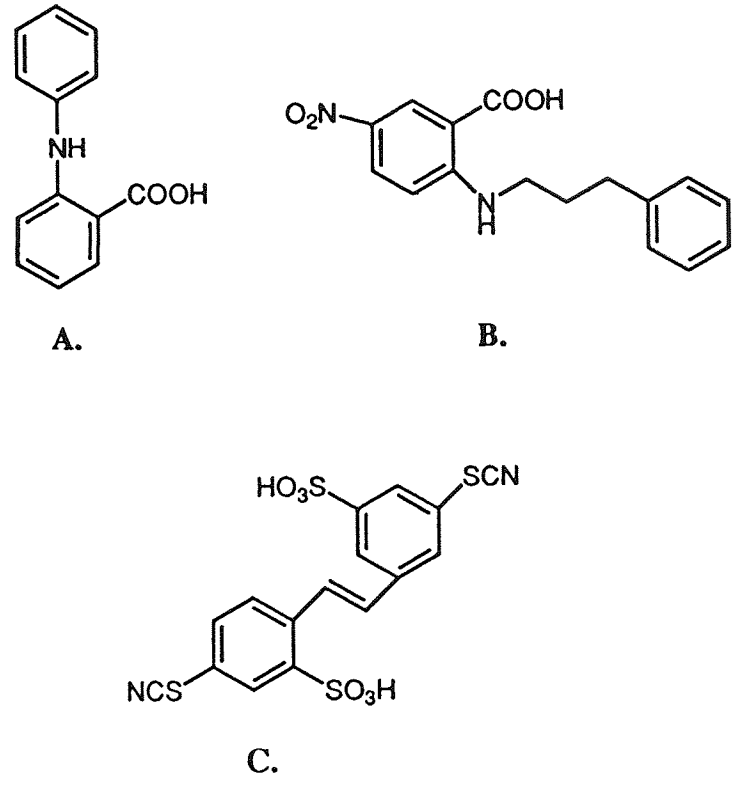

Figure 1.1 Structures of commonly used Cl^- channel blockers. *A, Diphenylamine-2-carboxylic acid (DPC); B, 5-nitro-2-(3-phenylpropylamino)benzoic acid (NPPB); C, 4,4'-diisothiocyanatostilbene-2,2'-disulphonic acid (DIDS).*

Most Cl^- channel blockers, particularly the stilbene derivatives, with very little molecular modification or at higher concentrations, will inhibit a variety of other Cl^--transporting proteins (Greger, 1990). Indeed, DIDS has been shown to irreversibly block the anion exchange of red blood cells by covalently binding to the anion transporters (Ship, Shami, Breuer & Rothstein, 1977).

Specific inhibitors for the volume-sensitive Cl^- channel associated with expression of P-glycoprotein also exist and are discussed below (1.3.5.4).

1.3.2. Cyclic AMP-dependent Cl^- channels:

Probably the most researched Cl^- channels are those that open in response to elevation of adenosine 3',5'-cyclic monophosphate (cyclic AMP). The underlying mechanism of channel activation is phosphorylation by cyclic AMP-dependent protein kinase (PKA). The most important member of this group of Cl^- channels is the cystic fibrosis transmembrane regulator (CFTR), the product of the CF gene (Riordan, Rommens, Kerem, Alon, Rozmahel, Grzelczak, Zielenski, Lok, Plavsic, Chou, Drumm, Iannuzzi, Collins & Tsui, 1989). A number of studies have comprehensively demonstrated that CFTR is a linear, cyclic AMP-activated 8 - 10 pS chloride channel (Anderson, Gregory, Thompson, Souza, Mulligan, Smith & Welsh, 1991; Cliff et al. 1992). The channel is voltage-independent and has an ion selectivity sequence of $Cl^- > Br > I^-$ (Anderson *et al.* 1991; Tabcharani, Rommens, Hou, Chang, Tsui, Riordan & Hanrahan, 1993). In addition to possessing intrinsic Cl^- channel activity, CFTR can influence the activity of other ion channels (Gabriel, Clarke, Boucher & Stutts, 1993).

As CFTR is a member of the ATP-binding cassette (ABC) transport proteins, this may be the result of transport of substances from the cytosol to the extracellular environment where they activate other channels (Schwiebert, Egan, Hwang, Fulmer, Allen, Cutting & Guggino, 1995). Other Cl^- channels activated by PKA include the group termed 'outwardly rectifying Cl^- channels' (ORCC) which possess a conductance of 30 - 70 pS and an anion selectivity of $SCN^- > I^- > Br^- > Cl^- > F^-$ (e.g. Halm, Rechkemmer, Schoumacher & Frizzell, 1998; Worrel, Cliff, Butt & Frizzell, 1989; Sepulveda, Fargon & McNaughton, 1991). Thus these channels are easily distinguished from those due to CFTR expression. In excised patches these channels can also be activated by unphysiologically strong deploarisations and are thus sometimes referred to as 'outwardly rectifying, depolarisation-induced Cl^- channels' (ORDIC; Solc & Wine, 1991). These types of channels appear to be widely distributed occurring not only in most epithelia (Gögelein, 1988) but in other cell types such as osteoblasts (Chesnoy-Marchais & Fritsch, 1989).

1.3.3. Ca^{2+}-activated Cl^- channels:

Another important class of Cl^- channels are activated by increases in the levels of intracellular Ca^{2+}. These channels are outwardly rectifying and exhibit an anion permeability sequence similar to ORCCs of $I^- > Br^- > Cl^-$ (Evans & Marty, 1986; Cliff & Frizzell, 1990; Anderson & Welsh, 1991). However unlike ORCCs, which have no obvious voltage-dependent properties, Ca^{2+}-dependent Cl^- channels show time-dependent inactivation at hyperpolarised potentials and time-dependent activation at depolarised potentials (e.g. Kubo & Okada, 1992). Single Ca^{2+}-dependent Cl^- channels

also have a much smaller single channel conductance (γ) of 1 - 3 pS (Taleb, Feltz, Bossu & Feltz, 1988). The mechanism by which intracellular Ca^{2+} opens these Cl^- channels is not clear. It may be by direct binding of Ca^{2+} to the channel protein, or via an interposed mechanism such as phosphorylation by a Ca^{2+}-dependent kinase (Nishimoto, Wagner, Schulman & Gardner, 1991; Worrell & Frizzell, 1991).

1.3.4. Voltage-dependent Cl^- channels:

As implied by the name these channels open in response to changes in membrane potential. A number of these channels have been cloned and form the ClC family of voltage-gated Cl^- channels (reviewed by Jentsch, 1993; Pusch & Jentsch, 1994; Jentsch, Günther, Pusch & Schwappach, 1995). These channels generally show a permeability sequence of $Cl^- > Br^- > I^-$, low single channel conductance (γ) values (< 10 pS) but exhibit a variety of rectification characteristics (ClC-0 is linear, ClC-1 is inwardly rectifying). The physiological functions of this cloned family of Cl^- channels is unclear, with the possible exceptions of ClC-1 (cloned from skeletal muscle) which may have a role in controlling muscle excitability, and ClC-2 which can be activated by cell swelling and thus may participate in volume regulation (see 1.3.5.5). Maxi-Cl^- channels are another type of voltage-gated Cl^- channel, these were first observed in primary cultures of skeletal muscle (Blatz & Magleby, 1983). They have since been shown to be present in most cell types including neuronal, blood, endothelia and epithelial cells (reviewed by Hurnák & Zachar, 1992). These channels possess a bell-shaped current-voltage relationship in physiological solutions i.e. the open probability reduces as the voltage is stepped away from 0 mV in both positive and negative

directions. The channels show a very high single channel conductance (γ) of between 200 - 450 pS and a variety of sub-conductance states. Maxi-Cl^- channels appear to be expressed at low density occurring in 5 - 20% of patches examined and only become active several minutes after excision, following large positive and negative voltage steps (Franciolino & Petris, 1990). Thus, the physiological significance of these channels remains undetermined, and has raised the possibility that under physiological conditions these channels are suppressed by an intracellular factor. Such a factor has been reported to be present in a variety of cell types, and shown to effectively inhibit epithelial Cl^- channels (Krick, Disser, Hazama, Burckhardt & Frömter, 1991).

1.3.5. Volume-sensitve Cl^- channels:

1.3.5.1 General properties:

Over the past decade volume-sensitive Cl^- currents have been discovered in an ever increasing number of cell types as their physiological role in maintenance of cell volume is slowly being established (discussed below). A summary of the properties of characterised volume-sensitive anion currents is shown in table 1.1. The currents typically activate in response to a reduction in extracellular osmolarity and the concomitant increase in cell volume. The currents show an outwardly rectifying current-voltage relationship and in a high percentage of cells, exhibit time-dependent inactivation at strongly depolarised potentials (not all currents however; see Table 1.1). The rate of inactivation is often variable and several studies have suggested the

Cell Type	Current Rectification	Anion Selectivity	Time-dependent inactivation	Blockers	Refs.
Human endothelial	Outward	I > Cl ~ Br > F > gluconate	✓	NPPB (29 μM) DIDS (120 μM) ATP (4.9, 8.2 mM) Tamoxifen (2.9μM) Verapamil (100 μM) DDFSK (60 μM) Arachidonate (weak)	1, 2
Human epithelial (Intestine 407)	Outward	SCN > I > Br > Cl > F > gluconate	✓	NPPB (25 μM) SITS (1.5, 6 μM) DPC (350 μM) Arachidonate (8μM)	3
Canine cardiac	Outward	-	X	NPPB 9-AC	4
F11 (neuronal)	Outward	I > Br > Cl > F > acetate	X	DIDS	5
Airway epithelia	Outward	I > Br > Cl	✓	DIDS	6
T-84 epithelia	Outward	-	✓	DNDS	7,8
Retinal pigment epithelia	Outward	-	X	DIDS SITS	9
Human neutrophils	Outward	SCN > I >Br ~ Cl > glucuronate	X	SITS	10
H69AR lung small cells	Outward	-	✓	DIDS	11,12
HeLa	Outward	SCN > I > Br >Cl > F > gluconate	✓	DIDS NPPB Verapamil DDFSK	13
Parotid acinar	Outward	SCN > I > Br > Cl > F > gluconate	✓ (weak)	SITS	14
Epididymal	Outward	I ~ Br > Cl	✓ (weak)	NPPB (120 μM) DPC (500 μM) DIDS (20, 120 μM)	15, 16
Osteoclasts	Outward	-	X	SITS DIDS DNDS	17
Ciliary epithelia	Outward	-	X	NPPB	18

Table 1.1. Properties of characterised volume-sensitive anion conductances. Time-dependent inactivation kinetics as assessed at depolarised potentials. IC_{50} values for blockers are indicated where determined in brackets. Where two values appear these represent the IC_{50}s determined at negative and positive potentials, and thus reflect voltage-dependent block. References: 1, Nilius, Sehrer & Droogmans, 1994a; 2, Nilius, Oike, Zahradnik & Droogmans, 1994b; 3, Kubo & Okada, 1992; 4, Tseng, 1992; 5, Pollard, 1993; 6, Chan, Goldstein & Nelson, 1992; 7, Worrell, Cliff, Butt & Frizzell, 1989; 8, Solc & Wine, 1991; 9, Botchkin & Matthews, 1993; 10, Stoddard, Steinbach & Simchowitz, 1993; 11, Jirsch, Deeley, Cole, Steward & Fedida, 1993; 12, Jirsch, Loe, Cole, Deeley & Fedida, 1994; 13, Díaz, Valverde, Higgins, Rucâreanu & Sepúlveda, 1993; 14, Arreola, Melvin & Begenisich, 1995; 15, Chan, Fu, Chung, Huang, Zhou & Wong, 1993; 16, Chan, Fu, Chung, Huang, Chan & Wong, 1994; 17, Kelly, Dixon & Sims, 1994; 18, Yantorno, Carré, Coca-Prados, Krupin & Civan, 1992.

mechanism responsible is voltage-dependent; however some single channel studies have shown that at positive potentials the mean open time and open probability of the channel is stable (McCann, Li, & Welsh, 1989; Solc & Wine, 1991). It has recently been shown that divalent cations, primarily Mg^{2+}, at physiological concentrations modulate volume-sensitive Cl^- currents and represent the mechanism responsible for time-dependent inactivation (Anderson, Jirsch & Fedida, 1995). Block of currents by cations is not an uncommon observation as cell-swelling activated Cl^- channels have previously been shown to be effectively inhibited by La^{3+} and Gd^{3+} (Ackerman, Wickman & Clapham, 1994), and intracellular block by Mg^{2+} ions is known to confer

the rectification properties of inwardly rectifying K^+ channels (Vandenburg, 1987). The anion permeability sequence of SCN > I > Br > Cl > F also seems to be characteristic of volume-sensitive Cl^- currents, but there are exceptions such as the current in human endothelial cells (Nilius, Seher & Droogmans, 1994) and neutrophils (Stoddard, Steinbach & Simchowitz, 1993).

Cell Type	Single Channel Conductance (γ) pS	Reference
T84 colonocytes	75	Worrell *et al.* 1989
Renal cortical collecting duct	305	Schwiebert, Mills & Stanton, 1994
Small cell lung carcinoma	53	Jirsch *et al.* 1994
Rabbit osteoclasts	19	Kelly *et al.* 1994
Cystic fibrosis and normal nasal epithelium	~ 50	Solc & Wine, 1991
C127 mouse mammary epithelium IEC-6 rat intestinal crypt	~ 70	Krouse, Haws, Xia, Fang & Wine, 1994
MDCK cells	~ 63	Banderali & Roy, 1992
PC12 (phechromocytoma)	~ 48	Cornett, Ubl & Kolb, 1993
Human endothelial cells	1.1	Nilius *et al.* 1994a
Human neutrophils	1.5	Stoddard *et al.* 1993
Human umbilical vein endothelium (HUVEC)	1.1	Nilius, Sehrer, Viana, De Greef, Raeymakers, Eggermont & Droogmans, 1994c
EN-aorta (endothelium)	1.5	Nilius *et al.* 1994c
COS-1 (monkey kidney)	0.4	Nilius *et al.* 1994c
HeLa (epithelia)	2.8	Nilius *et al.* 1994c
KB3 (epithelia)	3.2	Nilius *et al.* 1994c
3T3 (fibroblasts)	1.4	Nilius *et al.* 1994c
RBL-2H3	5.8	Nilius *et al.* 1994c
Jurkat (T-cell)	2.4	Nilius *et al.* 1994c
C3H 10T½ (fibroblasts)	0.2	Nilius *et al.* 1994c
L (connective tissue)	1.9	Nilius *et al.* 1994c
T84 cells	0.2	Ho, Duszyk & French, 1994
T-lymphocytes	~ 2	Lewis, Ross & Calahan, 1993

Table 1.2. Summary of single channel conductance values (γ) for volume-sensitive Cl^- currents in a variety of cell types. Conductance values are quoted for outward currents where channels showed an outwardly rectifying current-voltage relationship. Small conductance values (< 5 pS) were determined using stationary and non-stationary noise analysis of currents in whole-cell configuration (see relevant reference for details), larger currents were measured using conventional patch techniques.

As detailed by table 1.1 the currents are effectively inhibited by a variety of compounds but most notably the carboxylate and stilbene derivative Cl^- channel blockers (see 1.1). A number of studies have determined values of the conductance of the single channels responsible for whole-cell Cl^- currents (summarised in Table 1.2). As can be seen from table 1.2 these values appear to fall into two main categories; those with a single channel conductance of 50 pS or greater, and those with a conductance of less than 5 pS. There does appear to be some disagreement as to the conductance of the channels underlying the volume-sensitive current in T84 cells (Table 1.2). However, the channels reported by Worrell *et al* (1989) were also detected in cells under non-swelling conditions.

1.3.5.2. Mechanism of current activation:

The underlying mechanism by which volume-sensitive Cl^- currents are activated has been the focus of much attention. However, the data appears to be inconclusive and the proposed mechanisms vary substantially from cell type to cell type. There does

appear to be general consensus that increases in intracellular Ca^{2+} or levels of cyclic AMP are not responsible (e.g. Botchkin & Matthews, 1993; Kubo & Okada, 1992; Kelly *et al.* 1993; Chan *et al.* 1993). This conclusion has been based upon a number of findings: i) the differences between the kinetics and ion selectivity of currents activated by Ca^{2+}, cyclic AMP and hypotonicity (see above), ii) the lack of effect of inhibitors of protein kinase A or increased concentration of intracellular Ca^{2+} chelator upon volume-sensitive Cl^- current activation, and iii) in some cells where volume-sensitive Cl^- currents are present, increasing levels of cyclic AMP or intracellular Ca^{2+} directly are unable to elicit increases in membrane Cl^- permeability. Activation of kinases other than protein kinase A (PKA) have been implicated as possessing a role in osmosensing and subsequent activation of ionic conductances. Two studies have shown that hypotonic shock results in phosphorylation of intracellular proteins, particularly at tyrosine residues, and it has been suggested that this may be an important step in a cascade that terminates with activation of volume-sensitive ion channels (Tilly, van den Burghe, Tertoolen, Edixhoven & de Jonge, 1993; Galcheva-Gargova, Dérijard, Wu & Davis, 1994). In proximal tubule cells activation of a Cl^- current believed to participate in volume-regulation requires PKC and ATP for activation (Robson & Hunter, 1994). However, other studies have shown that non-specific kinase inhibitors such as H-8, or removal of intracellular ATP have failed to inhibit hypotonicity induced Cl^- current activation (Tseng, 1992; Jirsch *et al.* 1994). Nilius *et al* (1994b) have suggested a role of phospholipase A_2 (PLA_2) in volume-sensitive Cl^- current activation in human endothelial cells, a hypothesis based upon the inhibition of current activation by 4-bromophenacryl bromide (pBPB), a potent PLA_2 inhibitor. The identity of the metabolite responsible is unknown as addition of arachidonic acid, the major PLA_2

cleavage product, produced inconsistent effects. Cell swelling will produce an increase in membrane tension so it may be that the channels underlying volume-sensitive currents are stretch-activated. In renal cortical collecting duct cells application of negative pressure to the patch pipette has been demonstrated to induce activation of the same 305 pS channel activated by hypotonic shock (Schwiebert *et al.* 1994). A whole-cell study in cardiac myocytes using the cationic ampipath, dipyridamole (DPM), which has been shown to generate membrane tension (Jennings & Schultz, 1990), found that DPM rapidly produced increases in Cl^- permeability (Tseng, 1992). However, in human lymphocytes a converse finding was reported as DPM inhibited the volume-sensitive anion pathway (Sarkadi, Cheung, Mack, Grinstein, Gelfand & Rothstein, 1985). The cell cytoskeleton, particularly actin microfilaments, has been proposed to possess a role in volume-sensitive Cl^- current regulation (Jirsch *et al.* 1994; Mills, Schwiebert & Stanton, 1994; Schwiebert *et al.* 1994). Data to support this hypothesis has been obtained from studies employing actin disrupting agents, such as cytochalasins and dihydrocytochalasins. In renal cortical collecting duct cells dihydrocytochalasin B rapidly (4 min) produced activation of the 305 pS anion channel previously shown to open in response to hypotonic shock (Schwiebert *et al.* 1994). However, in small cell lung cancer cells treatment with cytochalasin D did not elicit any measurable current increases but did inhibit activation of the volume-regulated Cl^- current in response to hypotonic shock (Jirsch *et al.* 1994), suggesting effective uncoupling of the current and the volume response of the cells. Thus the exact role that actin microfilaments play in controlling volume-sensitive ionic conductances is unclear. It is interesting to note that a protein that can regulate volume-induced Cl^- currents in

Xenopus oocytes (pI_{Cln}; see 1.3.5.5) has an actin-binding domain (Krapivinsky, Ackerman, Gordon, Krapivinsky & Clapham, 1994).

1.3.5.3. The ClC-2 chloride channel:

A member of the ClC family of cloned voltage-gated Cl^- channels, ClC-2, has been shown to be activated in response to hypotonicity when expressed in *Xenopus* oocytes (Gründer, Thiemann, Pusch & Jentsch, 1992). It has been suggested that physiologically this channel has a role in cell volume regulation (see 1.4). There are however a number of biophysical differences between the current produced by this cloned variant and the currents from native channels in cells. The ClC-2 channel can not only be activated by cell swelling but also by unphysiologically strong hyperpolarisation (in excess of -100 mV). Other differences include a slightly inward-rectifying current-voltage relationship and a Cl^- over I^- ion selectivity ($Cl >> Br > I$). The reported single channel conductance of 3 - 5 pS does however agree with some values determined in cells (Table 1.2). Northern blot analysis has shown that ClC-2 appears to be ubiquitously expressed in all tissues (rat skeletal muscle, heart, brain, lung, kidney, pancreas, stomach, intestine and liver) and cell lines (NIH 3T3, T84, CFPAC-1, LLC-PK_1, CHO, Neuro-2a, PC12) investigated (Pusch & Jentsch, 1994). In some tissues (heart, skeletal muscle, T84 cells) expression has been further confirmed by additional cDNA cloning (Thiemann, Gründer, Pusch & Jentsch, 1992). Broad expression of ClC-2 suggests that it may fulfil an important cellular function, however as there are substantial differences between ClC-2 and other volume-regulated Cl^- conductances its *in vivo* role remains to be established.

1.3.5.4. P-glycoprotein:

Many cancer cells are intrinsically resistant to chemotherapy treatment or develop resistance during treatment. This resistance is normally non-selective, and cells become resistant to a wide variety of compounds, an effect that has led to the term 'multidrug resistance'. P-glycoprotein (P-gp), the product of expression of the MDR-1 gene, has been shown to actively transport chemotherapeutic substances from the cell cytosol and is a member of the ABC (ATP-binding cassette) family of transporters (reviewed by Doige & Ames, 1993). Prompted by the finding that CFTR, another ABC transporter, is a Cl^- channel, P-gp has been extensively tested for ion channel function. In cells transfected with MDR1 cDNA (encoding P-gp), substantial volume-sensitive Cl^- currents with characteristics similar to those reported for other volume-regulated currents were observed suggesting an association between P-gp expression and the currents (Valverde, Díaz, Sepúlveda, Gill, Hyde & Higgins, 1992; reviewed by Higgins, 1995). The volume-sensitive Cl^- currents associated with P-gp expression are inhibited by a variety of compounds that have been classified into four classes (Mintenig, Valverde, Sepúlveda, Gill, Hyde, Kirk & Higgins (1993). Class I compounds are cytotoxic drugs that are transported by P-gp such as daunomycin, and are only effective when present on the intracellular surface of the membrane in the presence of hydrolysable ATP. These compounds act to prevent channel activation rather than as a classical blocker. Class II compounds inhibit both the drug transport and Cl^- channel activity associated with P-gp; this effect has been reported for verapamil and dideoxyforskolin (DDFSK) but the most potent and specific of this class appears to be tamoxifen. The mechanism of block appears to be more consistent with

that of true channel blockers as they are effective from the extracellular surface. Class III compounds are typical Cl^- channel blockers such as NPPB and DIDS which block only channel activity, whilst class IV compounds (e.g. cyclosporin) block only drug transport. The differences between class III and class IV inhibitors suggest that the channel and transporter functions of P-gp are distinct and separable. A number of studies have suggested that P-gp is unlikely to be a channel itself and thus imply it must function as a channel regulatory protein. The most compelling result to support this hypothesis is work performed with HeLa cells which possess volume-activated Cl^- currents indistinguishable from those associated with P-gp expression (Díaz, Valverde, Higgins, Rucâreanu & Sepúlveda, 1994) yet do not express measurable levels of P-gp itself (Higgins, 1995). Volume-sensitive Cl^- currents in P-gp expressing cells have been shown to be sensitive to changes in PKC activity, with activation of PKC resulting in the prevention of channel activation (Hardy, Valverde, Goodfellow, Higgins & Sepúlveda, 1994). Expression of P-gp in HeLa cells confers PKC sensitivity on the endogenous volume-activated Cl^- currents, thus suggesting a channel regulatory function. The mechanism by which P-gp regulates channel activity is as yet undetermined.

1.3.5.5. I_{Cln} Cl current:

Another type of Cl^- current has resulted from expression cloning studies using MDCK cells as the source of mRNA. Injection of this mRNA into *Xenopus* oocytes results in expression of a 235-amino-acid protein and chloride selective outward currents (Paulmichl, Li, Wickman, Ackerman, Peralta & Clapham, 1992). This current, termed

I_{Cln}, possesses many of the characteristics of volume-sensitive Cl^- currents, but is inhibited by high concentrations of extracellular nucleotides (Paulmichl *et al.* 1992). As *Xenopus* oocytes have been shown to express a Cl^- current that responds to hypotonicity (Ackerman, Wickman & Clapham, 1994), the relationship between pI_{Cln} (the protein) and the volume-sensitive currents was investigated. Anti-I_{Cln} monoclonal antibodies were found to effectively inhibit the native hypotonicity-induced currents thus it has been suggested that pI_{Cln} is more likely to function as a regulatory protein than an ion channel (Krapivinsky *et al.* 1994).

1.4. Cell volume regulation:

Mammalian cells tend to gain volume passively as a result of the presence of membrane impermeant, charged intracellular molecules. This tendency of cells to swell must thus be counteracted by active processes to regulate cell volume otherwise cells will swell until eventually the membrane is compromised. The processes that cells utilise to maintain their volume has been the focus of much research and comprehensively reviewed (Hoffmann & Simonsen, 1989; Grinstein & Foskett, 1990). Much of this investigation has concentrated upon absorbing and secreting epithelia, as the large transcellular ion fluxes experienced by these cells represents a fierce challenge to cellular volume homeostasis (reviewed by Okada & Hazama, 1989). However, volume regulation appears to be a fundamental characteristic of all cell types. When cells are subjected to a reduction in extracellular osmolarity (hypotonic shock) they respond with rapid cell swelling followed by a slow readjustment of cell volume back towards basal levels. This process is termed a regulatory volume decrease (RVD). Conversely

when extracellular osmolarity is increased cells shrink prior to volume readjustment in a process termed regulatory volume increase (RVI). Here, only the mechanisms that lead to an RVD response are considered. The cellular RVD response to a hypotonic challenge has been extensively shown to result from the efflux of intracellular osmolytes, and accompanying osmotically obligated water. A number of studies have shown that RVD is associated with a reduction of the cellular content of K^+ and Cl^- ions (e.g. Bui & Wiley, 1981), suggesting these ions are extruded from the cell. Although cell volume reduction appears to be predominantly due to efflux of inorganic ions, efflux of organic osmolytes such as amino acids and taurine have also been demonstrated (Hoffman & Lambert, 1983; Garcia-Perez & Burg, 1991). Extrusion of K^+ and Cl^- in response to cell swelling occurs via activation of electroneutral K^+-Cl^- co-transport (Parker, 1983) or separate conductive pathways for each respective anion. The latter mechanism appears to be more common and results from activation of ion channels for each ion. Much of the evidence to support this conclusion has resulted from the inhibition of RVD by ion channel blockers selective for K^+ channels such as quinine, TEA, and 4-aminopyridine (Grinstein & Foskett, 1990), and those selective for Cl^- channels e.g. NPPB and DIDS (Kubo & Okada, 1992). More direct evidence has resulted from patch-clamp studies that have definitively demonstrated activation of Cl^- (see 1.3) and K^+ channels (e.g. Sackin, 1989; Davison, 1993) in response to hypotonic shock. In a variety of cell types Ca^{2+} has been shown to play a dominant role in the activation of RVD (reviewed by Pierce & Politis, 1990; McCarty & O'Neil, 1992). Removal of extracellular Ca^{2+} was found to substantially hinder the RVD response of UMR-106-01 osteosarcoma cells (Yamaguchi, Green, Kleeman & Muallem, 1989) and in Intestine 407 epithelial cells biphasic rises in cytosolic free Ca^{2+}

were observed in association with activation of K^+ and Cl^- conductances during RVD (Hazama & Okada, 1990). These observations have led to suggestions that the ionic conductances underlying the RVD process are Ca^{2+}-sensitive i.e. Ca^{2+}-dependent K^+ and Cl^- channels. A number of patch-clamp studies have shown that Ca^{2+}-sensitive K^+ channel activity is increased during RVD and that selective inhibitors of this channel such as charybdotoxin can effectively impair RVD (Christensen, 1987; Ubl, Murer & Kolb, 1988; Hazama & Okada, 1988; Davison, 1993). However, as discussed above, the volume-sensitive anion current involved in RVD in most cell types does not appear to open in response to elevation of intracellular Ca^{2+} (see 1.3). Similarly, in leukocytes the RVD process can occur independent of extracellular and intracellular Ca^{2+} suggesting neither conductance requires Ca^{2+} for activation (Grinstein & Foskett, 1990). This may suggest that although RVD generally seems to be accomplished by KCl efflux (and osmotically obligated water), the processes by which this is achieved may vary from cell type to cell type.

1.5. Intracellular Ca^{2+} homeostasis:

Ca^{2+} is an important cellular messenger responsible for coupling membrane excitability and extracellular signals to intracellular events such as muscle contraction and cellular secretion. Ion channels have a predominant role in controlling the amount of free Ca^{2+} present in the cell cytoplasm. This is achieved by two main pathways controlled by ion channels; entry of extracellular Ca^{2+} via voltage-gated and receptor-operated Ca^{2+} channels, and release of intracellular Ca^{2+} via Ca^{2+}-release channels present on the endoplasmic reticulum (ER). Voltage-gated Ca^{2+} channels have been extensively

researched and reviewed (see Tsien, 1983; Tsien & Tsien, 1990) and are thus not considered here.

Efflux of Ca^{2+} from intracellular stores (the ER) can occur in response to two types of intracellular stimuli. Elevation of intracellular Ca^{2+} alone can stimulate internal stores to release Ca^{2+} in a process termed 'Ca^{2+}-induced Ca^{2+} release' (CICR) (Endo, 1977). The second mechanism is in response to specific cytoplasmic agonists. Two groups of intracellular ligand-gated Ca^{2+}-release channels with significant structural and functional homologies have been distinguished, the inositol 1,4,5-trisphosphate receptors ($InsP_3R$) and the ryanodine receptors (RyR) (Berridge, 1993).

	$InsP_3$ receptor	Ryanodine receptor
Skeletal muscle	Minor	Dominant
Smooth muscle	Dominant	Minor
Neurones	Significant	Significant
$InsP_3$ (1 - 100 nM)	Opens	No action
Ryanodine	No action	Partial opener (at nM) Closes (> μM)
Caffeine	Inhibits	Opens
Ca^{2+}	Opens (< 300 nM) Inhibits (> 300 nM)	Opens
Ruthenium red	No action	Blocks
Heparin	$InsP_3$ antagonist	Potentiates

Table 1.3. Summary of the basic properties of the $InsP_3$ and ryanodine receptor Ca^{2+} release channels. *Adapted from Hille, 1992 and Berridge, 1993.*

Electrophysiologically, both classes of channel have been characterised using membrane vesicles isolated from the ER of a variety of cell types, which have been

incorporated into planar lipid bilayers. This technique allows the lipid bilayer to be voltage-clamped and the currents flowing through single channels to be measured (Miller, 1986). The basic properties of these two classes of Ca^{2+} release channels are summarised in table 1.3. Bilayer incorporation has shown that both channels are cation channels with a 5 - 10 fold preference for Ca^{2+} ions over small monovalent ions. As shown in table 1.3, both receptor/channels can be modulated by various pharmacological agents but their actions are not totally specific. Apart from antagonising the $InsP_3R$, heparin can also inhibit $InsP_3$ generation thus its usefulness in studies on intact cells is limited. Though caffeine is well known to release Ca^{2+} from ryanodine-sensitive stores there have been suggestions that it can have similar actions upon $InsP_3$-sensitive stores as well (Komori & Bolton, 1991). Recently, it has been shown that the RyR can be regulated by another putative cellular messenger, cyclic adenosine diphosphate ribose (cADPR) which also causes this store to release its sequestered Ca^{2+} (Galione, McDougall, Busa, Willmott, Gillot & Whitake, 1993). Thus these Ca^{2+} release channels are the basis of CICR (particularly the RyR), and the rises in intracellular Ca^{2+} levels that are seen with membrane receptor agonists that couple to the phosphoinositide cascade. Calcium oscillations that are frequently observed in cells (regenerative Ca^{2+} release) are also believed to be due to release by these channels, particularly in light of their CICR abilities, and thus they may represent a 'frequency-encoded second messenger system' (Berridge & Irvine, 1989).

Direct measurements of intracellular Ca^{2+} levels using fluorescent dyes has shown that rises in response to agonists linked to $InsP_3$ production occur as a consequence of not only mobilisation of intracellular stores but also extracellular Ca^{2+} influx (Tsien, Pozzan

& Rink, 1982). The mechanism by which this influx occurs appears to be by receptor-operated Ca^{2+} channels (ROCCs; reviewed by Fasolato, Innocenti & Pozzan, 1994). These channels can be opened in response to a variety of stimuli including depletion of intracellular Ca^{2+} stores and $InsP_3$ generation (summarised in table 1.4) thus the term 'receptor-operated' may be incorrect as some of the mechanisms by which these channels are opened is as yet undetermined.

Channel	Trigger	Conductance	Permeation	Cell type
Ca^{2+}-release-activated channel (I_{CRAC})	EGTA BAPTA $InsP_3$ ionomycin thapsigargin	20 fS (110 Ca^{2+})	$Ca^{2+}>Ba^{2+}>Mn^{2+}$	mast cells 3T3 fibroblasts hepatocytes endothelial oocytes
Second-messenger-operated channel	Ca^{2+} and $InsP_4$	2 pS (100 Mn^{2+})	Ba^{2+},Ca^{2+},Mn^{2+}	endothelial
	Ca^{2+}	4 - 25 pS (90 Ca^{2+})	Ca^{2+},K^+,Na^+	neutrophils
	$InsP_3$	8 pS (100 Ba^{2+})	Ba^{2+}, Ca^{2+}	T cells
	$InsP_3$	80 pS (55 Ba^{2+})	Ba^{2+}, K^+	neurones
	$InsP_3$	4 - 13 pS (100 Ca^{2+})	Ba^{2+}, Ca^{2+}	A413 cells
Receptor-operated channel	ATP	5 pS (100 Ca^{2+})	Ca^{2+},Na^+	smooth muscle

Table 1.4. Summary of the characteristics of Ca^{2+} channels activated by receptors or intracellular store depletion. *The concentration of the cation used to determine the conductance measurement is given in brackets. From Fasolato et al. 1994.*

As shown in table 1.4 the majority of these Ca^{2+} influx channels have a small conductance ranging from fS to low pS values. The pharmacology of these channels is

largely unknown, they are however insensitive to classical inhibitors of voltage-gated Ca^{2+} channels such as verapamil and dihydropyridines. The only characterised inhibitors are divalent and trivalent cations (Cd^{2+} and La^{3+}) and some imidazole derivatives such as SKF 96365 (Fasolato *et al.* 1994).

1.6. Aims of this investigation:

To establish and characterise cellular models in which the mechanisms underlying ion channel activation and modulation can be effectively studied and investigated in clonal and primary cultured cells.

Chapter 2.

GENERAL EXPERIMENTAL PROCEDURES

2.1. Cell Culture:

All cell lines were grown and maintained in Dulbecco's modified Eagle medium (DMEM) containing 25 mM D-glucose and 1 mM sodium pyruvate (GIBCO, Paisley, Scotland). The medium was further supplemented with 5% (L6) or 10% (ROS 17/2.8 and primary cultured osteoblasts) foetal calf serum, 2 mM glutamine (sterilised with a 0.22 μm filter prior to addition) and antibiotic-antimycotic mixture (200 U ml^{-1} penicillin, 200 μg ml^{-1} streptomycin and 0.5 μg ml^{-1} fungizone). Cultures were maintained at 37°C in a humidified 5% CO_2 in air atmosphere. Stock cultures were grown in either 75 cm^2 or 25 cm^2 culture flasks and sub-cultured at suitable intervals (4-7 days) when 80% confluence was attained. For experimental purposes cells were seeded on appropriate flasks and dishes as detailed later. All cell culture flasks and plates were tissue culture treated (collagen coating) and were obtained from Corning (New York, USA) or Bibby Sterilin Ltd. (Staffs., UK).

2.2. Inositol Phosphate Accumulation:

This assay measures the incorporation of radiolabelled *myo*-inositol into inositol phosphates to provide an indication of phospholipase C (PLC) activity. The detailed methodology was similar to that previously described (Jackson & Hanley, 1989).

Cells were grown to confluence in 24 well plates prior to labelling by replacing maintenance media with 5 μCi of [^{3}H]-*myo*-inositol (Amersham International, UK) added to 1 ml of supplemented DMEM (see 2.1 for composition). 24 - 48 hrs later the

incubation medium was removed and replaced with 1 ml Krebs-Hensleit buffer containing 0.3 % w/v bovine serum albumin (BSA) and incubated at 37°C for 30 min. Cells were preincubated with 10 mM LiCl in Krebs/BSA solution for 10 mins (to inhibit phosphatases) and then challenged with drugs for 30 min. Incubations were terminated by aspiration of the media and adddition of 1 ml of ice-cold (0 - 4°C) 20% v/v trichloracetic acid (TCA)/2mM EDTA solution to each well. The sample was left on ice for 15 min prior to centrifuging at 10,000g for 5 min to remove any protein. The supernatant was removed and neutralised by addition to 5 ml of a 1:1 1,1,2-trichloro-1,2,2-trifluorethane (freon)/tri-n-octylamine mixture. After vigorous shaking the mixture was allowed to separate into 2 distinct layers. The upper phase containing the [^{3}H] labelled inositol phosphates was carefully removed for analysis.

Radiolabelled inositol phosphates were analysed and separated by anion-exchange chromatography on columns of Dowex AG1-X8 resin (formate form, Biorad, UK) as described by Downes, Hawkins & Irvine (1986). Briefly, Dowex resin was prepared by soaking in distilled H_2O for 1 hr, changing the water 3 times to ensure any undersize resin particles were removed. After allowing the resin to sediment the volume was adjusted to provide a 50% v/v solution of Dowex resin. 1 ml of this solution was added to each chromatography column (Biorad, UK) and allowed to sediment. To separate inositol phosphates the sample for analysis was added to the top of the column and the following elution protocol was employed:

i) 2 x 4 ml dH_20 (to wash off any free inositol).

ii) 2 x 4 ml 60 mM Na-formate/5 mM di-sodium tetraborate (to remove glycerophosphoinositides).

iii) 1 x 4ml 1 M ammonium formate/0.1 M formic acid (to release inositol phosphates, up to $InsP_4$).

The final fraction was collected and added to 10 ml of scintillation cocktail (Hi-Safe III) before counting for [^{3}H] radiactivity by liquid scintillation counting (Packard 1900-TR, Packard, USA) using a tritium (β-emission) window for 5 min.

2.3. Electrophysiological Experiments.

2.3.1. Cells:

Cells were seeded onto uncoated glass coverslips (Chance Propper Ltd., Warley, UK), previously sterilised by immersion in 70% v/v ethanol and washed in DMEM, at a density of 1 x 10^4 cells ml^{-1}. Coverslips were placed in 6 wells plates until used in experiments 3 - 7 days after seeding. Prior to experiments the coverslip was broken into a number of small pieces, a new piece being used in each experiment so that cells did not receive multiple drug exposures.

2.3.2. Intracellular recording:

Cells were placed in a glass bottomed, perspex perfusion bath of approximately 4 ml volume (in-house fabrication) and perfused with Liley's saline by gravity at a flow rate

of 4 ml min^{-1} (see Solutions for composition). All experiments were performed at room temperature (20 - 24°C).

The perfusion bath was attached to the movable stage of a moving limb compound microscope (Carl Zeiss Jena, Germany). This was a microscope which moved the objective lens, not the specimen stage for focusing. The cells were observed using a 40 X long working distance (6.3 mm) Nomarski DIC objective (Nikon, Japan) and 10 X ocular lens, producing a total magnification of 400 X. Intracellular microelectrodes were manufactured from borosilicate glass capillaries (1.0 mm O.D. x 0.58 mm I.D.) containing an inner filament to aid filling (GC100F-15; Clark Electromedical Instruments, UK). The capillary was pulled in a single pull using a programmable needle/pipette puller (Kopf Model 750, David Kopf Instruments, USA) to form an electrode of 30 - 50 MΩ resistance when filled. The electrode was filled with 3 M KCl and inserted into an electrode holder (EH-3MR/1.0, Clark Electromedical Instruments) that contained a Ag/AgCl pellet. The holder was attached to the input stage of a biological amplifier (Model M-707, WPI, USA) that was held by a mechanical micromanipulator (Leitz, Germany) to allow fine positioning of the electrode. The perfusion chamber was attached to ground via a Ag/AgCl pellet electrode.

After the recording electrode was lowered into the saline and positioned above the cell to be impaled, tip potentials were negated using the amplifier DC offset such that the displayed potential was 0 mV. Tip potentials typically ranged between -20 and +40 mV. Cell penetration was achieved by rapidly forcing the recording electrode through the cell membrane with a swift downward movement of the manipulator. This

technique was found to have the highest success rate in achieving subsequent sealing of the membrane around the electrode and avoiding cell 'run down'. This occurs as a result of damage to the membrane such that cytoplasmic contents leak out and is seen as a slow fall in the membrane potential towards 0 mV. Experiments were performed on cells whose membrane potential did not fall below -60 mV during the 5 mins subsequent to cell penetration.

The output of the amplifier was displayed on a cathode ray oscilloscope (Tektronx D12, UK) and a flatbed chart recorder (Tekman, UK). Signals were also recorded onto videotape after digitisation via an analogue to digital converter (PCM-2, Medical System Corp., USA) for later off-line analysis. Analyses were performed by playback into an Apple Macintosh (Apple Computers, USA) using a MacLab 4 and Chart software (Analog Digital Instruments, Australia) sampling at 0.5 kHz.

Drugs were applied to the cell under study after dilution in Liley's saline via the perfusion system. The 'dead space' between the solution reservoirs and the bath accounted for a lag of approximately 2 min between the start of perfusion and the drug reaching the cell.

2.3.3. Patch-clamp recording:

Coverslips containing the seeded cells were placed in a Petri dish mounted on the specimen stage of an inverted microscope (Nikon TMS, Nikon, Japan) and continuously superfused with extracellular bathing solution by gravity at a flow rate of

4 ml min^{-1}. A peristaltic pump removed fluid to maintain a constant level in the recording chamber, typically around 1 mm deep. Drug and test solutions were applied directly to the cell under study by means of a multi-barrelled perfusion pipette system as described by Langton (1992). This allowed rapid exchange of the bathing medium surrounding the cell. Briefly, this consisted of 3 barrelled borosilicate capillary glass (1.2 mm O.D. x 0.69 mm I.D., 3GC120F-10, Clark Electromedical Instruments) that was pulled to a fine tip by heating with a glowing 4 turn nichrome wire. The tip was then cut using a glass knife and fire polished. The degree of fire polishing and the position of the cut relative to the shank of the pipette resulted in perfusion pipettes with different diameters and thus different flow rates. The flow rate routinely used was measured to be approximately 200 - 300 µl min^{-1}. Drug solutions were contained in 10 ml reservoirs that were connected to the perfusion pipette by 1.0 mm diameter polethylene tubing (Portex, UK) and a fine tube that was epoxied into the lumen of each of the pipette barrels. Flow from the reservoir was controlled by a low voltage switchable solenoid valve (LFAA 125, Lee Instac Products, UK). The perfusion pipette was placed between 200 and 500 µm from the cell under study, the distance dependent upon the pipette flow rate. This system changed the bathing medium surrounding the cell under study within 1 s as assessed by changes in pipette resistance when perfused with distilled water.

All experiments were performed at room temperature (20 - 24°C) using the patch-clamp technique (Hamill, Marty, Neher, Sakmann & Sigworth, 1981).

2.3.3.1. Whole-cell voltage-clamp:

Patch-clamp pipettes were manufactured from borosilicate glass capillaries (1.5 mm O.D. x 1.17 mm I.D., GC 150-15TF, Clark Electromedical Instruments) using a two-stage electrode puller (PB7, Narashige Instruments, Japan). Pipettes were fire polished with a glowing platinum glass coated wire to give a final resistance of 1 - 4 MΩ resistance when filled with pipette solution. Current changes were measured by a 0.1 mm diameter silver wire that was chlorided in the region it would come into contact with intracellular solution. The wire was chlorided at regular intervals (1 - 2 days) by the method of Purves (1981) using a switchable, low voltage (1 - 2 V) power supply and 0.1 M HCl. The wire was connected via a polycarbonate microelectrode holder to the input headstage of an Axopatch 1C patch-clamp amplifier (Axon Instruments, Foster City, CA, USA) mounted on a hydraulic micromanipulator (MO-203, Narashige Instruments). High resistance electrical seals (Giga-seal) were obtained by touching the patch pipette against the cell membrane surface and applying gentle negative pressure to the suction post of the microelectrode holder. After cancellation of capacitance transients due to the patch pipette, whole-cell mode was achieved by application of an electrical 'zap' (1 V amplitude, 0.1 - 0.5 ms duration), either alone or in conjunction with increased negative pressure, to the patch pipette. Cell capacitance and series resistance (typically 5 - 10 MΩ) were maximally compensated (80 - 90%) using the analog controls of the patch-clamp amplifier. Signals were filtered with an 8-pole Bessel type low pass filter at 1 or 2 kHz prior to digitisation at 2.5 kHz by a Labmaster DMA Tl-125 interface (Scientific Solutions, Solon, OH, USA). Currents were simultaneously stored on videotape using a pulse code modulator (PCM-2, Medical

System Corp.) and computer hard disk (386 DX, Olympus Technology, UK). Analysis was performed using WCP (J.Dempster, Strathclyde, UK) or pClamp 5.5.1 software (Axon Instruments), which was also utilised to generate voltage-clamp step protocols. The perfusion chamber was attached to ground via a Ag/AgCl pellet either directly, or isolated from the bath solution by a 3% w/v in 3 M KCl agar bridge.

2.3.3.2. Cell attached and excised patch experiments:

Experimental details for patch recording were similar to that described for whole-cell recording above. However, patch pipettes were coated with Sylgard 184 resin (Dow Corning, Belgium) to reduce the electrical capacitance of the patch pipette, and hence noise in the recording. This was performed by applying semi-cured resin (10:1, ratio of resin to hardener) to the 3 - 4 mm of the pipette shank preceeding the tip with a cocktail stick. The resin was completely cured using a Sylgard jig of the design of Sakmann & Neher (1983). Sylgarding was performed prior to fire-polishing so any resin that occluded the pipette tip would hopefully be removed by the polishing process. After polishing, pipettes had a resistance of 4 - 7 MΩ when filled with intracellular solution.

Cell attached patches were obtained by the process described above for giga-seal formation. Inside-out patches were formed by withdrawing the patch pipette from the cell surface after achieving a cell attached patch. Air exposure ensured that the patch was of inside-out configuration and not an isolated vesicle. This was simply performed by rapidly removing the patch pipette from the bathing solution into the air after patch

excision. Outside-out patches were formed by raising the patch pipette from the cell membrane subsequent to achieving whole-cell configuration. Where appropriate, after patch formation, the patch pipette was moved away from the cells at the bottom of the perfusion chamber to ensure that any substances released or secreted from the cells did not influence or contaminate the results.

2.4. Cell Volume Measurements.

Cells, grown to confluence on 15 cm diameter collagen coated culture plates, were released by 1% v/v trypsin/EDTA treatment (Gibco, Scotland) for 5 mins. After washing and resuspension in DMEM at a density of 8 x 10^6 cells ml^{-1}, cells were incubated in a humidified 5% CO_2 in air atmosphere at 37°C for 30 mins to allow recovery of ion gradients prior to cell volume measurement.

Cell diameter was measured by laser diffraction using a Malvern Mastersizer E (Malvern Instruments, Malvern, UK). To initiate experiments 0.5 ml of cell suspension was added to 10 ml of incubation medium of desired composition and osmolarity. Isotonic incubation medium consisted of (mM): NaCl, 140; KCl, 5; $MgCl_2$, 10; $CaCl_2$, 1.5; Hepes, 10; D-glucose, 5; bovine serum albumin, 0.1% w/v; pH 7.4 with HCl. Hypotonic incubation medium was obtained by dilution of isotonic solution to 50% with distilled water and supplemented with $CaCl_2$ to maintain extracelluar Ca^{2+} at a constant concentration unless otherwise specified. Prior to experiments all incubation solutions were filtered with a 0.22 μM filter (Whatman, New Jersey, USA) to remove any particles which could have corrupted the cell size analysis. Cells were routinely

resuspended at 5 min intervals to avoid any sedimentation that may occur within the sample cell during the course of an experiment.

Mean cell diameter distribution curves (2000 scans of the sample cell in a 4 s sample time) were recorded at various intervals over a 45 min period. Cell volumes were calculated from the mean cell diameter of each distribution curve (assuming cells were spherical) using equation 2.1, where r is the cell radius.

$$\text{Cell volume} = {}^{4}/_{3}\,\pi r^{3} \qquad \text{Equation 2.1.}$$

2.5. Solutions:

The composition of the buffers used in the experimental procedures are detailed below (mM):

Krebs-Hensleit buffer:

NaCl 120, KCl 5, $CaCl_2$ 2.5, KH_2PO_4 1, $NaHCO_3$ 25, $MgSO_4.7H_2O$ 1, D-glucose 12.

Liley's saline:

NaCl 137, KCl 5, $CaCl_2$ 2, $NaHCO_3$ 12, $NaHPO_4$ 12, MgCl 1, D-glucose 25.

Buffers were gassed with 5% CO_2/air mixture for 1 hr prior to use, or continuously throughout the duration of the experiment.

Patch-clamp solutions:

A variety of different solutions were used in patch-clamp experiments and are thus detailed in the results chapter to which they apply. All intracellular solutions were filtered with a 0.45 μM syringe filter (Whatman, New Jersey, USA) prior to filling of patch pipettes. Pipettes were filled using a fine capillary tube pulled from Nalgene tubing (3/16" i.d. x 5/16" o.d.) gently heated using the pilot light of a bunsen burner.

2.6. Data Analysis:

Results are routinely expressed as the mean ± the S.E.M. for n, number of observations. Where appropriate results were tested for significance using Student's paired or unpaired t-test; values of p less than or equal to 0.05 were deemed to be significantly different.

The 50% inhibitory concentration (IC_{50}) values for drugs were calculated by fitting the concentration-inhibition curves to a logistic equation (Equation 2.2) incorporating Hill coeffecients (n_H) using either the EBDA-LIGAND programme (Biosoft, Cambridge, UK) or MicroCal Origin (MicroCal Inc., Nortampton, MA, USA).

$$\text{Fraction Bound} = \frac{[\text{Drug}]^{n}H}{[\text{Drug}]^{n}H + IC_{50}} \qquad \text{Equation 2.2.}$$

Reversal potentials (E_{rev}) were obtained by fitting a second- or third-order polynomial to the current-potential (I-V) plots using the Levenburg-Marquardt algorithm. The resulting equation was solved using the Newton-Raphson iterative procedure. Where appropriate, peak currents were divided by the individual cell capacitance as indicated by the amplifier analogue compensation circuit, producing a current density (in $pApF^{-1}$) and thus a normalisation to cell size.

Chapter 3.

CHARACTERISATION OF A VOLUME-SENSITIVE CHLORIDE CURRENT IN RAT OSTEOBLAST-LIKE (ROS 17/2.8) CELLS

3.1. Background:

Osteoblasts have been shown to undergo substantial shape changes in response to stimulation by calciotropic hormones such as parathyroid hormone (PTH), vitamin D_3 and prostaglandin E_2 (Miller, Wolf & Arnaud, 1976). The osteoblasts, which normally form a continuous layer protecting the bone matrix, become dome-shaped and eventually become separated by an increased intercellular space. These morphological changes facilitate the bone resorbing action of osteoclasts and are thus a critical step in the process of bone resorption (Lindskog, Blomlöf & Hammarström, 1987).

It has been suggested that the alteration of osteoblast shape may involve a reduction in cell volume. Active regulation of cell volume has been demonstrated in the osteoblastic cell line, UMR-106-01, in response to a reduction in extracellular osmolarity. Hypotonic shock was also reported to produce an increase in intracellular Ca^{2+} levels and osteoblast hyperpolarization (Yamaguchi, Green, Kleeman & Muallem, 1989). Osteoblasts possess a wide variety of ionic channels including mechanosensitive non-selective cation channels which provide an entry pathway for Ca^{2+} (Duncan & Misler, 1989) and Ca^{2+}-sensitive K^+ channels (Dixon, Aubin & Dainty, 1984; Ferrier, Ward-Kesthely, Homble & Ross, 1987; Davidson, 1993). These K^+ channels are likely to open in response to elevated intracellular Ca^{2+} levels produced by cell swelling (via entry through mechanosensitive non-selective cation channels) and produce the reported cell hyperpolarization. However, for the osteoblast to accomplish a reduction in cell volume, this increased K^+ permeability is likely to be accompanied by an

increased Cl^- conductance, leading to efflux of KCl and thus osmotically obligated water.

In this chapter the effects of hypotonic shock upon membrane Cl^- permeability have been studied in the rat osteoblastic osteosarcoma cell line, ROS 17/2.8 cells

3.2. Methods:

Experiments were performed using the whole-cell, cell attached and excised patch configurations of the patch-clamp technique as described in the experimental procedures (2.3.2.2.) using Cl^- rich pipette and bathing solutions of composition detailed in table 3.1. The osmolarity of the solution was measured on the basis of freezing point depression using an osmometer (Knauer Instruments, Germany).

In experiments where reversal potentials or anion selectivity were determined, junction potentials were measured and corrected as described by Fenwick, Marty and Neher (1982). Briefly, junction potentials were measured by comparing the zero current voltage prior, and subsequent to the change in the bathing solution. During this procedure, a salt bridge was employed in the bath to eliminate changes in the reference electrode potential, though with the fast superfusion system (see 2.3.3.) employed in these experiments this was unlikely to occur.

In single channel experiments NMDG chloride isotonic bathing solution was used to both perfuse cells and as patch pipette solution. Cell swelling was achieved by either

application of normal NMDG chloride hypotonic solution (Table 3.1) or by dilution of isotonic solution to 50% v/v with distilled water.

A. N-methyl-D-glucamine (NMDG) chloride solutions (pH 7.4 - 7.5).

	Pipette*	Isotonic Bathing	Hypotonic Bathing†
NMDG-chloride	140	140	105
$MgCl_2$	1.2	0.5	0.5
$CaCl_2$	-	1.3	1.3
EGTA	1	--	--
HEPES	10	10	10
Osmolarity (mosmol l^{-1})	300	300	220

B. Choline chloride solutions (pH 7.3 - 7.4).

	Pipette*	Isotonic Bathing	Hypotonic Bathing
Choline Chloride	135	135	135
$MgSO_4$	2	5	5
$CaCl_2$	--	1.3	1.3
EGTA	1	--	--
HEPES	10	10	10
Mannitol	30	60	--
Osmolarity (mosmol l^{-1})	300	300	240

Table 3.1 Composition of solutions (mM) used in whole-cell recordings. **Unless indicated the pipette solution always contained 2 mM Na_2ATP and 0.5 mM Na_2 GTP. †For anion selectivity studies NMDG-chloride in this solution was replaced with*

either NaCl, NaSCN, NaI, NaBr, NaF or sodium gluconate. Any modifications to these solutions are detailed as appropriate.

Due to the non-inactivating nature of the current described in this chapter, leak currents were not subtracted and all current values are plotted are absolute with respect to the zero current level.

3.3. Materials:

N-phenylanthranilic acid (DPC) and 5-nitro-2-(3-phenylpropylamino)benzoic acid (NPPB) were purchased from RBI (Natick, MA, USA). Ionomycin was obtained from Calbiochem (Nottingham, UK), 12-O-tetradecanoylphorbol 13-acetate (TPA) and dipyridamole from Sigma (St.Louis, MA, USA). Tyrphostin A25 was supplied by Biomol (PA, USA). All above chemicals were added to the bathing solution from stock solutions in dimethyl sulfoxide (DMSO). The vehicle alone had no effect on whole cell Cl^- currents at the concentrations used (0.1 - 0.25%, n = 5). N-[2-(p-bromocinnamylamino)ethyl]-5-isoquinolinesulfonamide dihydrochloride (H-89, from Biomol) and 4,4'-diisothiocyanatostilbene-2-2'-disulphonic acid (DIDS, from Sigma) were directly dissolved in the test solution. Dihydrocytochalasin B (DHCB) was obtained from Sigma (USA), and dissolved in ethanol; ethanol (up to 1 % v/v) had no effect upon whole-cell chloride currents (n = 6).

3.4. Results:

3.4.1. Volume-sensitive chloride currents:

To ascertain if Cl^- channels sensitive to increases in cell volume were present in ROS 17/2.8 cells, pipette and bath solutions rich in Cl^- and containing N-methyl-D-glucamine (NMDG) or choline as the main cation, were used. When pipette and bath solutions were of equal osmolarity (300 mosmol l^{-1}) the zero current level was -0.3 ± 1.3 mV (n = 15), close to the holding potential of 0 mV. Alternating voltage steps to ± 40 mV of 800 ms duration applied at 5 s intervals (0.2 Hz) elicited currents of small amplitude (Fig. 3.1 prior to hypotonic shock). Similar results were obtained in response to voltage-clamp pulses of 320 ms duration to potentials between -80 and +80 mV from a holding potential of 0 mV (Fig. 3.2A and B for voltage protocol and currents respectively). The observed currents under these conditions were linearly related to voltage thus resembling a background leak conductance. In 11 cells with a mean capacitance of 36 ± 3 pF, the slope conductance was 2.1 ± 0.4 nS.

Under whole-cell voltage clamp single ROS 17/2.8 cells equilibrated with NMDG or choline chloride solutions responded to a reduction in extracellular osmolarity (hypotonic shock) with osmotic cell swelling that was clearly visible under the microscope. This was accompanied by instantaneous activation of sizeable, sustained inward and outward currents in response to hyperpolarising and depolarising pulses (Fig. 3.1). The currents developed over a period of minutes following a small lag

between onset of superfusion with hypotonic solution, and increases in basal conductance levels (routinely 10 - 20 s). Short (320 ms) voltage-clamp pulses between -80 and +80 mV (Fig. 3.2C) showed that at potentials more positive than +50 mV the current exhibited time-dependent inactivation that became progressively faster as the potential was clamped at increasingly positive potentials. The magnitude of this inactivation was however subject to a wide range of variation from cell to cell (compare figs 3.7A and 3.8A).

The effects of hypotonicity were readily reversed by returning the cell to isotonic conditions (Fig. 3.2D). The effects of hypotonicity upon membrane currents in 8 cells are summarised in Figure 3.3. At steady-state swelling the mean current at +80 mV (normalised to cell size) was 54.70 ± 6.61 $pApF^{-1}$ (n = 19). Returning the cells to isotonic conditions for 5 min reduced this value to 2.83 ± 0.33 $pApF^{-1}$, not significantly different from the basal value under isotonic conditions prior to osmotic swelling of 2.14 ± 0.36 $pApF^{-1}$ ($p > 0.05$, Student's paired t-test). This reduction in conductance occurred concomitantly with reductions in cell volume that were visible under the microscope.

The currents did not appear spontaneously when ROS 17/2.8 cells were bathed in isotonic solution (n = 279), however when the same cells were subject to a hypotonic challenge, increases in conductance were always observed.

3.4.2. Current kinetics and characteristics:

The magnitude of pulse-induced instantaneous currents was found to be strongly dependent upon pre-potential level. The steady-state inactivation induced by depolarised potentials is summarised in figure 3.4A as an H-infinity curve (Hille, 1992). This suggests that the current will be entirely active over the complete 'physiological voltage range' i.e. potentials between -90 and + 40 mV. Instantaneous currents evoked by a constant positive voltage-clamp step to +100 mV were increased as the conditioning pulse became progressively more negative (Fig. 3.4B), an effect that was observed even 20 s after restoring the cell to a holding potential of 0 mV; this property has been noted previously, and termed 'history dependency' by Kubo and Okada (1992). This implies that hyperpolarisation is required to remove the inactivation induced by strong depolarisations.

The current did not appear to exhibit any notable activation kinetics at negative potentials. The only exception to this was when the current had been previously inactivated by a strong depolarisation (as in Fig. 3.4B), but this, however represents removal or relief from inactivation, as opposed to 'true' activation.

Dependence upon pre-potential level suggested that an accurate current-voltage relationship could not be evaluated using an alternating pulse protocol as shown in Fig. 3.2A as the inactivation induced by a previous depolarising pulse would not be removed when the cell was returned to a holding potential of 0 mV. To overcome this each command pulse of the alternating step protocol (Fig. 3.2A) was preceded by a

conditioning prepulse to -100 mV for 500 ms. This ensured complete alleviation of any inactivation induced by the previous voltage step. Using this modified voltage protocol, the resulting whole-cell current-voltage (I - V) relationship in symmetrical choline chloride solutions is shown in Figure 3.5. The current exhibits marked outward rectification with mean conductances of 85.5 ± 11.4 nS and 14.4 ± 2.6 nS (n = 15) at +80 and -80 mV respectively. This corresponds to a rectification ratio of approximately 6.

The mean zero-current (reversal potential) obtained using voltage-ramp stimuli (over a 2 s period; see 3.4.3.) was -0.1 ± 0.6 mV (n = 15), extremely close to the expected value of 0 mV predicted by Nernstian theory for a perfectly Cl^- selective channel under these conditions.

3.4.3. Ionic selectivity of the current:

The anion selectivity of the channel was examined by applying a voltage-ramp stimulus between -80 and +80 mV over a 2 s period (dmV/dt = 80 mV s^{-1}), in hypotonic bathing solutions in which NMDG chloride was replaced with the sodium salt of other anionic species (Fig. 3.6A, B & C). From the current-voltage curves obtained under maximal current activation the reversal potentials (E_{rev}) were evaluated. Ion permeabilities relative to Cl^- were calculated using the Goldman-Hodgkin-Katz equation (Equation 3; Hille, 1992), assuming that the currents were carried solely by anions (see Table 3.2).

Table 3.2. Effects of Cl^- ion replacement upon reversal potentials (E_{rev}) of volume-sensitive anion currents in ROS 17/2.8 cells.

Anion	E_{rev} (mV)†	P_x/P_{Cl}*	n
SCN^-	-15.7 ± 1.7	2.19 ± 0.15	10
I^-	-12.0 ± 0.6	1.87 ± 0.04	5
Br^-	-5.6 ± 1.2	1.45 ± 0.07	5
F^-	+10.8 ± 1.4	0.75 ± 0.04	5
Gluconate$^-$	+46.0 ± 1.1	0.17 ± 0.01	5

E_{rev} obtained from I-V plots as detailed in experimental procedures (section 2.6). †*Values corrected for junction potentials (around 5 mV for gluconate, but < 1 mV for other anions).* **Relative ion permeabilities calculated from Goldman-Hodgkin-Katz equation as follows, where x is the replacement anion:*

$$E_{rev} = \frac{RT}{F} \ln \frac{[Cl]_i + (P_x/P_{Cl})[x]_i}{[Cl]_o + (P_x/P_{Cl})[x]_o}, \qquad \text{Equation 3.1}$$

and where R, T and F have their usual thermodynamic meaning.

The reversal potential with hypotonic NaCl solution in the bath was -2.1 ± 0.8 mV (n = 15), not significantly different from that obtained with hypotonic NMDG chloride (-0.6 ± 0.9 mV (n = 9); p > 0.3, Student's unpaired t-test). This is consistent with the conductance exhibiting anion selectivity, ruling out permeation by cations as it is unlikely that the channel would show similar permeabilities to Na^+ and $NMDG^+$.

3.4.4. Sensitivity to Cl^- channel blockers:

The effects of the Cl^- channel blockers NPPB, DIDS and DPC on the volume-regulated Cl^- conductance were tested. The stilbene derivative DIDS rapidly (within 30 s) suppressed the current in a concentration-dependent manner (Fig. 3.9). In the presence of DIDS, the rate of inactivation of the current at strongly depolarised potentials was accelerated (Fig. 3.7B). The blockade produced by DIDS was voltage-dependent; the outward current was substantially more sensitive than the inward current (Fig. 3.7). The half -maximum inhibitory concentration (IC_{50}) for the outward current was 81 μM at +80 mV. Due to the incomplete concentration-inhibition curve (Fig. 3.9), it was difficult to obtain an accurate fitted IC_{50} for the inward current at -80 mV. If it was assumed that DIDS blocked to the same extent as at +80 mV, an IC_{50} value of 298 μM was obtained.

The carboxylate analogue Cl^- channel blocker NPPB, also inhibited the Cl^- current in a concentration-dependent manner (Fig. 3.9), however, both inward and outward currents were equally affected by NPPB with an IC_{50} value of 64 μM (Fig. 3.8). Interestingly, the volume-activated Cl^- currents were relatively insensitive to another carboxylate analogue Cl^- channel blocker, DPC. At 500 μM (the highest concentration tested), DPC produced only modest inhibition of the current (22.5 ± 4.0%, n = 5). Block by both DIDS and NPPB were totally reversible upon return to hypotonic solution free from the blocker within 2 min.

It has been shown that the L-type calcium channel blocker, verapamil, can also inhibit the volume-sensitive Cl^- channel that is associated with the expression of the P-glycoprotein gene (Valverde *et al.* 1992). Verapamil (200 μM) produced only minor inhibition (4.9 ± 1.8%, n = 5) of the osmotic swelling induced Cl^- current in ROS 17/2.8 cells.

3.4.5. Second messenger independence:

Osmotic swelling, produced by hypotonic shock, induced Cl^- currents even though 1 mM EGTA was present in the patch pipette to chelate intracellular Ca^{2+}. The calcium independence of the Cl^- current was further demonstrated by the presence of the Ca^{2+} ionophore, ionomycin. Superfusion with 1 μM ionomycin failed to produce a significant increase from basal chloride conductance levels under isotonic conditions in cells which subsequently responded to a hypotonic challenge with large, outwardly rectifying Cl^- currents (Fig. 3.10). In 4 cells tested, the peak current at +80 mV was 56.4 ± 34.9 pA under control isotonic conditions, and 126.0 ± 106 pA subsequent to ionomycin treatment for 2 min (not significantly different, Student's unpaired t-test).

Osmotic swelling has been reported to produce an increase in the levels of cyclic AMP and inositol phosphates in osteoblasts (Sandy, Meghji, Farndale & Meikle, 1989). However, as shown in Table 3.3., the magnitude of currents induced by osmotic swelling were unaffected by inclusion of H-89, a selective inhibitor of cAMP-dependent protein kinase (protein kinase A), in the pipette solution at 1 μM. Dialysis of ROS 17/2.8 cells with cyclic AMP directly (up to 50 μM) failed to produce any

increase in basal chloride conductance; external application of 0.1 μM 12-*O*-tetradecanoylphorbol-13 acetate (TPA), an activator of protein kinase C, for 5 min was also without effect (mean peak currents at +80 mV: control, 24.0 ± 1.2 pA; 50 μM cAMP, 24.5 ± 17.1 pA; 0.1 μM TPA, 39.5 ± 9.4 pA; n = 4).

Condition	Isotonic (pA)	Hypotonic (pA)	n
Control	78.3 ± 13.6	2488.1 ± 323.1	23
No nucleotides	126.0 ± 46.5	2480.0 ± 639.0	5
H-89 (1 μM)	38.6 ± 7.9	2191.3 ± 602.0	4
Tyrphostin A25 (200 μM)	49.3 ± 11.8	3222.0 ± 870.0	4

Table 3.3. Effects of H-89, tyrphostin A25 and no nucleotides (absence of ATP and GTP from patch pipette solution) upon chloride currents in ROS 17/2.8 cells under isotonic and hypotonic conditions. *Cells were dialysed under isotonic conditions with NMDG chloride solutions with patch pipette solution modified as indicated for 5 min (10 min for nucleotide free solution) after establishing whole-cell mode. Measurements are the peak current for a command pulse to +80 mV for 300 ms (holding potential 0 mV) under isotonic conditions, and 2 min after switching to hypotonic conditions. Data expressed as mean ± S.E.M. of the indicated number of observations (n). All values non-significant from respective control values (Student's t-test with Bonferroni correction).*

Tyrosine phosphorylation has been shown to play a role in the osmoregulation of ionic conductances in Intestine 407 cells (Tilly, Van den Burghe, Tertoolen, Edixhoven & de

Jonge, 1993). Dialysis with a pipette solution containing 200 μM tyrphostin A25, a selective tyrosine kinase inhibitor, was without effect upon basal chloride conductance levels, or the magnitude of the volume-sensitive Cl^- currents in response to hypotonic shock (Table 3.3).

All results presented above were obtained with pipette solutions containing 0.5 mM GTP and 2 mM ATP. To determine if nucleotides were required for activation of volume-sensitive Cl^- currents, experiments were conducted with pipette solutions devoid of both nucleotides. The absence of ATP and GTP was found to be without effect upon the development of the current in response to hypotonic shock (Table 3.3).

Osteoblasts have been shown to possess a type of phospholipase A_2 that is directly sensitive to cell deformation and mechanical stress (Binderman, Zor, Kaye, Shimshoni, Harell & Sömjen, 1988). As the major product of this enzyme, arachidonic acid, has been shown to activate ionic conductances in a variety of cell types (Ordway, Singer & Walsh, 1991), it was possible that it may be the mechanism of volume-sensitive Cl^- current activation in ROS 17/2.8 cells. However, arachidonate (25 μM applied externally for 5 min) failed to elicit a significant increase in chloride conductance from baseline levels in cells that responded to a subsequent hypotonic shock with large volume-sensitive Cl^- currents (Mean peak current at +80 mV: control, 71.4 ± 27.8 pA; 25 μM arachidonate, 105.6 ± 42.7 pA; hypotonic shock, 3073.1 ± 1220.0 pA; n = 4).

Studies using the actin disrupting cytochalasin family of compounds have suggested that the cell cytoskeleton may have a role in controlling ionic conductances (Mills,

Schwiebert & Standaert, 1994; Cornet, Ubl & Kolb, 1993; Suzuki, Miyazaki, Ikeda, Kawaguchi & Sakai, 1993). Recently a regulatory protein, pI_{Cln}, has also been successfully cloned which can control the volume-sensitive Cl^- current in *Xenopus* oocytes and has a putative actin-binding domain (Krapivinsky *et al.* 1994). The effects of dihydrocytochalasin B (DHCB) upon chloride permeability are summarised in Table 3.4.

Dialysis of cells with a pipette solution devoid of nucleotides (ATP is a co-factor in actin repolymerisation) and 1 μM DHCB for 10 min produced a modest increase in chloride permeability from a basal value at +80 mV of 46.4 ± 8.9 pA to 518 ± 236.2 pA (n = 7). This effect was however small compared to the increase observed when the same cells were subject to a subsequent hypotonic shock for 2 min (2894.1 ± 678 pA).

Condition	Control (Isotonic) (pA)	Hypotonic (pA)	n
Control	69.3 ± 12.9	3210.9 ± 582.6	12
1 μM DHCB 5 min	183.1 ± 53.2	3350.8 ± 783.0	9
1 μM DHCB 1 hr	40.0 ± 10.6	6159.6 ± 1804.1	4
10 μM DHCB 18 hrs	163.2 ± 60.9	5341.4 ± 2167.0	6
Vehicle (Ethanol 0.5% v/v) 18 hrs.	155.6 ± 60.0	2996.2 ± 540.2	4

Table 3.4. Effects of dihydrocytochalasin B (DHCB) upon chloride conductance in ROS 17/2.8 cells. *All experiments performed using NMDG chloride pipette and bath solutions, values are peak currents at +80 mV (Mean ± S.E.M.). DHCB incubated with cells in bath solution, except for 18 hr exposure when the medium in which the cells were maintained was supplemented.*

As ROS 17/2.8 cells visibly swelled when subjected to hypotonic shock it is plausible that increases in membrane tension may induce activation of the volume-sensitive Cl^- current i.e. it is stretch-sensitive. The anionic ampipath dipyridamole (DPM) preferentially inserts into the outer leaflet of the membrane bilayer, creating a membrane shape change ('crenation') that is similar to the changes that occur as a result of cell swelling (Jennings & Schultz, 1990). Dipyridamole has been shown to produce increases in membrane Cl^- conductance in canine cardiac cells, an effect suggested to be due to activation of volume-sensitive Cl^- channels (Tseng, 1992). Dipyridamole had no effect upon Cl^- conductance in ROS 17/2.8 (Fig. 3.11), though all cells tested subsequently responded to hypotonic shock with large amplitude Cl^- currents (n = 4).

3.4.6. Single channel recording:

In 8/8 cell attached patches from cells that had been previously hypotonically swollen, there was no evidence of any single channel activity at positive pipette potentials. Positive pipette potentials produced hyperpolarisation of the patch under the pipette providing an inward driving force for cations. As the major cation in the pipette solution ($NMDG^+$) is theoretically impermeant this ensures minimum contamination from any stretch or volume-sensitive cation currents. Similar lack of channel activity was observed in 4 patches that were formed on control cells, subsequently subjected to hypotonic shock for 10 min. Application of substantial (high enough to produce patch

disruption) negative pressure by mouth to the suction post of the pipette holder also proved ineffective at eliciting measurable single channel activity.

In 5/8 excised inside-out patches there was substantial single channel activity (see Fig. 3.12A). The channel was of high conductance, and appeared to show reduced activity as the potential was stepped away from 0 mV. The current-voltage relationship was linear in symmetrical 140 mM NMDG chloride (Fig. 3.12B), yielding a mean single channel (γ) conductance of 381 ± 15 pS (n = 5). The channel also seemed to exhibit subconductance states (see Fig. 3.12A, +20 mV pulse) though this was not further characterised in this study.

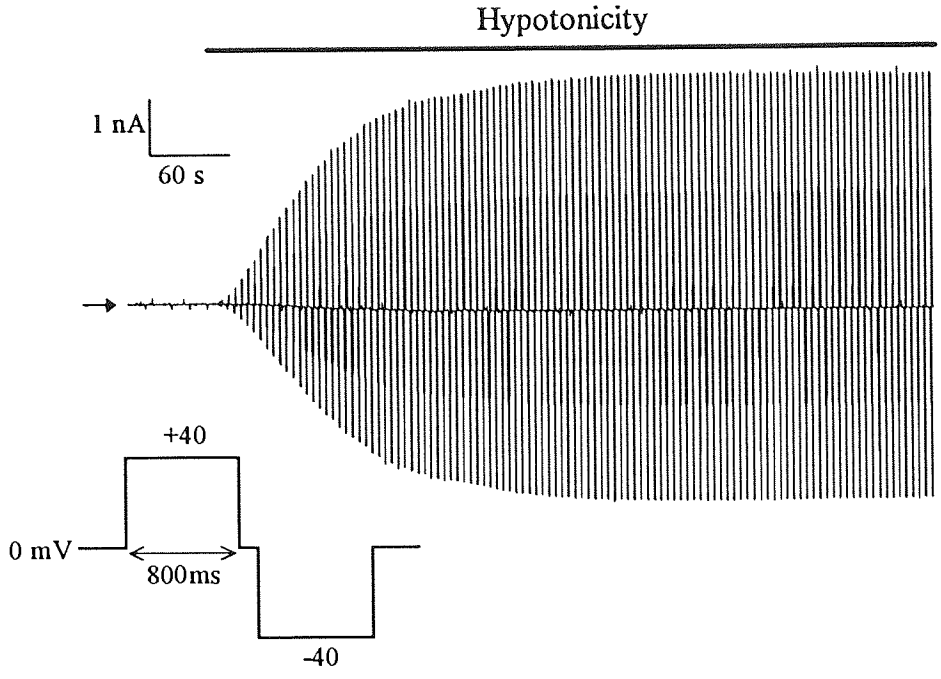

Figure 3.1. Effects of hypotonic shock upon whole-cell chloride currents. *Single ROS 17/2.8 cell equilibrated with NMDG chloride solution. Cell was subject to hypotonic shock 2 min after breakthrough into whole-cell configuration (as indicated by solid bar), arrow denotes zero current level. Inset shows voltage protocol applied at 0.2 Hz. Trace representative of 148 similar experiments.*

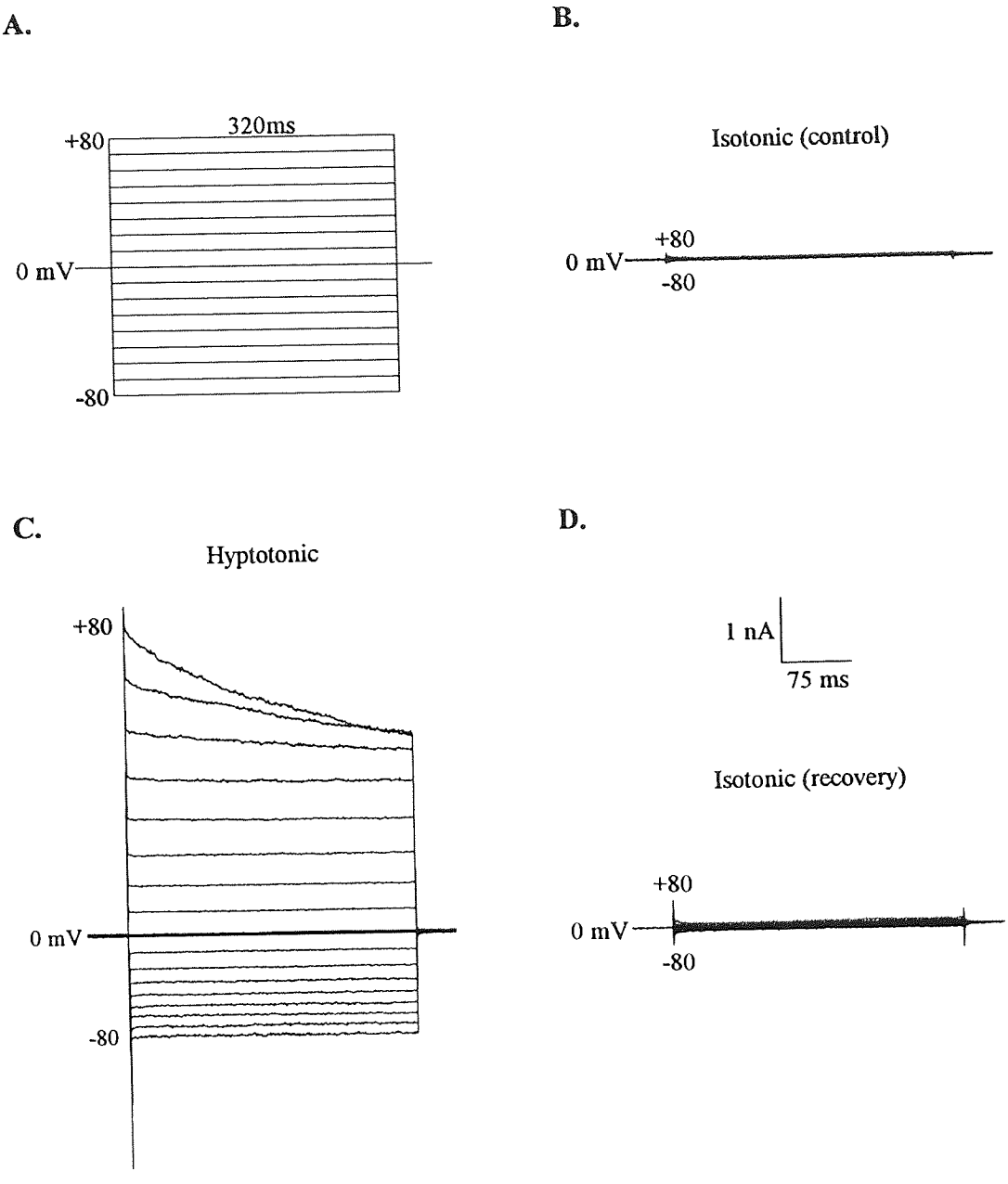

Figure 3.2. Reversible activation of anion currents in single ROS 17/2.8 cell by hypotonic shock. *A, alternating pulse protocol. B, basal currents in isotonic NMDG chloride 2 min after establishing whole-cell voltage clamp mode. C, Cl^- currents upon steady osmotic swelling induced by a hypotonic challenge (3 min) in same cell as B. D, recovery 5 min after returning cell to isotonic NMDG chloride bathing solution. Trace representative of 18 similar experiments.*

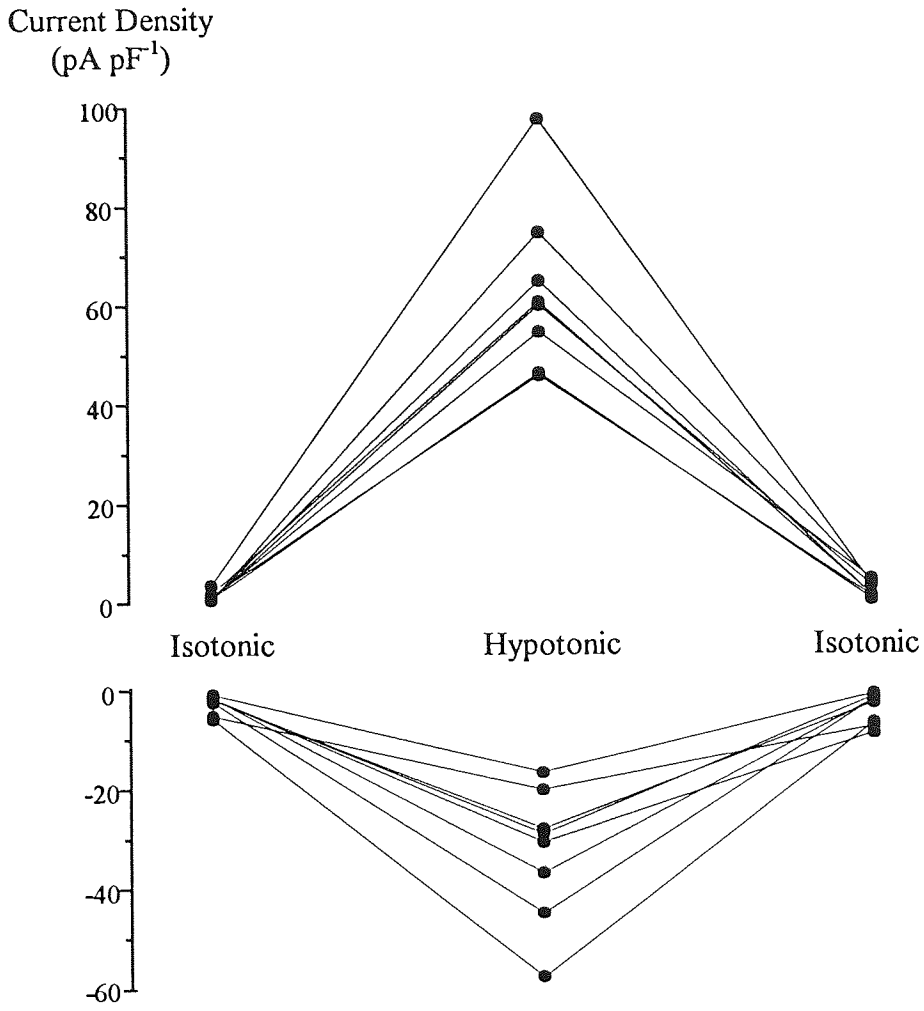

Figure 3.3. Reversibility of hypotonicity-induced increases in chloride permeability in ROS 17/2.8 cells. *Peak currents in single ROS 17/2.8 cells, equilibrated with NMDG chloride solutions, were measured at -80 and +80 mV prior, 3 min subsequent to hypotonic challenge, and 5 min after return to isotonic conditions. Peak currents are normalized to cell size and are thus expressed as current densities in pA* pF^{-1} *(ordinate).*

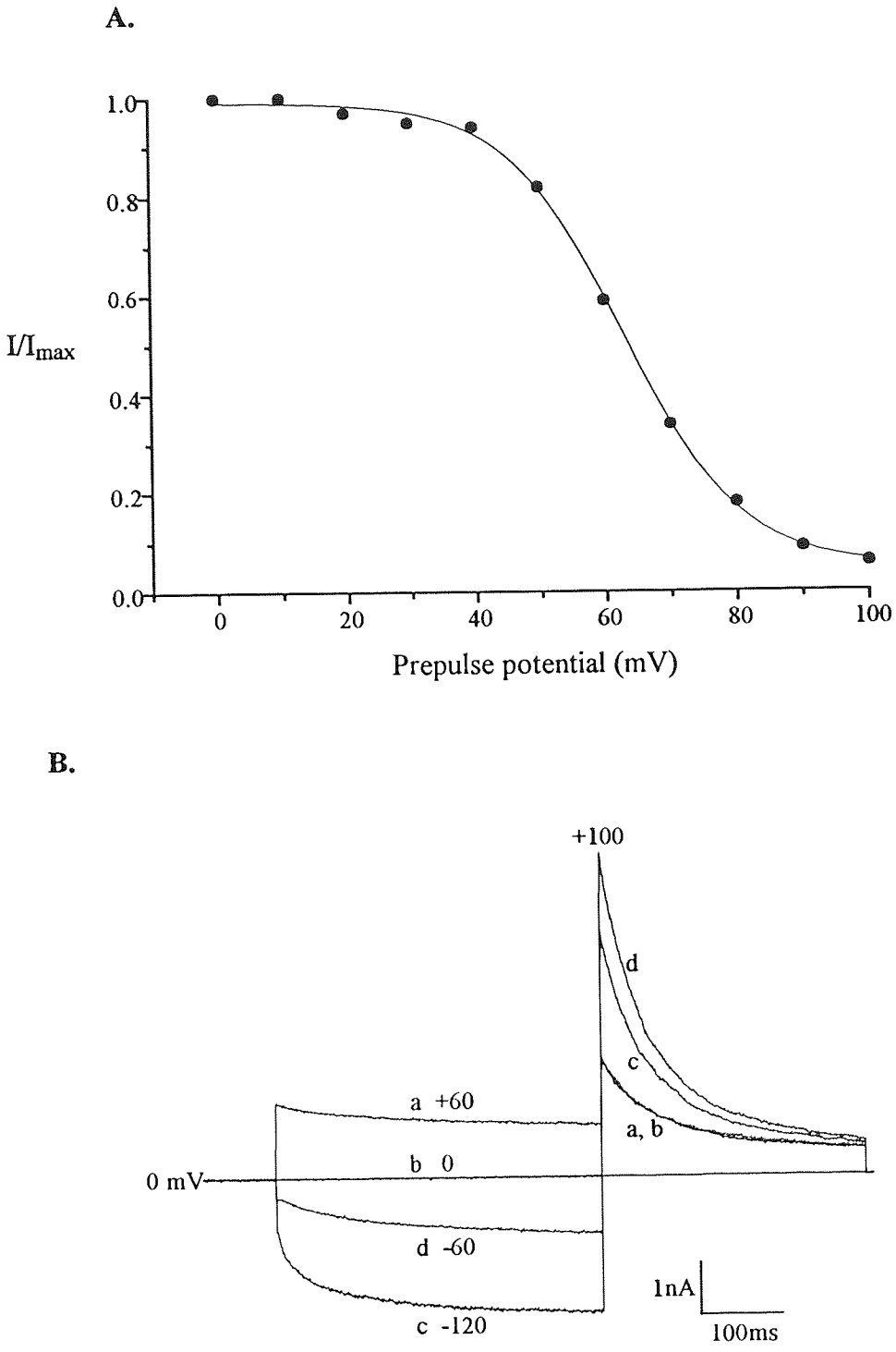

Figure 3.4. Effects of conditioning pulses upon whole-cell Cl^- currents in single osmotically swollen ROS 17/2.8 cells equilibrated with choline chloride solutions.

A, steady-state inactivation (H-infinity) curve; curve constructed from normalised peak currents at +100 mV (480 ms test step) after cell was held at indicated prepulse potential for 1.7 s (holding potential -80 mV). Curve represents Boltzmann function fitted to the raw data (V_h = 62.9 mV, slope factor = 8.9 mV), representative of 3 other experiments. B, hyperpolarization is required to remove inactivation; pulses to +60 mV (a), 0 mV (b), -60 mV (c) and -120 mV (d) remove inactivation induced by prepulse to +100 mV to differing degrees, as assessed by current response to a subsequent +100 mV step. Data from a single cell, representative of six experiments.

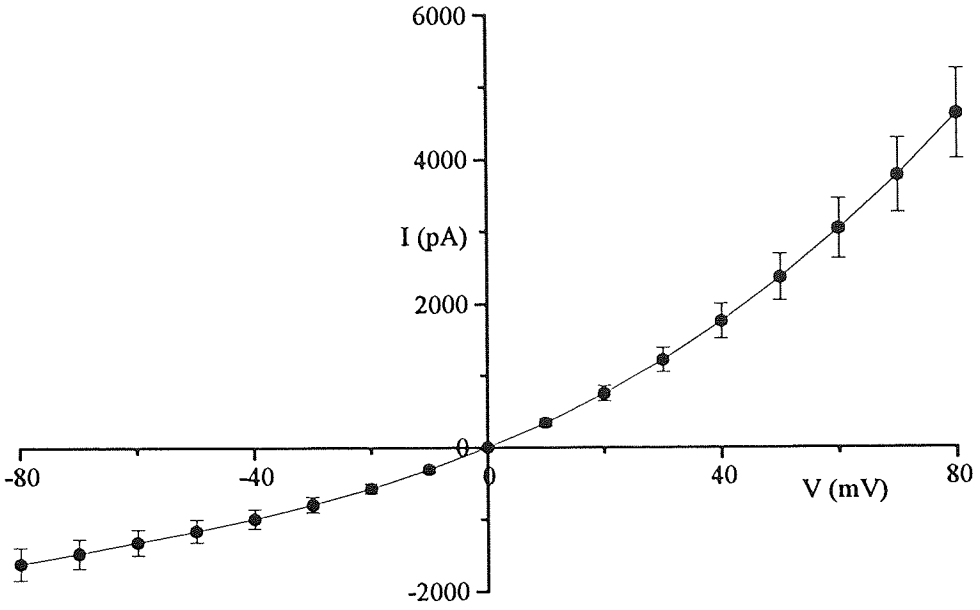

Figure 3.5. Current-voltage relationship of volume-sensitive Cl^- currents. *Instantaneous currents were measured in osmotically swollen ROS 17/2.8 cells, equilibrated with symmetrical choline chloride solutions, using an alternating pulse protocol (as in Fig. 3.2A) but with a prepulse to -100 mV preceding each command potential. Each point represents the mean current of 17 cells, 3 min after onset of hypotonic challenge, with S.E.M. shown by vertical bars. Peak currents were measured within 10 ms of onset of the voltage pulse.*

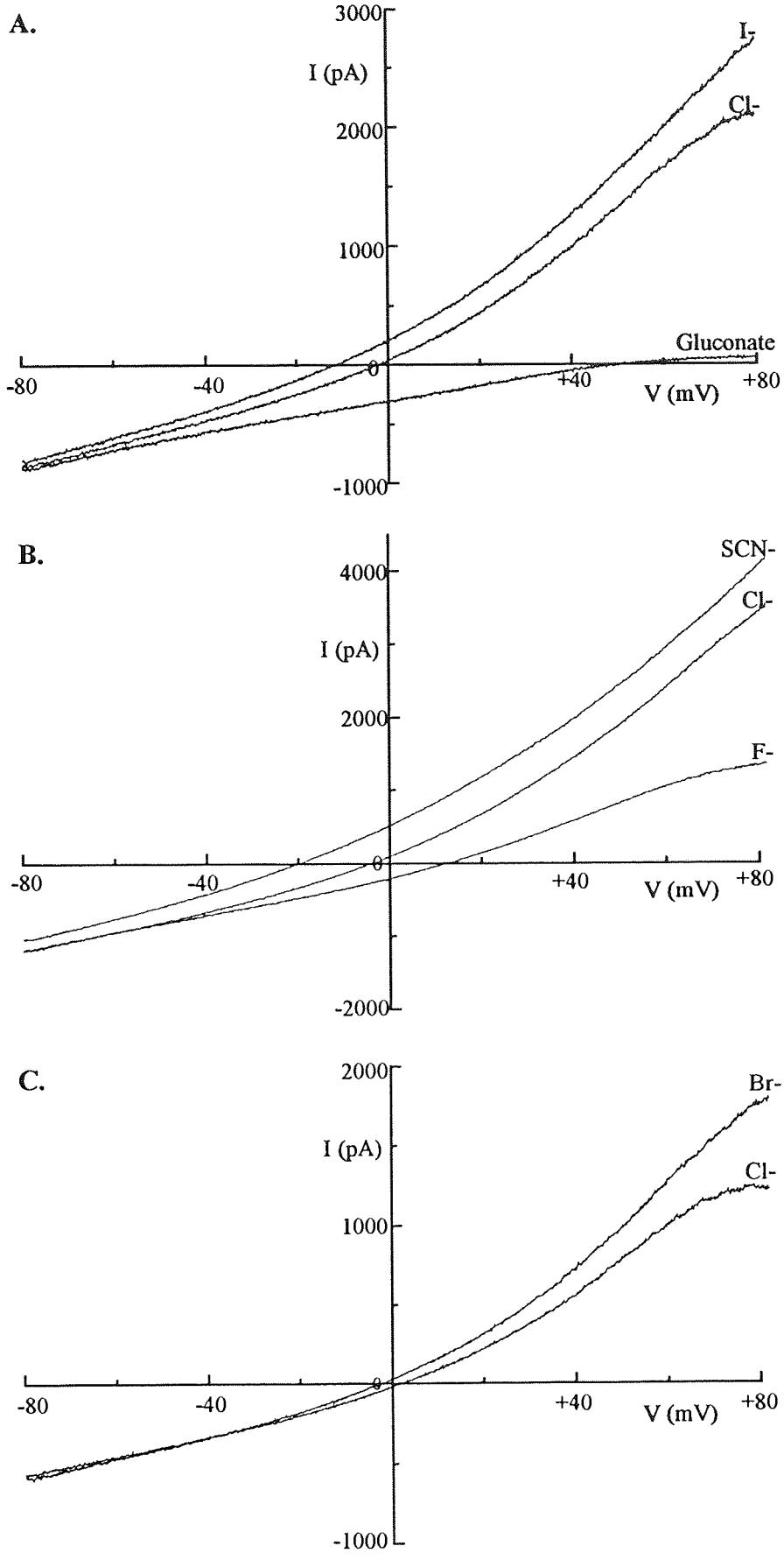
A.
3000
I (pA)
2000
1000
-1000
I-
Cl-
Gluconate
-80
-40
0
+40
+80
V (mV)
B.
4000
I (pA)
2000
-2000
SCN-
Cl-
F-
-80
-40
0
+40
+80
V (mV)
C.
2000
I (pA)
1000
-1000
Br-
Cl-
-80
-40
0
+40
+80
V (mV)

Figure 3.6. Effects of anion substitution on current-voltage curves measured by ramp voltage-clamp stimulus. *Voltage ramps from -80 to +80 mV applied over 2 s, after steady current activation was observed in osmotically swollen single ROS 17/2.8 cells. Cells superfused with hypotonic medium (Table 3.1; NMDG chloride solution) in which NaCl was replaced with sodium salt of indicated ion:*

A; I^-, Cl^-, gluconate$^-$.

B; SCN^-, Cl^-, F^-.

C; Br^-, Cl^-.

Data representative of 4 - 16 experiments.

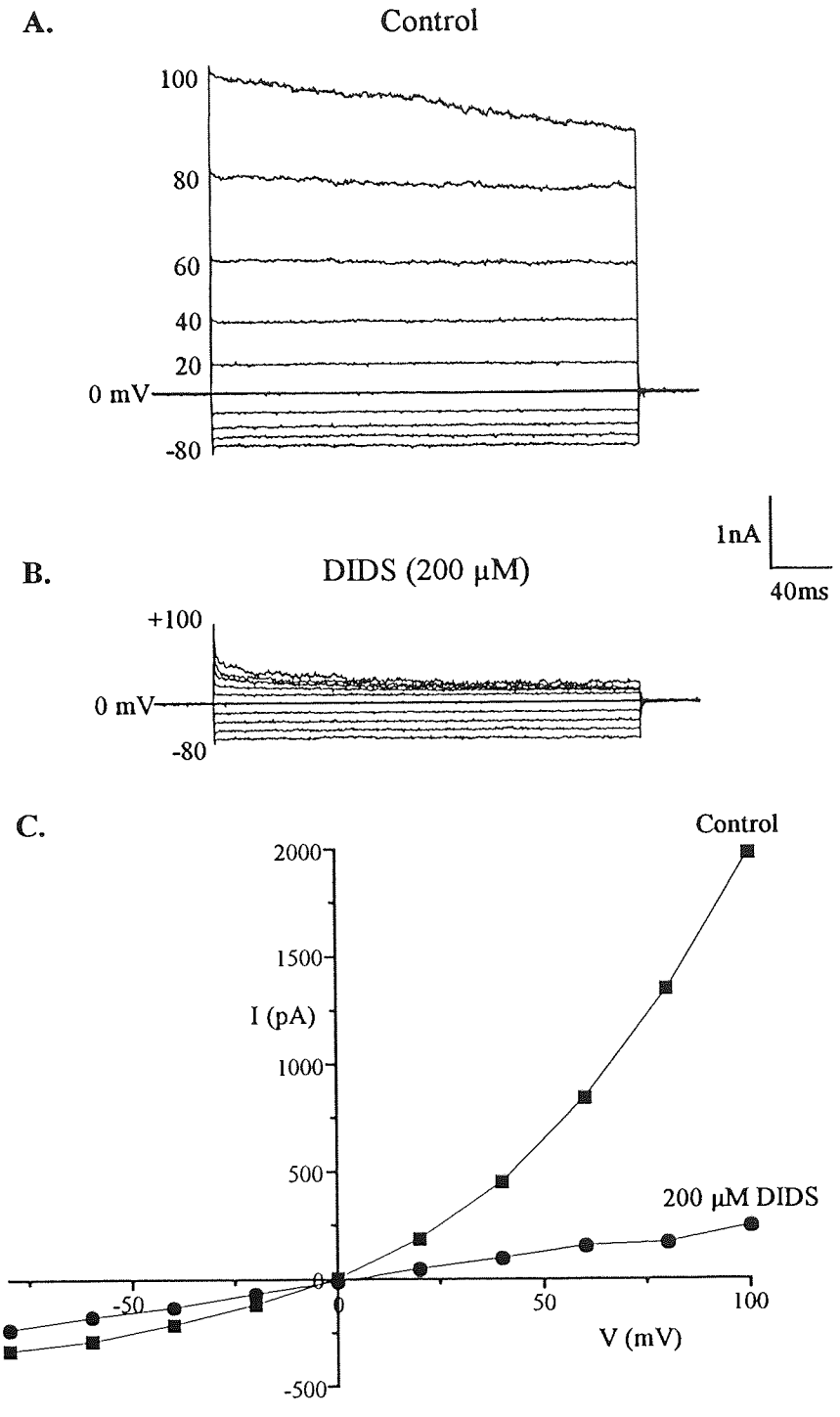

Figure 3.7. Effects of DIDS upon whole-cell volume-sensitive Cl^- currents in ROS 17/2.8 cells. *Currents elicited in osmotically swollen cell (NMDG chloride solutions) by command pulses to indicated potential of 320 ms duration from a holding potential of 0 mV, prior (A) and 30 s subsequent to addition of DIDS (B). C, current-voltage relationship for traces shown in A and B. Data representative of six experiments.*

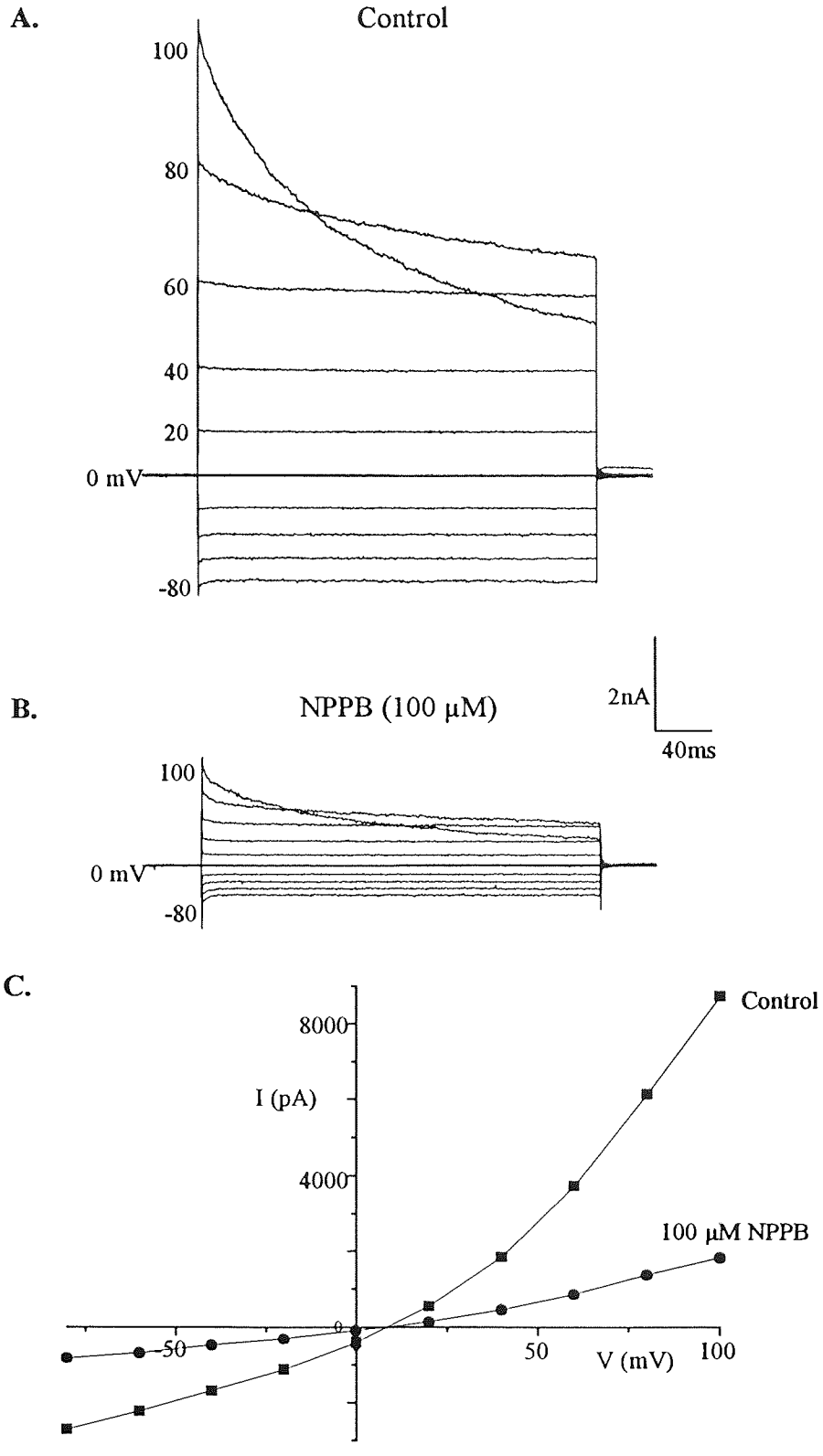

Figure 3.8. Effects of NPPB on whole-cell volume-sensitive Cl^- currents in ROS 17/2.8 cell. Currents elicited in osmotically swollen cell (NMDG chloride solutions) by command pulses to indicated potential of 320 ms duration from a holding potential

of 0 mV, prior (A) and 30 s subsequent to addition of NPPB (B). C, current-voltage relationship for traces shown in A and B. Data representative of six experiments.

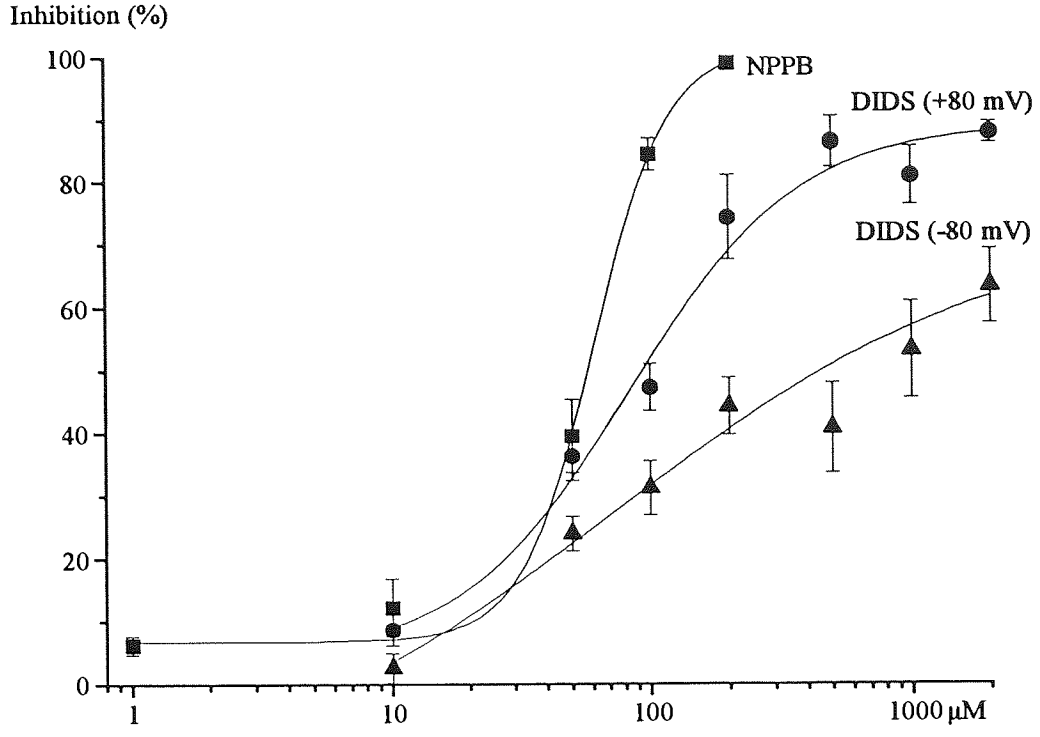

Figure 3.9. Concentration-inhibition curves of NPPB (■) and DIDS (●) on outward Cl^- currents (at +80 mV) in osmotically swollen ROS 17/2.8 cells. *Effect of DIDS on inward currents (at -80 mV, ▲) is also shown. Currents were measured prior and 30 s subsequent to application of blocker. Ordinate represents the percentage inhibition after application of the blocker against steady current before drug application. Each symbol represents the mean value of 4 - 12 experiments with S.E.M. (vertical bars). Curves represent fit to the data (using Equation 2.2) with the following parameters from MicroCal Origin program: IC_{50}, 64 µM (NPPB), 81 µM (DIDS, +80 mV), 298 µM (DIDS, -80 mV); Hill coeffecients, 3.8 (NPPB), 1.87 (DIDS, +80 mV), 0.5 (DIDS, -80 mV); maximal inhibition, 100% (NPPB), 88% (DIDS, +80 and -80 mV).*

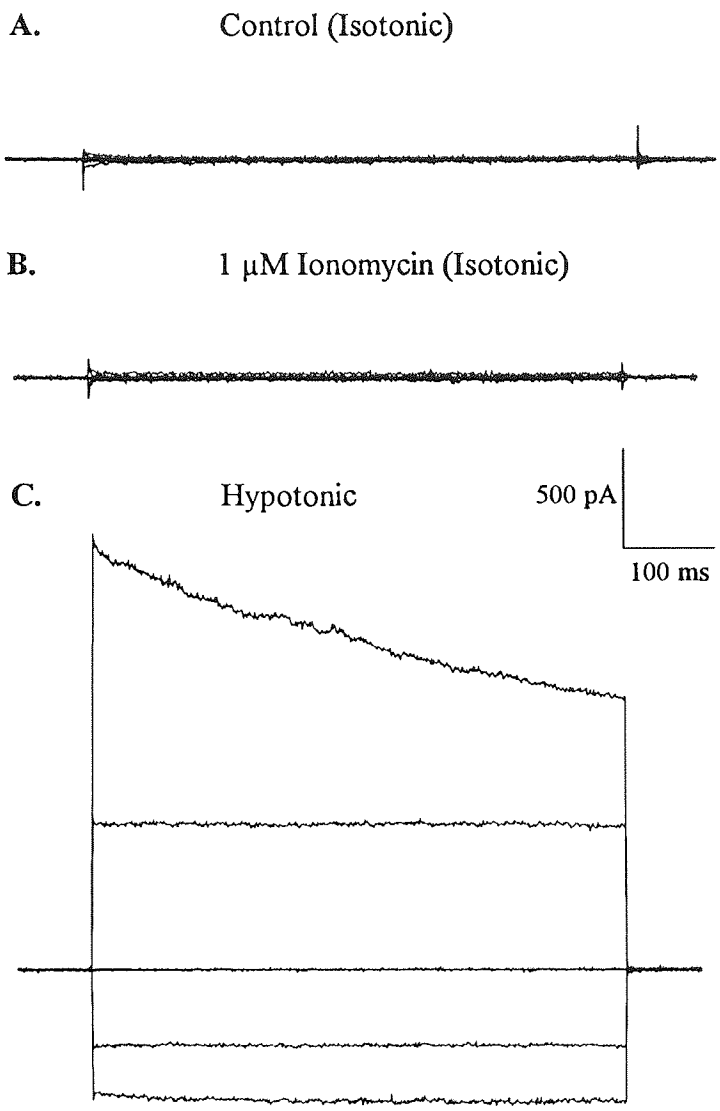

Figure 3.10. Effects of 1 μM ionomycin upon Cl⁻ conductance in ROS 17/2.8 cells. *Currents elicited by 1 s voltage steps between -80 and +80 mV (40 mV increments) from a holding potential of 0 mV under A; control isotonic conditions, B; 2 min superfusion with 1 μM ionomycin, C; 2 min hypotonic shock. Traces representative of 3 similar experiments.*

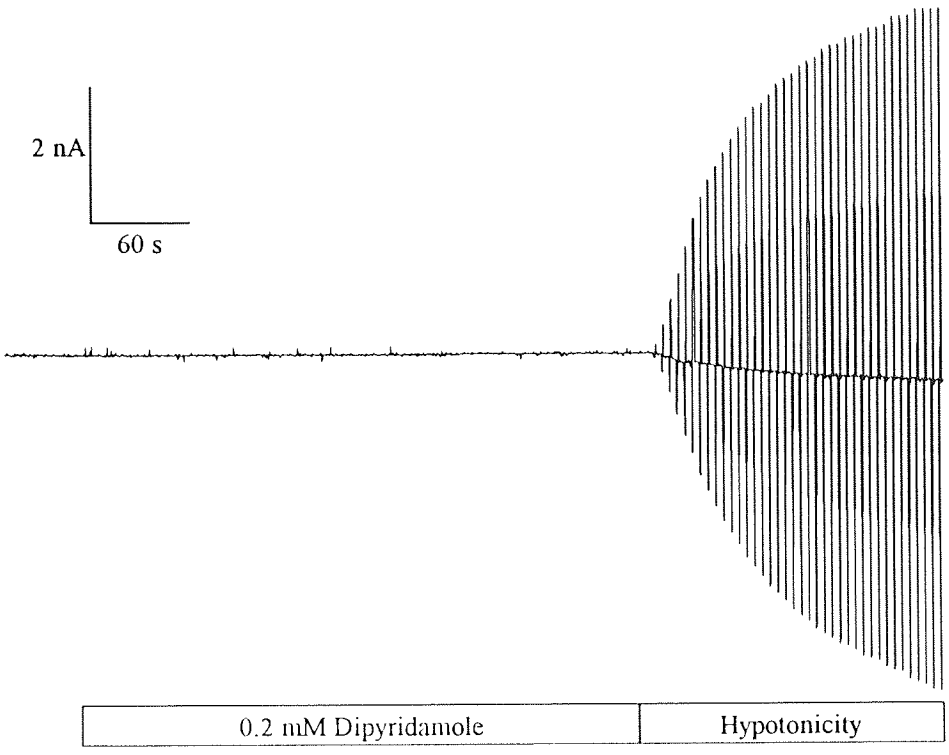

Figure 3.11. Effects of 0.2 mM dipyridamole upon chloride permeability in single ROS 17/2.8 cell equilibrated with NMDG chloride solutions. *Cell subject to alternating voltage protocol to ± 40 mV from a holding potential of 0 mV at 0.2 Hz (as Fig. 3.1.). Dipyridamole applied by fast perfusion system under isotonic conditions as indicated above; cell subsequently hypotonically challenged to confirm presence of volume-sensitive Cl^- current. Data representative of 3 other experiments.*

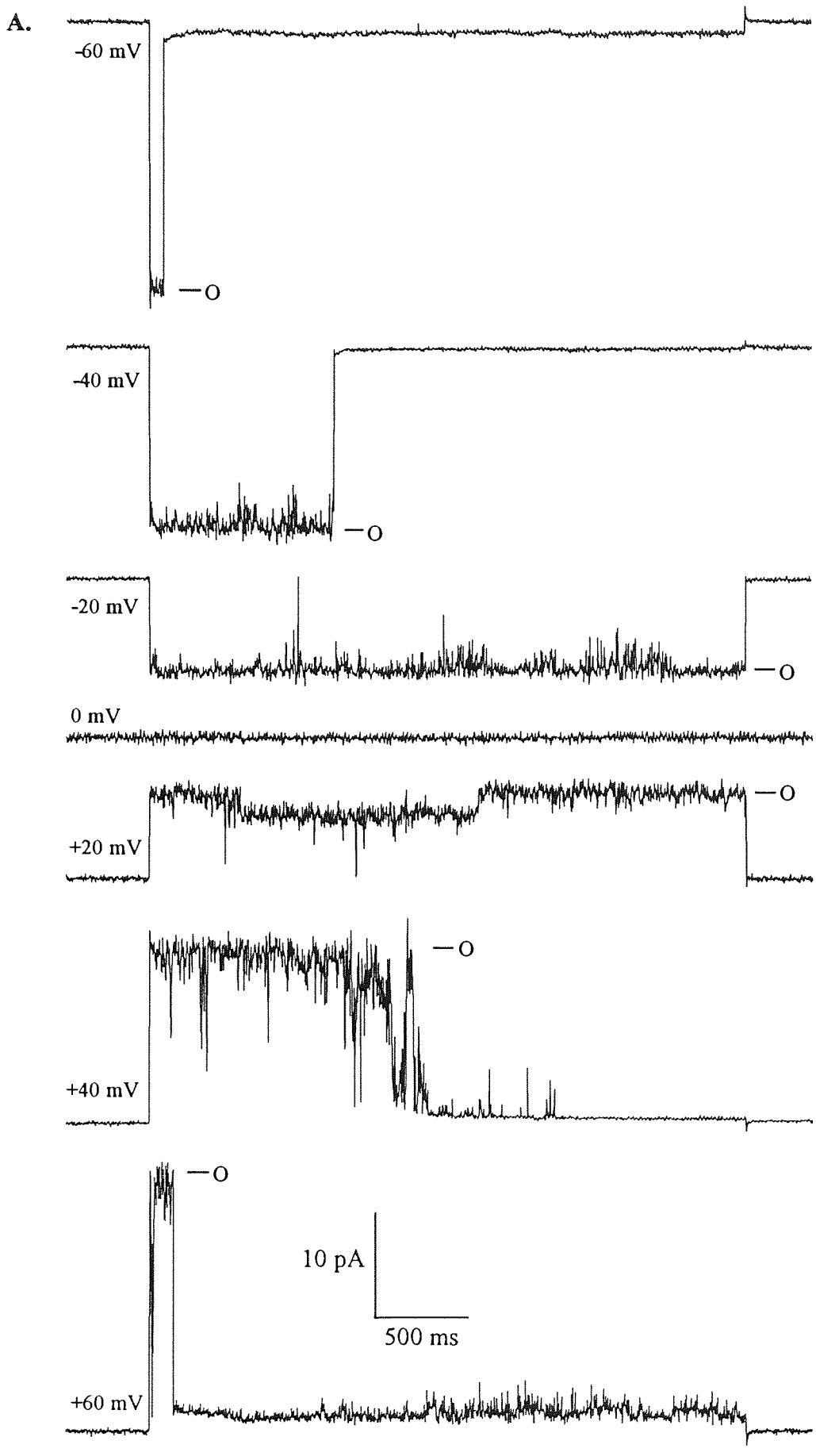
A.
-60 mV
—O
-40 mV
—O
-20 mV
—O
0 mV
+20 mV
—O
—O
+40 mV
—O
10 pA
500 ms
+60 mV

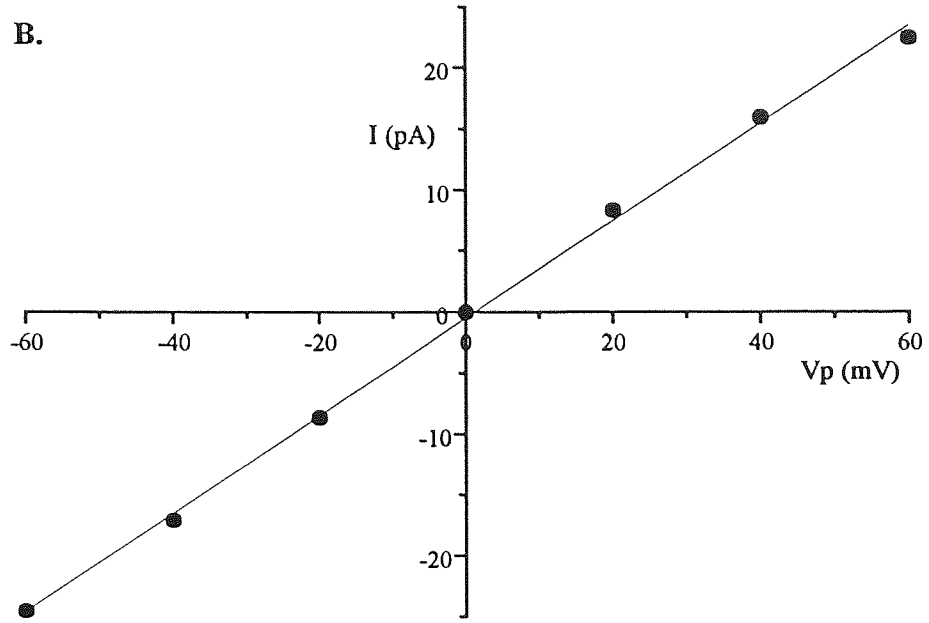

Figure 3.12. High conductance anion channel (Maxi-Cl) in excised inside-out patch from ROS 17/2.8 cell. *A, Voltage pulses applied for 3.2 s to indicated potential (pipette potential, Vp) from a holding potential of 0 mV, records digitized at 0.5 kHz and low pass filtered at 1 kHz. Pipette and bath solutions were symmetrical 140 mM NMDG chloride. Inside-out configuration confirmed by air exposure subsequent to patch excision, level of channel opening indicated (O). Note subconductance state during the +20 mV test step. Open probability (P_{open}) decreases as voltage moves away from 0 mV: P_{open}; -60 mV, 0.03; -40 mV, 0.31; -20 mV, 1.0; +20 mV, 1.0; +40 mV, 0.47; +60 mV, 0.04. B, Current-voltage relationship for channel shown in A. I - V relationship is linear producing a calculated single channel conductance (γ) of 399 pS. Data representative of 5 similar experiments.*

3.5. Discussion:

3.5.1. Properties of volume-sensitive Cl^- conductance:

The results shown above suggest that ROS 17/2.8 cells possess a Cl^- conductance that is activated in response to cell swelling induced by hypotonic shock. The instantaneous whole-cell current of swollen cells was of large amplitude and showed marked outward rectification (Fig. 3.5). The current was maintained in the active state over the entire physiological range of membrane potentials, but exhibited inactivation during large depolarisations (over +50 mV) (Figs 3.2C, 3.4B, 3.8A and 3.10C). The inactivation was time-dependent, becoming more rapid and severe as membrane potential became increasingly depolarised. It has been suggested that this effect occurs as a result of modulation by divalent cations (such as Ca^{2+} and Mg^{2+}) from the external side by impeding the influx of Cl^- ions (Anderson, Jirsch & Fedida, 1995). The conductance in ROS 17/2.8 cells appears to be anion selective, as Cl^- was the only permeant ion used in the experiments reported above. This view is supported by the fact that observed reversal potentials were close to the theoretical value for a perfectly selective Cl^- channel, and also the effect of chloride replacement by gluconate. Gluconate in the extracellular solution attenuated outward currents and shifted the reversal potential to a more positive value, behaviour expected for a less permeable anion on inward currents (Fig. 3.6A and Table 3.2). The anion selectivity sequence determined from reversal potentials was $SCN^- > I^- > Br^- > Cl^- > F^- >$ gluconate$^-$, corresponding to Eisenman's sequence I (Wright & Diamond, 1977). This suggests that the major determinants of selectivity are cationic binding sites within the channel that form weak

electrostatic interactions with the permeating anion. This sequence is in good agreement with the permeability sequences of volume-sensitive anion currents reported in a number of epithelial cell lines such as HeLa, Intestine 407 and T84 cells (Worrell *et al.* 1989; Kubo & Okada, 1992; Díaz *et al.* 1993).

The swelling-induced Cl^- conductance in ROS 17/2.8 cells was sensitive to two structurally unrelated Cl^- blockers (Figs 3.7 and 3.8). Blockade produced by the stilbene derivative DIDS was notably voltage-dependent, the outward currents being more prominently suppressed than the inward currents (Fig. 3.7). DIDS also facilitated inactivation of the outward current (Fig. 3.7C), which may reflect time-dependent block. Both effects of DIDS were noted for the cyclic AMP-dependent Cl^- reported in primary cultured rat osteoblasts (Chesnoy-Marchais & Fritsch, 1989). These were explained by the hypothesis that DIDS reversibly blocks the open channel, and that being negatively charged, DIDS should enter the channel more easily when the membrane potential is more depolarised. The carboxylate analogue, NPPB, was also effective at inhibiting volume-sensitive Cl^- currents in ROS 17/2.8 cells. Unlike DIDS, both inward and outward currents were equally susceptible to blockade by NPPB (Fig. 3.8). Lack of voltage-dependency is perhaps surprising as NPPB is also negatively charged at physiological pH (Greger, 1990). This suggests that NPPB and DIDS elicit their inhibitory effects by quite different mechanisms, and it has been suggested that NPPB modulates channel gating rather than acting as a blocker (Alton & Williams, 1992).

3.5.2. Mechanism of current activation:

Hypotonic cell swelling is known to elevate the cytosolic free Ca^{2+} concentration in the osteoblastic cell line UMR-106-01 (Yamaguchi *et al.* 1989). Increases in intracellular cyclic AMP and inositol phosphate levels have been observed in association with osmotic swelling and also mechanical deformation in many cell types, including osteoblasts (Sandy *et al.* 1989; Baquet, Miejer & Hue, 1990; Watson, 1990). Therefore, it is feasible that these second messengers may be involved in activation of volume-sensitive Cl^- currents. However in ROS 17/2.8 cells, swelling-induced Cl^- currents were found to be independent of intracellular Ca^{2+}, cyclic AMP, protein kinase C and tyrosine kinase (Table 3.3). The lack of effect of absence of nucleotides from the patch pipette solution also suggest that kinases are unlikely to be involved in the activation of volume-sensitive Cl^- currents in these cells. Failure of dihydrocytochalasin B (Table 3.4) or arachidonate to induce consistent increases in Cl^- permeability suggest that detachment from the F-actin cytoskeletal network, or increased levels of arachidonate are not important steps in volume-sensitive Cl^- current activation in ROS 17/2.8 cells.

3.5.3. Comparison with other chloride conductances:

Osteoblasts have previously been shown to possess two distinct types of anion channel, activated by either voltage changes (Chesnoy-Marchais & Fritsch, 1994; Ravesloot, Van Houten, Ypey, & Nijweide, 1991) or cyclic AMP (Chesnoy-Marchais & Fritsch, 1989). The cyclic AMP-dependent Cl^- current described in rat primary osteoblasts has

similar properties to the volume-sensitive Cl^- current reported above; both are outwardly rectifying and sensitive to block by DIDS. The results, however, show that volume-sensitive whole-cell Cl^- currents could be activated in the presence of an inhibitor of cyclic AMP-dependent protein kinase (H-89, Table 3.3) and that dialysis with cyclic AMP itself failed to elicit a measurable increase in Cl^- conductance. This suggests that not only is activation of the volume-sensitive current totally independent of cyclic AMP, but that ROS 17/2.8 cells do not express the cyclic AMP-dependent channel.

There have been two reports of anion conductances in osteoblasts that respond to membrane potential. The first, characterised in primary rat calvarial osteoblasts, is activated by hyperpolarization, sensitive to block by DIDS and NPPB, and is osmosensitive (Chesnoy-Marchais & Fritsch, 1994). However, in contrast to the anion current described above in ROS 17/2.8 cells, this conductance is reduced by external hyposmolarity. A second type of voltage-gated anion conductance has been studied in excised patches from chick osteoblasts (Ravesloot *et al.* 1991). The channel was of large conductance (around 400 pS) and was active only at potentials close to 0 mV. This type of channel, commonly termed 'maxi-Cl', is likely to be the channel observed in excised inside-out patches from ROS 17/2.8 cells reported in this investigation (Fig. 3.12). It is however, unlikely to be the channel underlying the whole-cell volume-sensitive Cl^- current as it exhibits a markedly different current-voltage (I-V) relationship, though it could be argued that this may be the result of patch excision. Perhaps stronger evidence is provided by the lack of channel activity in cell-attached patches from hypotonically swollen ROS 17/2.8 cells (see 3.4.6). Maxi-Cl channels

appear to be expressed in a wide variety of cell types including L6 skeletal myocytes (Hurnák & Zachar, 1992), BC_3H_1 myoblasts (Hurnák & Zachar, 1993), T lymphocytes (Pahapill & Schlichter, 1992), alveolar epithelia (Kemp, MacGregor & Olver, 1993) and neuroblastoma (Bettendorf, Kolb & Schoffeniels, 1993) yet their physiological function remains as yet unclear.

The characteristics of the swelling-induced Cl^- currents in ROS 17/2.8 cells are similar to those of volume-regulated conductances reported in other cell types such as epididymal cells (Chan *et al.* 1993), sweat duct cells (Solc & Wine, 1991), parotid acinar cells (Arreola *et al.* 1995) and intestinal, colonic and airway epithelial cells (Worrell *et al.* 1989; Chan *et al.* 1992; Kubo & Okada, 1992). These currents all exhibited outwardly rectifying I-V relationships and time-dependent inactivation at depolarised potentials. Such kinetics contrast those of both the Ca^{2+}-activated Cl^- channel, which activates upon depolarisation and inactivates upon hyperpolarization, and the ohmic Cl^- channel which exhibits neither time-dependent activation nor inactivation (Anderson & Welsh, 1991). The anion permeability sequence of $SCN^- > I^- > Br^- > Cl^- > F^-$ > gluconate$^-$ demonstrated by the volume-sensitive current in ROS 17/2.8 cells is distinct from that published for the cAMP-dependent Cl^- current in a number of cell types (see 1.3.22). This sequence also suggests that the channel underlying the conductance in ROS 17/2.8 cells is not the cloned ClC-2 protein. The ClC-2 Cl^- channel can be reversibly activated by extracellular hypotonicity and appears to be ubiquitously expressed, however in contrast to the conductance in ROS 17/2.8 cells it shows Cl^- over I^- specificity (Gründer *et al.* 1992).

The volume-activated Cl^- current in ROS 17/2.8 cells was found to be sensitive to the Cl^- channel blockers DIDS and NPPB. Similarly, swelling-induced Cl^- currents in colonic and intestinal epithelia, sweat duct cells and epididymal cells are reported to be inhibited by NPPB and stilbene-derivatives, including DIDS (Solc & Wine, 1991; Chan *et al.* 1992; Kubo & Okada, 1992; Chan *et al.* 1993). The volume-regulated conductances in epididymal cells and Intestine 507 cells were substantially more sensitive to block by DPC (IC_{50} values of 120 and 350 μM respectively) than the current in ROS 17/2.8 cells (Kubo & Okada, 1992; Chan *et al.* 1993). This may indicate that the observed swelling-induced conductance in these cells is different from that observed in ROS 17/2.8 cells.

Volume-activated Cl^- currents in ROS 17/2.8 cells were resistant to block by verapamil and did not require intracellular ATP for activation (Table 3.3). This suggests that the channel responsible for the conductance in these cells is unlikely to be that associated with the expression of the multidrug-resistance P-glycoprotein (MDR-1) gene (Valverde *et al.* 1992).

Single channel studies have suggested that in certain cell types such as epithelial cancer cells and normal nasal epithelia that hypotonic shock activates a Cl^- channel with a conductance (γ) of around 50 pS (Jirsch *et al.* 1994; Solc & Wine, 1991). The lack of any measurable single channel activity in cell-attached patches from hypotonically swollen ROS 17/2.8 cells (see 3.4.6) suggest that this is unlikely to be the channel underlying whole-cell Cl^- currents in these cells. However, in a variety of cells expressing volume-sensitive Cl^- currents that are outwardly rectifying, show a higher

permeability for I^- than Cl^- and which are sensitive to block by NPPB (e.g. T84, HeLa, COS-1, 3T3), noise analysis has shown that the single channel conductances range between 0.2 and 5 pS (Ho *et al.* 1994; Nilius *et al.* 1994c). Thus, the volume-activated Cl^- current in ROS 17/2.8 cells may belong to this lower conductance class of channels.

3.6. Conclusions:

During osmotic swelling ROS 17/2.8 cells exhibit reversible activation of large amplitude, outwardly rectifying Cl^- currents. The current appears to be anion selective with a permeability sequence of $SCN^- > I^- > Br^- > Cl^- > F^-$ > gluconate$^-$, and effectively inhibited by the Cl^- channel blockers DIDS and NPPB. The current occurs independent of Ca^{2+}, cyclic AMP, arachidonic acid, tyrosine kinase and intracellular nucleotides; Cl^- current activation could not be mimicked by activation of protein kinase C, F-actin filament disruption by dihydrocytochalasin B or generation of membrane tension using the anionic ampipath, dipyridamole. Single channel recordings from swollen ROS 17/2.8 cells suggest that the channel responsible for whole-cell Cl^- currents may be of small conductance.

Chapter 4.

VOLUME-SENSITIVE CHLORIDE CURRENT IN PRIMARY CULTURED MOUSE CALVARIAL OSTEOBLASTS.

4.1. Background:

The potential for unlimited cell division of some cells in culture makes it possible to isolate one cell and, by mitosis, obtain a population of cells that, if propagated indefinitely, is defined as a clonal cell line. Cells with this ability can be derived in two related ways; firstly, by primary culture of differentiated cells (i.e. isolate them directly from the parent organism) and then transforming them using carcinogenic stimuli such as chemicals, viruses, or radiation, and secondly, by deriving the cells directly from tumours. Clonal cell lines have a distinct advantage over primary cultured cells as they theoretically provide an indefinite source of homogenous cells, thus obviating the need for continued isolation of primary cells. Unfortunately there are disadvantages, the majority being due to the genetic instability of immortalised cell lines which tend to show genetic drifts during their *in vitro* life. This can provide substantial experimental problems if the cells change their phenotypic characteristics such that the normal compliment of cell receptors etc. is altered.

In chapter 3 it was shown that clonal cell line, ROS 17/2.8 expresses a volume-sensitive Cl^- current. The ROS 17/2.8 cell line was derived from a rat osteosarcoma induced by the transplantable rat osteogenic sarcoma R3559/52A (Majeska, Rodan & Rodan, 1980) and exhibits an osteoblastic phenotype as assessed by receptors for pararthyroid hormone (PTH) and expression of high alkaline phosphatase activity. A variety of other osteoblastic clonal cell lines are available including UMR 106-01, Saos-2 and MC2T3-E1. Although all these cell lines are expected to exhibit similar phenotypes there are pronounced differences, especially in the receptors that each

expresses e.g. UMR 106-01, Saos-2 and MC3T3-E1 cells possess receptors for calcitonin gene-related peptide (CGRP) and vasoactive intestinal polypeptide (VIP) whereas ROS 17/2.8 cells have neither (Bjurholm, 1991).

To assess if the volume-sensitive Cl^- current present in ROS 17/2.8 cells described in chapter 3 is a peculiarity of the clonal cell line and not characteristic of osteoblasts, the effects of hypotonic shock upon primary cultured mouse osteoblasts was investigated.

4.2. Methods:

4.2.1. Isolation of primary calvarial osteoblasts.

The method of cell isolation utilised is a modification of the explant technique of Chenoy-Marchais and Fritsch (1988). Neonatal (2 - 3 days old) MF-1 (outbred) mice, bred in-house, were killed by cervical dislocation and the head removed. The outer layers of skin covering the skull were carefully removed to expose the calvarial bones. Using a fine pair of scissors the parietal bones at the top of the skull were removed in a single piece and placed in a Petri dish containing sterile DMEM. Any visible tissue or blood vessels were carefully removed with fine forceps. The two major anterior calvaria were removed by cutting within the confines of the suture lines to produce two small rectangles of bone. This ensured that the mixed population of progenitor cells that form the suture lines are not included in the isolation. Under a dissection microscope the periosteal membranes on the upper and lower surfaces of the calvaria were carefully removed using a pair of fine forceps. The calvaria were then cut into

small pieces and placed upon sterile coverslips in 6 well plates containing DMEM. Osteoblasts were used in experiments 5 -7 days later, during which time they had migrated from the surface of the bone to the coverslip.

4.2.2. Histological staining for alkaline phosphatase activity:

Intense alkaline phosphatase activity is a well-known indicator of osteoblastic phenotype (Rodan & Rodan, 1984), and thus provides an easy method to confirm osteoblast identity. In this method, cells are incubated with napthol AS-MX phosphate and a diazonium salt (Fast Red) in an alkaline buffer. Napthol AS-MX, formed at the sites of phosphatase activity, produces an insoluble azo pigment which is seen associated with the cell membrane.

Cells were first fixed using 4% w/v paraformaldehyde in Krebs-Hensleit solution for 5 min. This was removed and the cells washed twice with Krebs-Hensleit solution at 5 min intervals prior to addition of the alkaline phosphatase stain. This consisted of 1 mg ml^{-1} 'fast red' TR salt and 0.27 mg ml^{-1} napthol AS-MX phosphate made up in 0.1 M Tris HCl, pH 8.2 (all Sigma, USA). The stain was made immediately prior to use as over long periods of time (> 1 hr) it can autodevelop. The stain was removed from the cells after 5 min and replaced with dH_2O; alkaline phosphatase positive cells are stained pink when observed under a microscope.

4.2.3. Patch-clamp recording:

Experiments were performed using the whole-cell mode of the patch-clamp technique as detailed in section 2.3.2.2 of the experimental procedures. All other experimental details and the solutions used in whole-cell recording are as detailed in section 3.2.

4.3. Materials:

Paraformaldehyde, 'fast red' TR salt and napthol AS-MX phosphate were all obtained from Sigma (USA).

4.4. Results:

4.4.1. Primary cultured calvarial osteoblasts:

The cellular morphology of calvarial osteoblasts is shown in figure 4.1A. Subsequent to migration from the bone explant to the surface of the coverslip, cells appeared elliptical with single or multiple longitudinal projections. As shown in figure 4.1B the majority of these cells stained positive for alkaline phosphatase activity, as indicated by the pink/red stain, suggesting they were likely to be of osteoblastic phenotype.

4.4.2. Volume-sensitive Cl⁻ currents:

Under whole-cell voltage clamp, primary osteoblasts equilibrated with symmetrical isotonic NMDG chloride solutions, exhibited small currents linearly related to voltage in response to 320 ms duration voltage clamp pulses between -80 and +80 mV (Fig. 4.2A). In 7 cells, with a mean cell capacitance of 22 ± 3 pF, the slope conductance was 1.0 ± 0.3 nS. When cells were subject to hypotonic shock, there was visible cell swelling that was accompanied by instantaneous activation of large amplitude inward and outward currents in response to hyperpolarising and depolarising pulses (Fig. 4.2B.). At strongly depolarised potentials the current exhibited marked time-dependent inactivation, there was however no evident activation kinetics. The current-voltage (I-V) relationship was clearly outwardly rectifying and reversed at 3.2 ± 0.8 mV (n = 7). The effects of hypotonic shock were readily reversed upon returning the cells to isotonic conditions (Fig. 4.2C). In 7 cells the mean current at +80 mV under steady swelling was 77.6 ± 14.2 $pApF^{-1}$; however, on return to isotonic bathing conditions (for 5 min) this value fell to 3.9 ± 0.6 $pApF^{-1}$, close to the basal value under isotonic conditions prior to hypotonic challenge of 2.2 ± 0.5 $pApF^{-1}$.

Using the alternating voltage pulse protocol with a conditioning prepulse to -100 mV as detailed in section 3.4.2 and symmetrical choline chloride solutions, an accurate I-V relationship was determined as shown in Fig 4.3. The current rectified in the outward direction with mean conductances of 38.9 ± 9.7 nS and 12.3 ± 2.3 nS (n = 5) at +80 and -80 mV respectively. The mean reversal potential (E_{rev}) was -0.4 ± 0.5 mV,

identical to that predicted by Nernstian theory of 0 mV for a perfectly selective Cl^- channel under these conditions.

4.4.3. Ionic selectivity of the current:

The ionic selectivity of the volume-regulated current in primary osteoblasts was investigated by applying a voltage-ramp stimulus between -80 and +80 mV (as in 3.4.3), in hypotonic bathing solutions in which NMDG chloride was replaced with the sodium salt of a variety of anions (Fig. 4.4). From the current-voltage curves the reversal potentials (E_{rev}) were evaluated and permeabilities relative to Cl^- (see Table 4.1) were calculated using the Goldman-Hodgkin-Katz equation (Equation 3.1).

Table 4.1.. Effects of Cl^- ion replacement upon reversal potentials (E_{rev}) of volume-sensitive anion currents in primary cultured mouse calvarial osteoblasts.

Anion	E_{rev} (mV)†	P_x/P_{Cl}*	n
SCN^-	-15.5 ± 1.9	2.17 ± 0.17	4
I^-	-10.5 ± 2.2	1.78 ± 0.15	4
Br^-	-6.5 ± 1.0	1.51 ± 0.06	4
F^-	+14.0 ± 0.4	0.66 ± 0.01	4
$Gluconate^-$	+45.8 ± 2.1	0.17 ± 0.02	4

E_{rev} obtained from I-V plots as detailed in experimental procedures (section 2.6).
†Values corrected for junction potentials (around 5 mV for gluconate, but < 1 mV for other anions).

The reversal potential with hypotonic NaCl bathing solution was 1.7 ± 0.7 mV (n = 12), not significantly different from that obtained with standard hypotonic NMDG chloride extracellular solution of 3.2 ± 0.8 mV (n = 7; Student's unpaired t-test, $p > 0.05$); this is consistent with the current showing anion selectivity. As shown by table 4.1 the exhibited anion sequence was $SCN^- > I^- > Br^- > Cl^- > F^- >$ gluconate$^-$.

4.4.4. Sensitivity to Cl^- channel blockers:

The volume-sensitive Cl^- conductance in ROS 17/2.8 cells was effectively inhibited by the Cl^- channel blockers NPPB and DIDS, but resistant to block by DPC (see chapter 3). The effects of these blockers at 100 μM were thus assessed upon the swelling induced Cl^- conductance present in murine primary calvarial osteoblasts.

As shown in figure 4.5 100 μM NPPB when applied extracellularly for 30 s produced substantial inhibition of the volume-sensitive current. This block appeared to occur independent of voltage, the mean inhibitory effects of NPPB in 5 cells being 72.8 ± 7.0% and 81.8 ± 2.8% at -80 and +80 mV respectively. DIDS also effectively inhibited the current (Fig. 4.6), however these effects were notably voltage-dependent with the outward current being more susceptible to block than the inward current. The mean inhibition produced by DIDS at -80 mV was 32.0 ± 4.4% (n = 4) compared to 54.7 ± 3.9% at +80 mV. DIDS was also found to facilitate the rate of inactivation exhibited by the current at strongly depolarised potentials (Fig. 4.6, +80 mV voltage step). DPC was a relatively ineffective inhibitor of the volume-sensitive Cl^- current, 100 μM

producing only 15.9 ± 3.3% and 20.7 ± 3.7% (n = 4) inhibition at -80 and +80 mV respectively.

A.

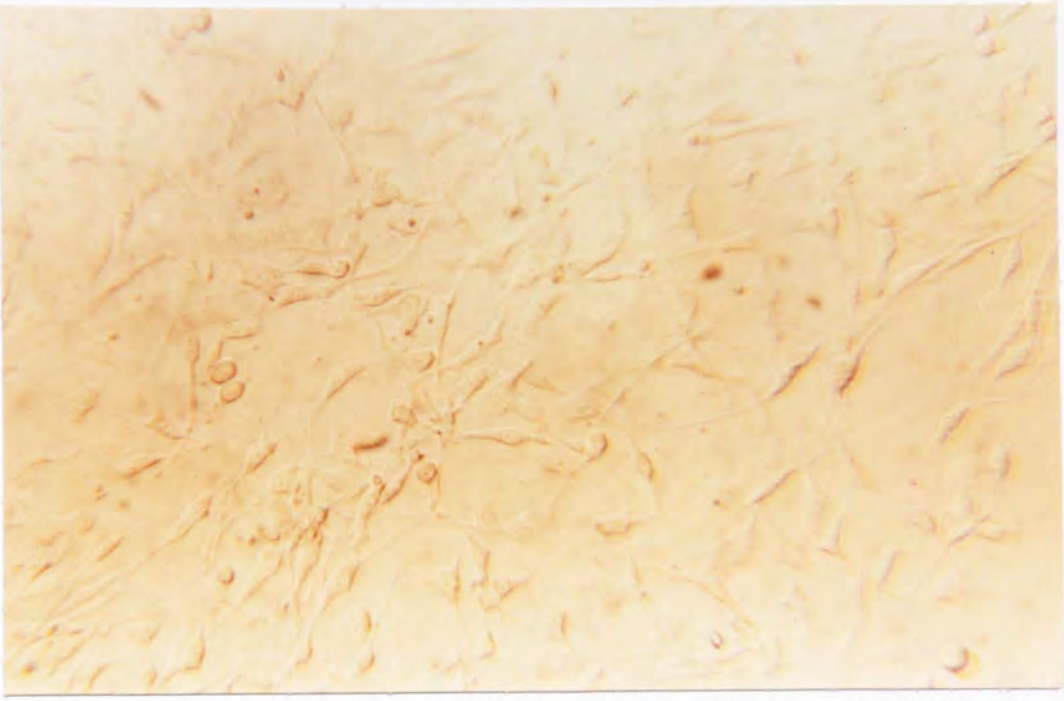

B.

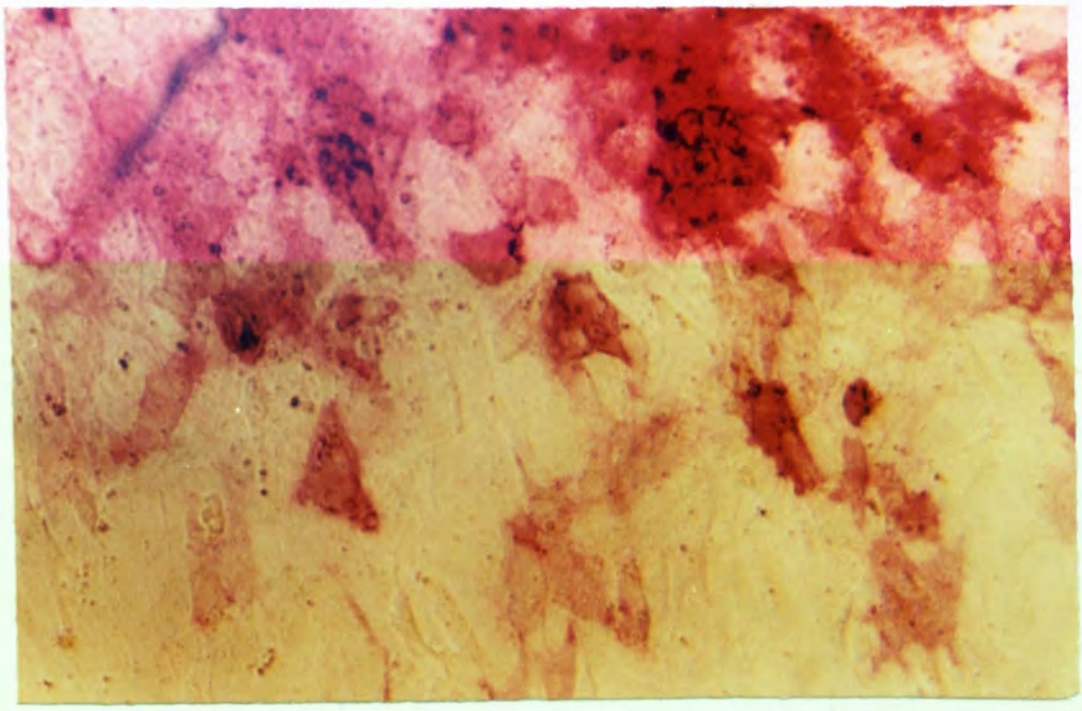

Figure 4.1. Morphological appearance and histological staining of primary cultured mouse calvarial explant osteoblasts. *A, cell morphology at X400 magnification. B, results of histological staining for alkaline phosphatase activity (red/pink colour is positive), at X400 magnification. Cells were fixed in paraformaldehyde prior to staining with napthol AS-MX phosphate at pH 8.2 as detailed in methods.*

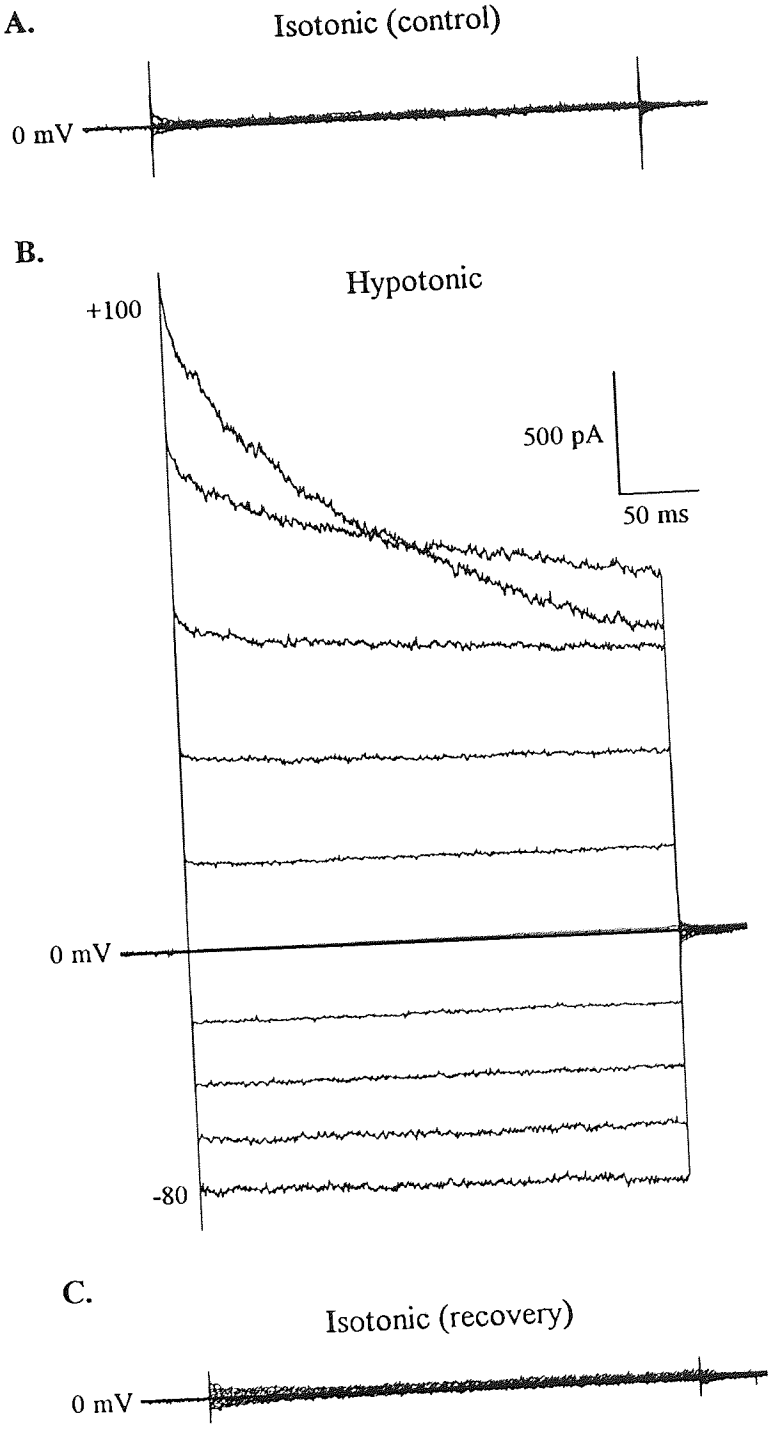
A.
Isotonic (control)
0 mV
B.
Hypotonic
+100
500 pA
50 ms
0 mV
-80
C.
Isotonic (recovery)
0 mV

Figure 4.2. Reversible activation of volume-sensitive Cl^- currents in primary cultured mouse calvarial osteoblasts. A, Basal currents elicited in single cell equlibrated with isotonic NMDG chloride solutions, by voltage pulses between -80 and +100 mV (20 mV increments, preceded by a 500 ms prepulse to -100 mV). B, Cl^- currents in the same cell upon steady osmotic cell swelling induced by a hypotonic challenge (3 min). C, recovery 5 min after returning cell to isotonic NMDG chloride bathing solution. Data representative of 10 similar experiments.

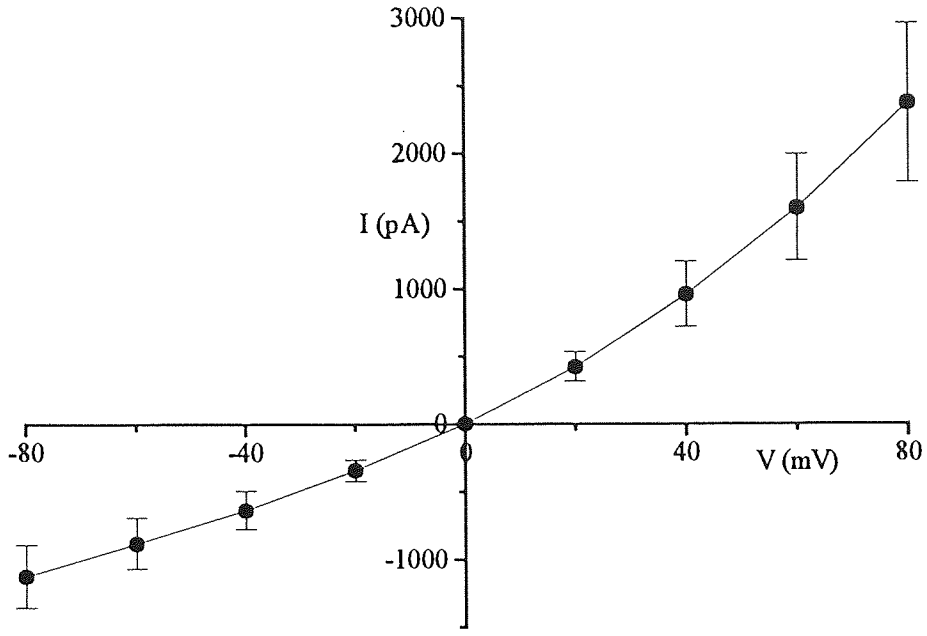

Figure 4.3. Current-voltage relationship of volume-sensitive Cl^- currents in primary cultured mouse osteoblasts under symmetrical 135 mM Cl^- solutions. *Peak instantaneous currents were measured in osmotically swollen mouse calvarial osteoblasts, equilibrated with symmetrical choline chloride solutions, using an alternating pulses protocol as detailed in fig. 4.1. Each point represents the mean current of 5 cells, 3 min after superfusion with hypotonic bathing solution, with S.E.M. shown by vertical bars. Peak currents measured within 10 ms of onset of voltage pulse.*

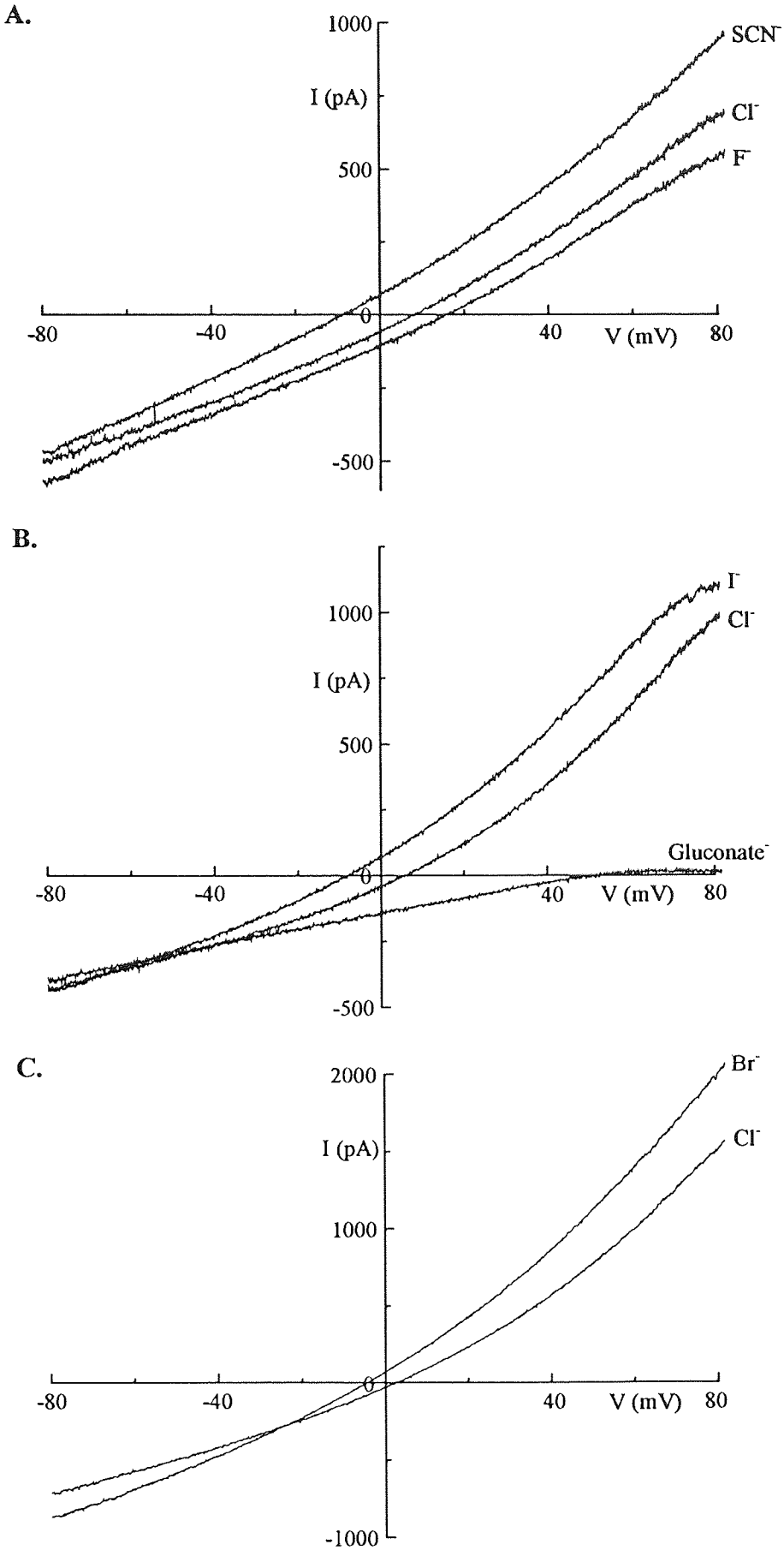
A.
1000
I (pA)
500
-500
SCN-
Cl-
F-
-80
-40
0
40
V (mV)
80
B.
1000
I (pA)
500
-500
I-
Cl-
Gluconate-
-80
-40
0
40
V (mV)
80
C.
2000
I (pA)
1000
-1000
Br-
Cl-
-80
-40
0
40
V (mV)
80

Figure 4.4. Effects of anion substitution on current-voltage curves assessed by ramp voltage-clamp stimulus in primary mouse calvarial osteoblasts. Voltage ramps between -80 and +80 mV were over a 2 s period after steady current activation was observed in single osmotically swollen mouse calvarial osteoblast. Cells superfused with hypotonic medium (NMDG chloride solution; Table 3.1) in which NaCl was replaced with the sodium salt of the indicated anion:

A, SCN^-, Cl^-, F^-.

B, I^-, Cl^-, $gluconate^-$.

C, Br^-, Cl^-.

Data representative of 4 - 12 experiments.

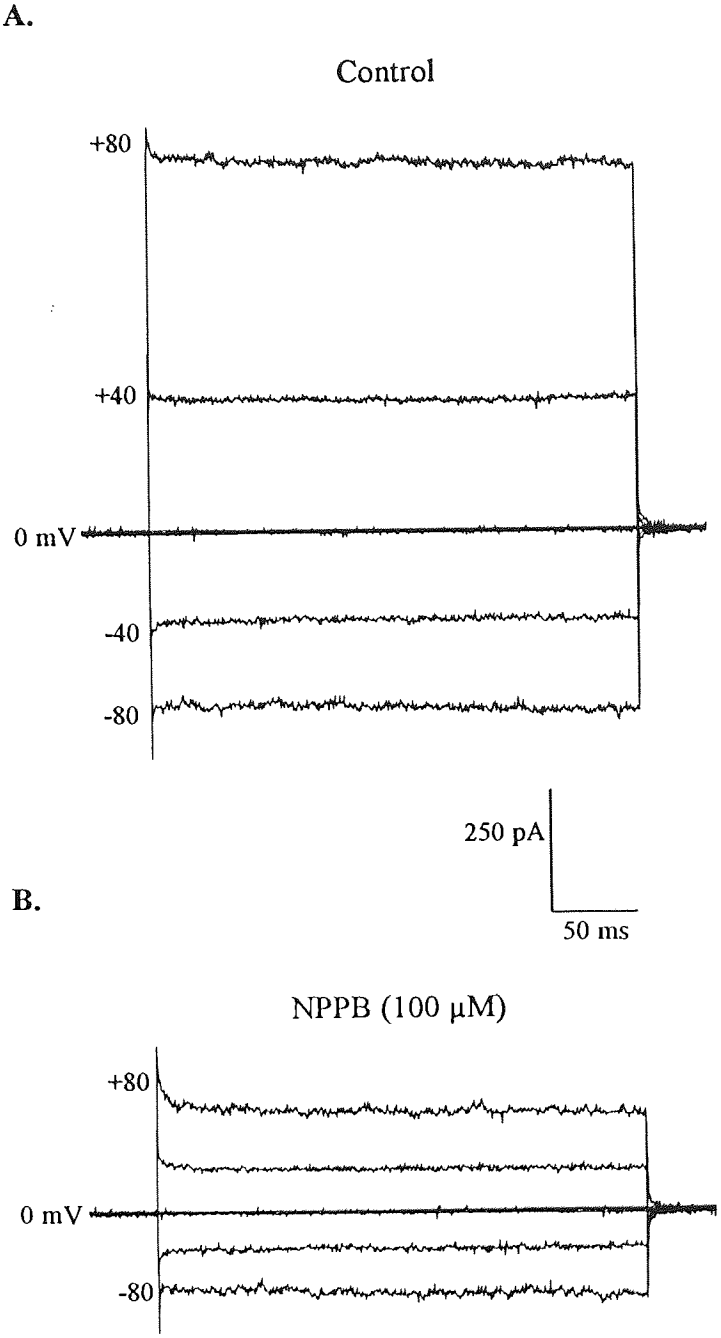

Figure 4.5. Effects of 100 µM NPPB upon whole-cell volume-sensitive Cl^- currents in primary cultured mouse calvarial osteoblasts. *Currents elicited in osmotically swollen cell (NMDG chloride solutions) by 320 ms command pulses to indicated potential from a holding potential of 0 mV, prior (A) and 30 s subsequent to addition NPPB (B). Cell representative of 3 similar experiments. Inhibition by 100 µM NPPB at -80 mV, 71.2 %; at +80 mV, 77.8 %.*

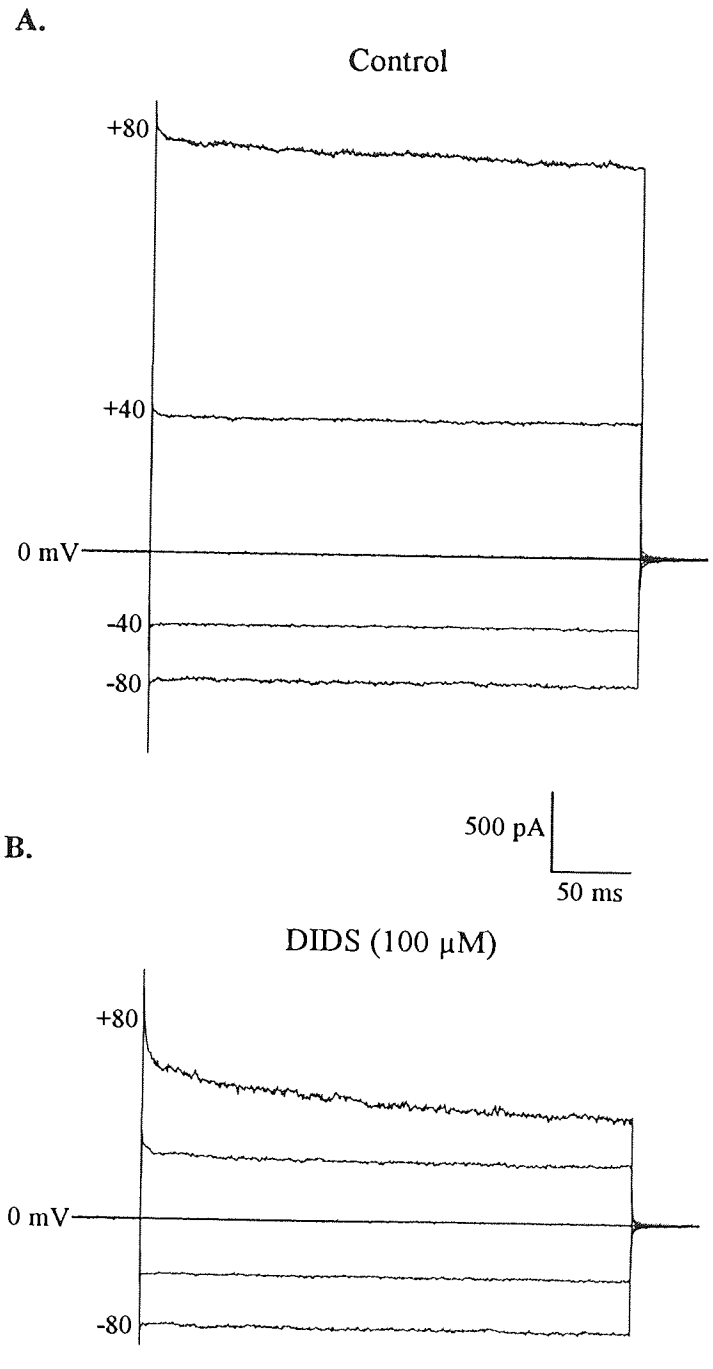

Figure 4.6. Effects of 100 μM DIDS upon whole-cell volume-sensitive Cl^- currents in mouse primary cultured calvarial osteoblasts. *Currents elcited in single osmotically swollen (NMDG chloride solutions) osteoblast by voltage command pulses to indicated potential from a holding potential of 0 mV, prior (A) and 30 s subsequent to addition of 100 μM DIDS (B). Cell representative of 3 similar*

experiments. Note voltage-dependence of inhibition; inhibition at -80 mV, 21.9 %; at +80 mV, 65.2 %.

4.5. Discussion & Conclusions:

The characteristics of the chloride current activated by hypotonic shock in mouse primary cultured calvarial osteoblasts are summarised in table 4.2 below.

Characteristic	Primary Cultured Mouse Calvarial Osteoblasts	ROS 17/2.8 cell line
Reversible current activation in response to hypotonic shock.	✓	✓
Rectification	Outward	Outward
Time-dependent inactivation†	✓	✓
Anion selectivity sequence	SCN > I > Br > Cl > F > gluconate	SCN > I > Br > Cl > F > gluconate
Sensitivity to block by: NPPB DIDS DPC	 ✓ ✓ (voltage-dependent) × (weak block)	 ✓ ✓ (voltage-dependent) × (weak block)

Table 4.2. Characteristics of the currents activated by hypotonic shock in mouse primary cultured osteoblasts and ROS 17/2.8 cells. *†Time-dependent inactivation assessed at strongly depolarised potentials (> +50 mV).*

As can be seen the characteristics of the volume-sensitive Cl^- currents in primary osteoblasts and ROS 17/2.8 cells are identical in terms of kinetics, selectivity sequences and pharmacology. This suggests that the conductances are likely to be due to a similar or identical channel, and that this current is 'physiologically' present in osteoblasts. Thus, the ROS 17/2.8 cell line provides a suitable model in which to further characterise this conductance.

Chapter 5.

MODULATORY EFFECTS OF ARACHIDONIC ACID UPON THE VOLUME-SENSITIVE CHLORIDE CURRENT IN RAT OSTEOBLAST-LIKE (ROS 17/2.8) CELLS.

5.1. Background:

Arachidonic acid has been shown to be an important cellular messenger in a wide variety of cell types (Irvine, 1982). Its biological actions are widespread and varied, including activation of protein kinase C (Murakami & Routenburg, 1985) and potentiation of NMDA receptor currents (Miller, Sarantis, Traynelis & Attwell, 1992). Physiologically, arachidonate can be produced in eukaryotic cells by at least three distinct mechanisms; as a product of the cleavage of certain membrane phospholipids by phosholipase A_2 (PLA_2), sequential action of phospholipase C (PLC) and diacylglycerol lipases, or through the action of diacylglycerol lipase on phosphatidic acid generated by activation of phospholipase D (PLD). Arachidonate can be processed by cyclo-oxygenases, lipoxygenases and cytochrome P-450 enzymes, yielding a variety of structurally diverse biologically active metabolites that can function not only as potential autocrine factors but also interact with specific cell surface receptors (e.g. prostaglandin E_2) (Needleman, Turk, Jakschik, Morrison & Lefkowith, 1986).

Arachidonate has been reported to possess a broad spectrum of effects upon ion channels that include both activation (Ordway, Walsh & Singer, 1989) and potentiation of currents, as well as inhibition (Chesnoy-Marchais & Fritsch, 1994a). The mechanisms by which these effects occur are still not fully understood. Excised patch experiments have shown that arachidonate can activate ion channels in the absence of cytosolic cell components suggesting a direct effect not involving arachidonate metabolism. Modulation of ion channels by arachidonate metabolites has also been

clearly documented (e.g. Kurachi, Ito, Sugimoto, Shimizu, Miki & Michio, 1989). Recently, it has been suggested that endothelium-derived hyperpolarising factor (EDHF) is a cytochrome P-450 metabolite of arachidonate that acts to open Ca^{2+}-activated K^+ channels (Hecker, Bara, Bauersachs & Busse, 1994).

Arachidonate has strongly concentration-dependent effects upon ionic conductances in osteoblasts; at low concentrations (< 5 μM) arachidonate produces inhibition of the L-type Ca^{2+} current and the delayed rectifier K^+ current. At higher concentrations (> 5 μM) it produces the converse effects (Chesnoy-Marchais & Fritsch, 1994a). The effects of arachidonate upon chloride channels have not been so widely investigated. In Ehrlich ascites tumour cells, measurements of cell volume strongly suggest that the Cl^- transport pathway responsible for a regulatory volume decrease (RVD) in response to hypotonic shock is sensitive to inhibition by arachidonate (Lambert, 1987). Electrophysiological investigation has shown that arachidonate rapidly and effectively (IC_{50} = 8 μM) inhibits the volume-regulatory Cl^- current present in cultured human epithelial cells (Hazama & Okada, 1993).

In this chapter the effects of exogenously applied arachidonate upon the volume-regulated Cl^- conductance in ROS 17/2.8 cells has been investigated.

5.2. Methods:

Experiments were performed using the whole-cell configuration of the patch-clamp technique as described in experimental procedures (2.3.2.2) with NMDG chloride bath and pipette solutions (see Table 3.1 for composition).

The inactivation exhibited by the volume-sensitive Cl^- current in ROS 17/2.8 cells at strongly depolarised potentials (> +50 mV) was quantified in these experiments. This was most consistently achieved ($R > 0.99$) using a single exponential function Y (equation 5.1) to yield a time constant (τ_{inact}), where A_0 and A_1 are the current values at the beginning and end of the fitting region.

$$Y = A_0 + A_1^{-t/\tau_{inact}} \qquad \text{Equation 5.1.}$$

The fitting region commenced at least 5 ms after the onset of the voltage pulse to ensure that the fit was free from contamination by any uncompensated capacitance transients, and continued until 5 ms prior to the end of the command pulse.

5.3. Materials:

Arachidonic, oleic and elaidic acids were dissolved in ethanol to produce stock solutions of 25 mM that were aliquoted and stored under argon at -20°C. Stock solutions were thawed prior to use and diluted into the appropriate external solution to

provide final concentrations between 1 and 250 μM. The vehicle alone (ethanol) did not have any significant inhibitory effects upon whole-cell volume-sensitive Cl^- currents even at 1% v/v (n = 5). SKF525A (proadifen HCl) and metyrapone HCl were dissolved in distilled water prior to dilution into internal solution. Cimetidine, indomethacin, nordihydroguaretic acid (NDGA), 12-O-tetradecanoylphorbol-13-acetate (TPA) and forskolin were all dissolved in dimethyl sulfoxide (DMSO) and diluted as appropriate. At the concentrations used (0.1 - 0.25% v/v) DMSO was without effect upon whole-cell Cl^- currents when applied both intra- and extracellularly (n = 5). Ethoxyresorufin and piperonyl butoxide were dissolved in ethanol to produce stock solutions. All drugs were obtained from Sigma (St.Louis, Ma, USA) with the exception of cimetidine and piperonyl butoxide which were the kind gift of Dr.M.Coleman (Aston University).

5.4. Results:

5.4.1. Effects of extracellular arachidonic acid on the volume sensitive Cl^- current in ROS 17/2.8 cells:

As shown in figure 5.1 addition of extracellular arachidonate produced two distinct effects upon the volume-sensitive Cl^- current elicited by hypotonic shock in ROS 17/2.8 cells. Firstly, there was a rapid block that reached steady-state within 10 - 15 s of arachidonate application. The inhibition occurred independent of membrane potential (inhibition by 100 μM arachidonate; -40 mV, 34.7 ± 3.1%; +40 mV, 32.1 ± 3.1%; n = 11) though it was strongly reliant on the concentration of arachidonate (Fig.

5.3). Due to the incomplete concentration-inhibition curve it was difficult to obtain an accurate fitted IC_{50} value, but if it was assumed that the inhibition would eventually reach 100%, an IC_{50} value of 177 μM was obtained. A second phase of inhibition was also observed that developed with a much slower time course (Fig 5.1 & 5.4). This block developed following a characteristic latency period of 90 to 130 s after commencing arachidonate superfusion. The delay in the onset of the second phase of inhibition was not substantially affected by increasing the arachidonate concentration (at 25 μM, 131 ± 14 s, n = 16; 100 μM, 93 ± 6 s, n = 4), however the time for the inhibitory response to reach steady state after onset was reduced with increasing concentration (at 10 μM, 335 ± 40 s, n = 6; 25 μM, 243 ± 15 s, n = 15; 50 μM, 108 ± 13 s, n = 7; 100 μM, 119 ± 6 s, n = 4). In common with the rapid initial inhibition of the current by arachidonate, the second phase of inhibition was not voltage-dependent (Fig. 5.1 & 5.2). The second phase of inhibition however occurred at lower concentrations of arachidonate, being detectable at 1 μM and complete blockade routinely observed at 50 μM. The calculated IC_{50} value of 10 μM (Fig. 5.3) was thus significantly lower than that for the rapid phase of inhibition (177 μM). Both inhibitory effects were reversed upon reperfusion with hypotonic solution free from arachidonate (Fig. 5.1). In 6/7 cells, membrane currents had returned to control levels within 5 min of arachidonate removal even when the inhibition had been produced by concentrations as high as 100 μM.

As shown in figure 5.2, arachidonate did not only affect the peak of the volume-sensitive Cl^- current, it also elicited kinetic modifications. These were manifest as an acceleration of the inactivation present at strong depolarisations, and also the induction

of inactivation at depolarised potentials where it was previously absent (eg. +40 mV). In 7 cells application of 25 μM arachidonate reduced the monoexponential fit time constant (t_{inact}) for the +100 mV test step from a control value of 272.0 ± 29.7 ms to 81.8 ± 23.4 ms (n=7) within 5 - 10 min. By correlating the peak amplitude and the inactivation time constant prior and during superfusion with 25 μM arachidonate (Fig. 5.4), it is clear that acceleration of inactivation accompanies the second slower phase of current inhibition.

5.4.2. Evidence that arachidonate's effects are not mediated via enzymatic metabolites or protein kinases.

To determine whether metabolic pathways mediated the effects of arachidonate, the effects of arachidonate were studied in the presence of inhibitors of cyclo-oxygenase, lipoxygenase and cytochrome P-450, enzymes responsible for processing arachidonate. As shown in table 5.1A internal dialysis with a variety of inhibitors for periods of up to 15 min prior to arachidonate application, had no significant effect upon the inhibition of the volume-sensitive Cl^- current by arachidonate with the exception of 10 μM NDGA which reduced the initial inhibition by arachidonate. As this inhibition was not reproduced by a higher concentration (100 μM) this result may reflect a very low potency or just an anomalous result. The magnitude of the control Cl^- currents elicited by hypotonic shock prior to arachidonate application were generally unaffected by the inhibitors. Piperonyl butoxide significantly reduced the current density (Table 5.1A) whereas metyrapone potentiated the current. As both of these compounds are broad spectrum cytochrome P-450 inhibitors it seems unlikely they would produce contrary

effects, thus these results may reflect non-specific effects of piperonyl butoxide and metyrapone.

A. Current Inhibition.

Condition	Initial Inhibition (%)	Steady-State Inhibition (%)	Peak Current (pA/pF)	n
Control (25 μM arachidonate)	9.4 ± 0.8	86.5 ± 2.2	53.4 ± 4.3	22
10 μM Indomethacin	9.1 ± 2.8	91.0 ± 6.4	59.9 ± 11.2	4
10 μM NDGA	5.3 ± 0.8*	87.8 ± 1.4	60.9 ± 14.9	5
100 μM NDGA	5.9 ± 2.0	91.6 ± 3.6	52.1 ± 5.2	4
100 μM SKF525A	10.2 ± 2.4	86.4 ± 4.6	48.0 ± 6.8	6
10 μM Ethoxyresorufin	8.5 ± 2.7	81.8 ± 0.6	48.0 ± 15.9	4
500 μM Metyrapone	11.4 ± 1.0	75.5 ± 9.7	70.2 ± 7.0*	4
500 μM Piperonyl Butoxide	7.2 ± 2.6	78.3 ± 5.3	30.3 ± 7.1*	6
1 mM Cimetidine	8.3 ± 2.7	86.7 ± 2.7	52.2 ± 14.7	4
No ATP & GTP	8.9 ± 1.5	77.5 ± 5.2	67.1 ± 9.7	4

B. Kinetic Modifications.

Condition	Before (Control)	After 25μM AA	n
Control	272.0 ± 29.7	81.8 ± 23.4	7
10 μM Indomethacin	233.6 ± 39.7	80.9 ± 29.3	4
100 μM NDGA	211.3 ± 41.3	72.6 ± 15.4	4
100 μM SKF525A	256.8 ± 46.3	113.3 ± 22.5	4
10 μM Ethoxyresorufin	169.8 ± 22.3	65.6 ± 18.0	4
500 μM Metyrapone	201.5 ± 32.1	94.8 ± 29.9	4
500 μM Piperonyl Butoxide	204.2 ± 41.4	98.5 ± 21.8	4
1 mM Cimetidine	190.5 ± 50.7	100.5 ± 32.1	4
No ATP & GTP	261.0 ± 73.9	113.5 ± 56.2	4

Table 5.1: Effects of inhibitors of cyclo-oxygenase (indomethacin), lipoxygenase (NDGA), cytochrome P-450 (SKF525A, ethoxyresorufin, metyrapone, piperonyl butoxide and cimetidine) and no nucleotides (absence of ATP and GTP from patch pipette solution) upon the effects of 25μM arachidonate upon volume-sensitive chloride currents in ROS 17/2.8 cells. Cells were dialysed under isotonic conditions with patch pipette solution modified as indicated above for 5 - 15 min after breakthrough into whole-cell configuration. After this period cells were subject to hypotonic shock for 2 - 3 min prior to addition of 25μM arachidonate. A, percentage initial and sustained phases of inhibition were measured using an alternating voltage pulses as described in Fig. 5.1., values are for the +40 mV step as are current density values. B, kinetic modifications were assessed using 320 ms voltage pulses to +100 mV (as Fig. 5.2.) and subject to a monoexponential fit to yield a single time constant (τ_{inact}), prior and subsequent to arachidonate application. Data expressed as mean ± S.E.M. of the indicated number of observations (n). denotes significantly different from control value using Student's unpaired t-test with Bonferroni correction, except in B where arachidonate significantly reduced τ_{inact} in all cases.*

Table 5.1B shows the effects of the arachidonate processing enzyme inhibitors upon the acceleration of inactivation induced by arachidonate. The inactivation shows a large amount of variation as can be seen from the control values, but in the presence of all inhibitors arachidonate still produced a substantial reduction in the time constant (τ_{inact}) for inactivation.

Other effects of arachidonate include direct activation of protein kinase C (PKC) and stimulation of adenylate cyclase, leading to an increase in cyclic AMP levels. To ascertain if either was the underlying mechanism by which arachidonate was exerting its inhibitory effects, forskolin and 12-O-tetradecanoylphorbol-13-acetate (TPA) were used. Volume-sensitive Cl^- currents were unaffected by 1 μM forskolin (n = 4) or 0.5 μM TPA (n = 3) treatment for 5 - 10 mins. Even when the EGTA concentration of the internal solution was lowered from 1 to 0.05 mM to reduce internal calcium buffering capacity and thus provide intracellular calcium required as a cofactor for PKC activity, TPA was still an ineffective inhibitor (n = 4). The lack of dependence upon intracelluar nucleotides (Table 5.1A & B) provides further evidence to suggest that arachidonate's actions are not mediated via activation of a kinase. The kinetic modifications induced by arachidonate were unaffected by exclusion of nucleotides and could not be mimicked by either forskolin or TPA.

Latencies between addition of arachidonate, onset of inhibition and steady-state inhibition were also unaffected by the inhibitors detailed above.

5.4.3. Effect of intracellular arachidonate upon the volume-sensitive Cl^- current:

In a number of cell types the effects of fatty acids upon ion channels have been shown to possess a 'sidedness' of effect, being only effective when applied to the extracellular surface of the membrane (e.g. Honoré, Bahranin, Attali, Lesage & Lazdunski, 1994; Poling, Karanian, Salem & Vicini, 1995). To test if this was the case with the inhibition of the volume-sensitive Cl^- current in ROS 17/2.8 cells arachidonate was applied

internally. This was achieved by supplementing normal pipette solution with 50 μM arachidonate and dialysing the cell for 5 min after establishing whole-cell recording, prior to a subsequent hypotonic shock. Intracellular arachidonate significantly reduced the peak current density at +40 mV from a control value of 63.7 ± 3.0 $pApF^{-1}$ (n = 65) to only 14.0 ± 4.6 $pApF^{-1}$ (n = 8, $p < 0.001$, Student's unpaired t-test) suggesting it was effective from the intracellular side of the membrane. It was not possible to assess if internal arachidonate induced any kinetic modification of the current as this technique did not allow control inactivation time constants to be determined.

In 3 out of the 8 cells tested with internal arachidonate the currents were of sufficient magnitude to ascertain whether the current was now refractory to inhibition by extracellularly applied arachidonate. As shown in figure 5.5 external 50 μM arachidonate still produced two distinct phases of inhibition; one with rapid onset (15s) and another occurring approximately 2 min later. In the 3 cells tested these amounted to 21.9% and 77.6% inhibition of the peak current respectively. Figure 5.5 also shows that upon superfusion with hypotonicity the current shows a decrease in baseline chloride levels before increasing. This was a common occurrence in cells which had been dialysed for long periods of time (> 10 min) prior to hypotonic shock and may reflect another type of Cl^- current present in ROS 17/2.8 cells that is inhibited by hypotonicity. A similar observation has recently been reported in primary cultured rat osteoblasts (Chesnoy-Marchais & Fritsch, 1994).

5.4.4. Effects of oleic and elaidic acids upon the volume-sensitive Cl^- current:

In an attempt to ascertain whether these modulatory effects were specific to arachidonate or could be mimicked by other fatty acids the effects of another *cis* unsaturated fatty acid, oleic acid were investigated. Unlike arachidonate, which has 20 carbon atoms and four double bonds at positions 5,8,11 and 14 (relative to the carboxyl carbon of the acyl chain), oleic acid has only 18 carbons and a single double bond at position 9. Superfusion with oleic acid at 25 μM for 5 - 10 min produced only modest inhibition of the volume-sensitive Cl^- current; this amounted to a rapid inhibition at +40 mV of only 1.4 ± 0.6% and a steady-state inhibition of 10.8 ± 5.7% (n = 4). The inactivation kinetics of the current were unaffected. Elaidic acid, the *trans* isomer of oleic acid, at 25 μM was without measurable effect either upon the current amplitude or kinetics (n = 3). At concentrations higher than 25 μM both fatty acids were found to compromise patch-clamp seals after only 1 - 2 min superfusion, making it impossible to assess if any inhibition would occur at higher concentrations. The reason for this phenomenon remains unexplained.

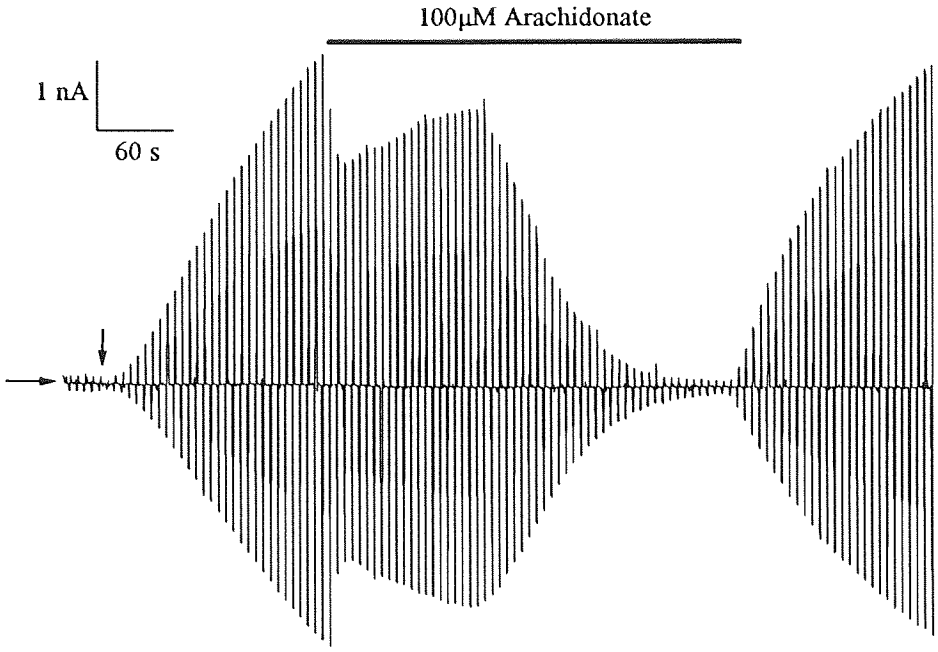

Figure 5.1. Effects of extracellular 100 μM arachidonate upon volume-sensitive Cl^- currents in ROS 17/2.8 cells. *Currents measured by applying alternating voltage-clamp pulses to ± 40 mV from a holding potential of 0 mV at 0.2 Hz to single ROS 17/2.8 cell equilibrated with NMDG chloride solutions. The hypotonic challenge was administered at time indicated by the vertical arrow; arachidonate applied by fast superfusion system as shown by solid bar 3 min after onset of hypotonic challenge. Zero current level indicated by horizontal arrow, data representative of four similar experiments.*

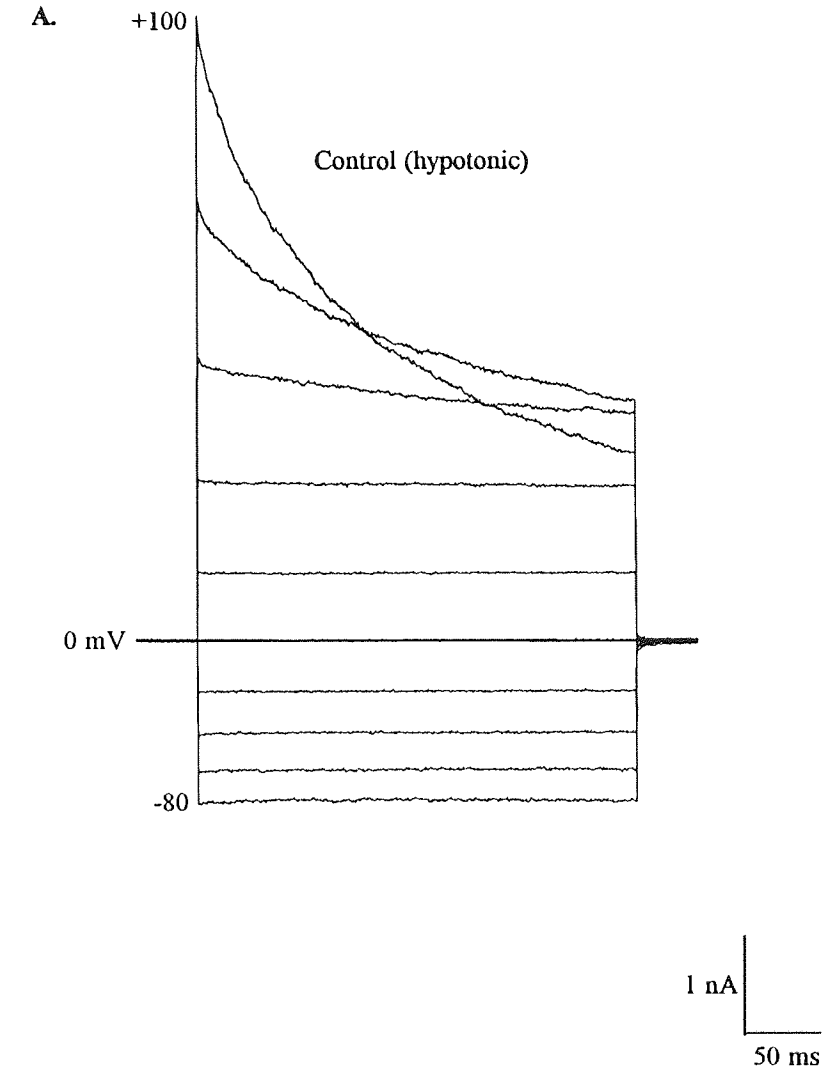
A.
+100
Control (hypotonic)
0 mV
-80
1 nA
50 ms
B.
25 μM arachidonate
(5 min)
+100
0 mV
-80

C.

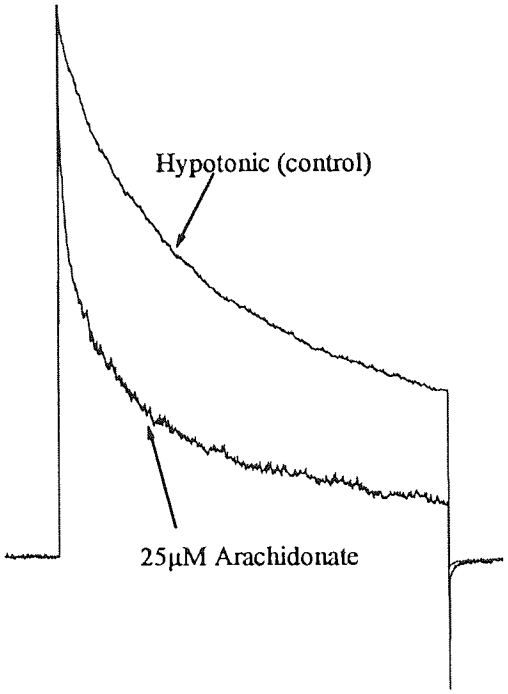

D.

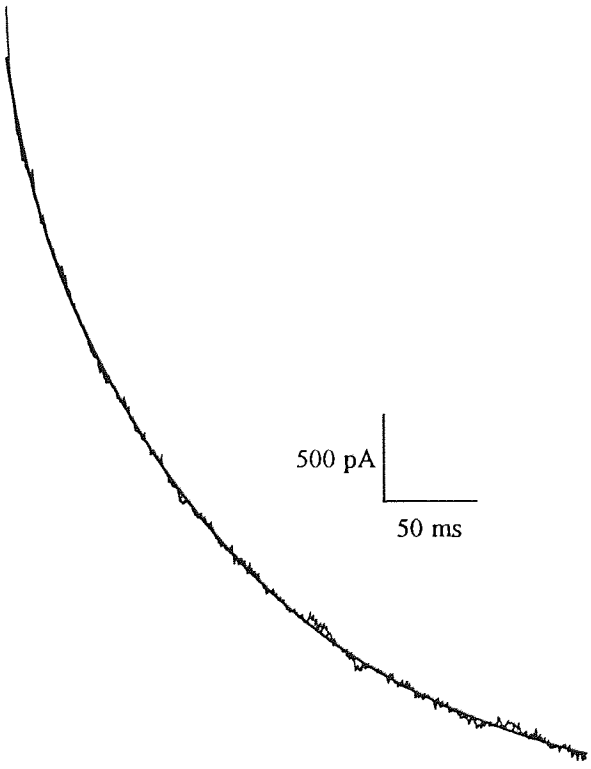

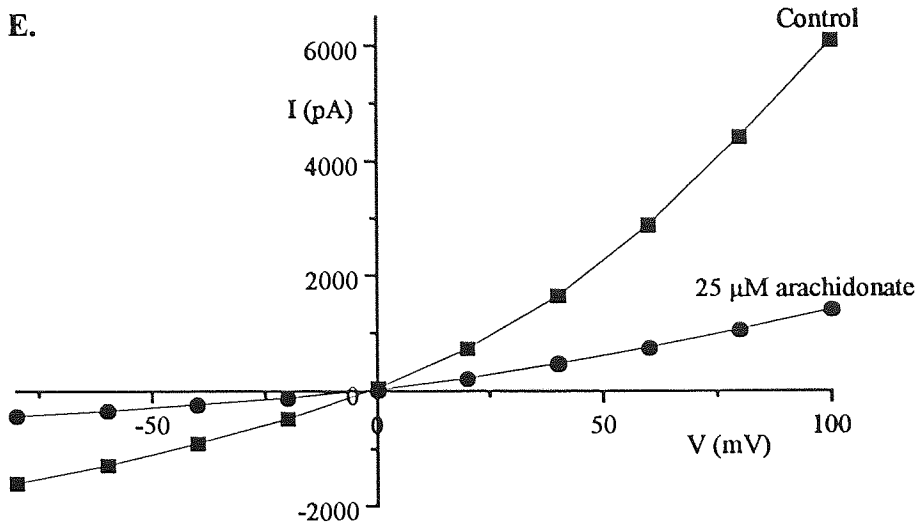

Figure 5.2. Effects of 25 μM arachidonate upon the inactivation kinetics of the volume-sensitive Cl^- current in ROS 17/2.8 cells. *A, B; currents elicited by voltage-clamp pulses to potentials between -80 and +100 mV (20 mV increments, preceded by a 500 ms conditioning prepulse to -100 mV) for 320 ms from a holding potential of 0 mV applied to a single osmotically swollen ROS 17/2.8 cell in the absence (A) and 5 min after onset of arachidonate superfusion (B). C, acceleration of current inactivation is shown more clearly when the current in the presence of arachidonate is scaled to control current (+100 mV voltage pulse; scale factor 3.16): τ_{inact}; control, 118.0 ms; 25 μM arachidonate, 64.3 ms; peak current inhibition, 77.7%. D, example of monoexponential fit to the inactivation exhibited by the current at +100 mV (control trace in C). E, current-voltage (I-V) relationship for currents shown in A and B, prior (■) and subsequent (●) to arachidonate superfusion. Data from a single cell representative of 8 other experiments.*

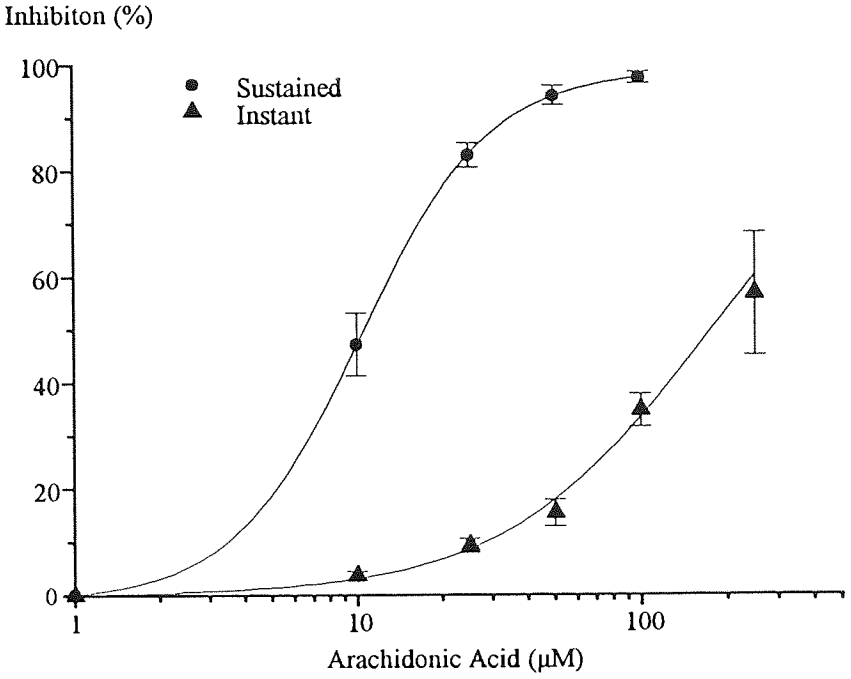

Figure 5.3. Concentration-inhibition curves of arachidonate on volume-sensitive Cl^- currents in osmotically swollen ROS 17/2.8 cells. *Instantaneous inhibition (▲) was measured within 15 s of arachidonate application, sustained (●) was measured at steady-state inhibition. Ordinate represents the percentage inhibition after application of arachidonate against steady state current prior to drug challenge. Symbols represent the mean value of 4 -21 experiments with S.E.M. (vertical bars). Curves show fits to the data (using equation 2.2) with the following parameters from MicroCal Origin: IC_{50}, 10.4 μM (sustained), 177.1 μM (instant); Hill coeffecients (n_H), 1.9 (sustained), 1.2 (instant); maximal inhibition, 100% in both cases.*

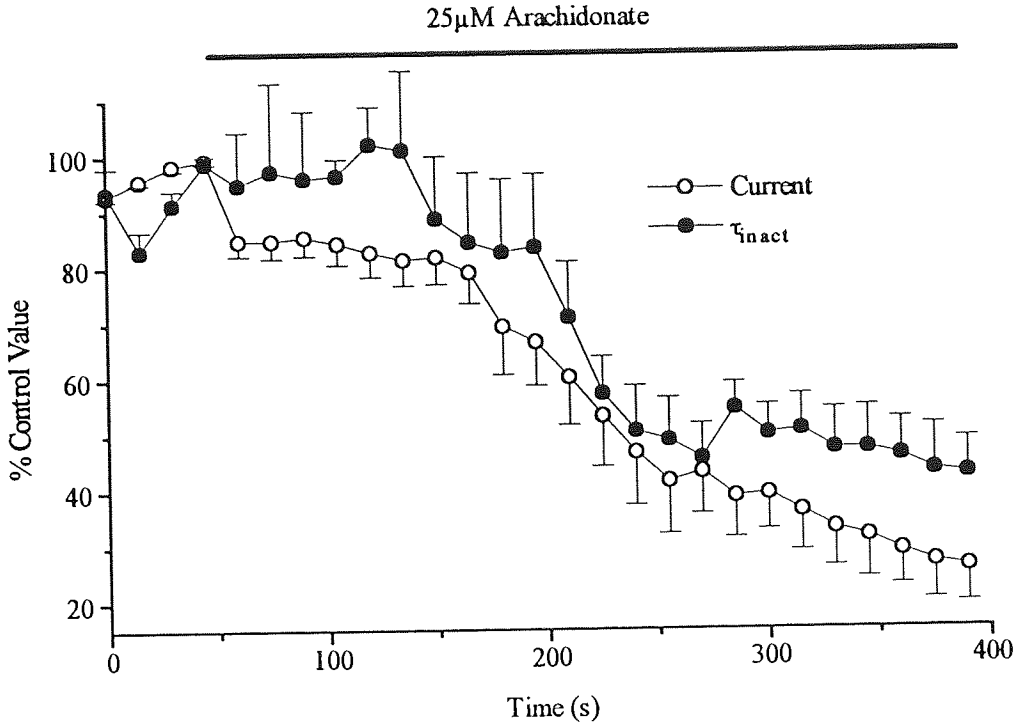

Figure 5.4. Time courses of the effects of 25 μM arachidonate upon peak currents and inactivation kinetics of volume-sensitive Cl^- currents. *Currents elicited by a depolarising voltage-clamp pulse to +100 mV for 320 ms from a holding potential of 0 mV preceded by a conditioning prepulse to -100 mV for 500 ms. Pulses were applied at 15 s intervals to osmotically swollen ROS 17/2.8 cells 60 s prior and 360 s subsequent to superfusion with 25 μM arachidonate as indicated by solid bar. Inactivation kinetics were analysed as detailed in section 5.2 to yield a single time constant (τ_{inact}). Symbols represent the mean with S.E.M. (vertical bars) of 4 cells, results were normalised to peak current and time constant prior to arachidonate application (mean peak current 12474 ± 2041 pA; mean peak time constant 262.2 ± 58.9 ms).*

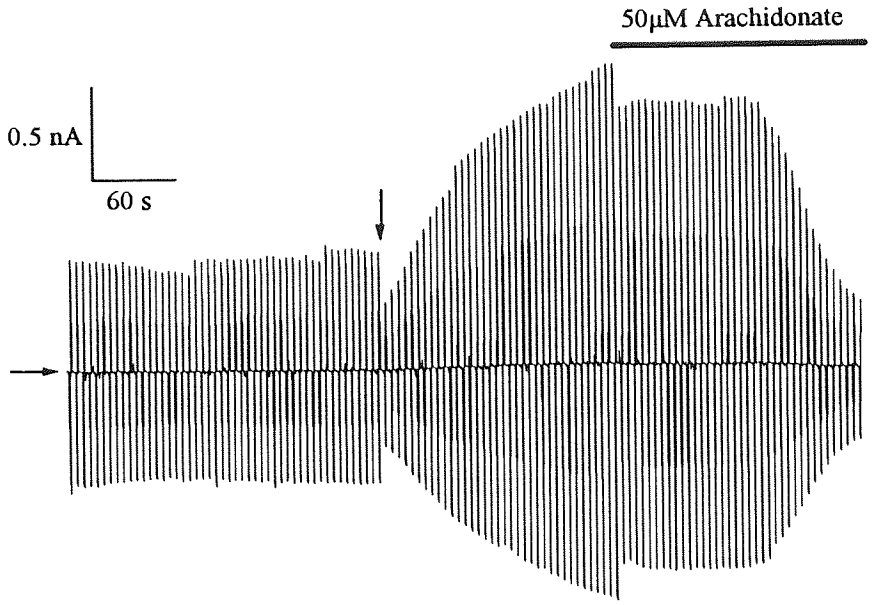

Figure 5.5. Effects of extracellular superfusion with arachidonate upon volume-sensitive Cl^- current in ROS 17/2.8 cell previously dialysed with intracellular arachidonate. *Currents were elicited by voltage pulses to ± 40 mV (holding potential 0 mV) applied at 0.2 Hz in a single ROS 17/2.8 cell equilibrated with NMDG chloride solution. The pipette solution was supplemented with 50 μM arachidonate, whole-cell mode established 1 min prior to start of record. Hypotonic challenge administered at time indicated by vertical arrow (zero current level indicated by horizontal arrow). Extracellular arachidonate applied as indicated by solid bar. Data representative of two similar experiments.*

5.5. Discussion:

5.5.1. Effects of arachidonate upon the volume-sensitive Cl^- current in ROS 17/2.8 cells:

The major finding of the present study is that arachidonate effectively and reversibly inhibits the volume-sensitive Cl^- current in ROS 17/2.8 cells. This inhibition occurs in two distinct phases (Fig. 5.1); a rapid inhibition that occurs within 5 - 10s of arachidonate exposure, preceding a slower phase that starts to develop approximately 2 min later and reaches steady-state after a further 100 - 300s (depending upon the arachidonate concentration). Accompanying the second phase of inhibition is an acceleration of the time-dependent inactivation exhibited by the current at depolarised potentials (Figs 5.2 & 5.4). Similar effects upon the inactivation kinetics of this conductance occur with the Cl^- channel blocker DIDS (see 3.4.4.). As the inhibition produced by DIDS was also notably voltage-dependent it was suggested that this effect reflected time-dependent, reversible association of the negatively charged blocker with the channel at depolarised potentials. The inhibitory effects of arachidonate are not sensitive to membrane potential (Fig. 5.2) even though at physiological pH it also is negatively charged, thus this explanation may not be valid for arachidonate. The second phase of inhibition occurred at much lower concentrations than the initial phase of inhibition (IC_{50}s; 10 μM and 177 μM respectively) which may reflect differences in the mechanisms by which the two phases of blockade are produced. This makes arachidonate a significantly more potent

inhibitor of the volume-sensitive Cl^- current in ROS 17/2.8 cells than the recognised Cl^- channel blockers NPPB and DIDS (IC_{50}s of 64 μM and 81 μM respectively).

5.5.2. Mechanism of arachidonate action:

Fatty acids have been demonstrated to interact directly with ion channels (Ordway, Singer & Walsh, 1991). However, the possibility that the action of arachidonate is mediated through oxygenated metabolites or second messenger systems must be considered. Various inhibitors of cyclo-oxygenase, lipoxygenase and cytochrome P-450 were tested in this study and found to be ineffective against the inhibitory effects of arachidonate upon the volume-sensitive Cl^- current (Table 5.1). This suggests that arachidonate does not have to be metabolised to elicit its effects. The phorbol ester TPA was unable to mimic the effects of arachidonate suggesting that PKC activation is not involved. This hypothesis is further supported by the lack of dependence upon intracellular nucleotides and the lack of current inhibition by oleic acid which can also directly activate PKC (Murakami & Routenburg, 1985). Forskolin was also ineffective at reproducing arachidonate's effects implying an elevation of cyclic AMP levels is not the underlying mechanism. These results suggest that the inhibitory effects of arachidonate appear to be direct ie. does not involve known second messenger systems, protein phosphorylation or conversion of arachidonate to bioactive metabolites. *Cis* unsaturated fatty acids are known to partition into and fluidize membranes (Klausner, Kleinfeld, Hoover & Karnovsky, 1980) changing their physical properties and those of proteins resident in them (eg. ion channels). The observation that oleic acid, another *cis* unsaturated fatty acid, was without effect upon the volume-

sensitive Cl^- conductance suggest that changes in membrane lipid structure are unlikely to mediate the effects of arachidonate. This observation also suggests some degree of selectivity for arachidonate; however, the effects of more fatty acids would need to be investigated to validate this fully. A possible explanation is the existence of a specific fatty acid binding domain of the chloride channels underlying this current, perhaps similar to a putative site that has been identified in the NMDA receptor structure (Petrou, Ordway, Singer & Walsh, 1993).

It has been proposed that fatty acids can 'flip' from one bilayer leaflet to the other and are thus not confined to the side of the membrane to which they are applied, a process that occurs rapidly for unionised fatty acids ($t_{1/2}$ < 2 s) but much slower ($t_{1/2}$ of minutes) for ionised fatty acids (Kamp & Hamilton, 1992). It is thus tempting to speculate that the two phases of inhibition of the volume-sensitive Cl^- current reported in this study are due to unionised and ionised arachidonate traversing the cell membrane and interacting with a site on the cytosolic face of the membrane. Indeed dialysis experiments suggested that arachidonate was effective at inhibiting the volume-sensitive Cl^- conductance from the intracellular side of the membrane. However, internally applied arachidonate did not render the current refractory to subsequent superfusion with external arachidonate (Fig.5.5) indicating that this is unlikely to be the explanation for the two inhibitory phases. Other studies have shown a distinct 'sidedness' of effect of fatty acids implying they do not freely permeate biological membranes (Poling *et al.* 1995; Honoré *et al.* 1994; Zachar & Hurnak, 1994; Anderson & Welsh, 1990) thus it may be that arachidonate can directly modulate the

volume-sensitive Cl^- current in ROS 17/2.8 cells from both sides of the membrane, but with unequal potencies or by different mechanisms.

5.5.3. Comparison with the effects of fatty acids upon other chloride conductances:

Inhibitory effects of arachidonate upon Cl^- currents have previously been observed in human placental brush-border membrane vesicles (Vatish & Boyd, 1993), airway epithelia (Anderson & Welsh, 1990; Hwang, Guggino & Guggino, 1990) and L6 myoblasts (Zachar & Hurnak, 1994). Conversely, arachidonate has also been shown to activate small conductance Cl^- channels in rabbit parietal cells (Sakai, Okada, Morii & Takeguchi, 1992). These experiments were performed using either $^{36}Cl^-$ flux or single channel analysis, thus the whole-cell current kinetics were not investigated. Kubo & Okada (1992) similarly have reported that the volume-sensitive Cl^- current in Intestine 407 epithelial cells is sensitive to blockade by arachidonate but do not mention any kinetic modifications. This block occurred rapidly, reaching steady-state in 10 - 20 s and could be mimicked by oleic acid. This suggests that the mechanism by which arachidonate inhibits the volume-regulatory Cl^- current in Intestine 407 cells differs from that described here in ROS 17/2.8 cells. In human umbilical vein endothelial cells arachidonate was found to have inconsistent effects upon the Cl^- current induced by hypotonic shock, producing either potentiation, inhibition or total lack of effect (Nilius *et al.* 1994).

The effects of arachidonate upon the volume-sensitive Cl^- conductance in ROS 17/2.8 cells we report above are strongly reminiscent of the effects fatty acids upon the

delayed-rectifier K^+ channel. Concomitant inhibition and acceleration of inactivation kinetics of this current by arachidonate and related unsaturated fatty acids have been widely reported in a variety of cell types including neuroblastoma cells, pinealocytes, cardiac cells and Chinese hamster ovary (CHO) cells transfected with cloned mKv1.1 and mKv1.2 K^+ channels (McEvoy, Owen & Garratt, 1995; Garratt & Owen, 1995; Gubitsoi-Klug, Yu, Choi & Gross, 1995; Honoré *et al.* 1994; Poling *et al.* 1994; Rouzaire-Dubois, Gérard & Dubois, 1991). These effects have been suggested to be due to time-dependent open channel block by the polyunsaturated fatty acid.

5.6. Conclusion:

Arachidonate effectively inhibits the whole-cell volume-regulated Cl^- conductance in ROS 17/2.8 cells. This occurs in two distinct phases separated by a latency period of around 120 s, with considerably different IC_{50} values of 10 and 177 μM. The effects of arachidonate appear to be direct as they do not appear to involve second messengers or conversion of arachidonate to a bioactive metabolite.

Chapter 6.

REGULATORY VOLUME DECREASE (RVD) IN RAT OSTEOBLASTIC (ROS 17/2.8) CELLS.

6.1. Background:

Most cell types, including osteoblasts, actively respond to a decrease in extracellular osmolarity with rapid cell swelling that precedes a period of volume regulation where cells attempt to restore their volume to basal levels (Yamaguchi *et al.* 1989). This regulatory volume decrease has been widely shown to involve activation of parallel conductive pathways for K^+ and Cl^-, leading to KCl efflux that is accompanied by osmotically obligated water (for reviews see Hoffman & Simonsen, 1989; Grinstein & Foskett, 1990).

A number of studies have suggested that compounds which can affect the RVD response to hypotonic shock do so as a consequence of inhibitory effects upon the ionic conductances responsible for KCl efflux (Lambert, 1987; Sarkadi *et al.* 1985; Kubo & Okada, 1992). These compounds include Cl^- channel blockers and polyunsaturated fatty acids such as arachidonate. As the volume-sensitive Cl^- current in ROS 17/2.8 cells is effectively inhibited by both the Cl^- channel blockers, NPPB and DIDS (see chapter 3), and also arachidonate (see chapter 5), the effects of these compounds upon the RVD response to hypotonic stimulation were assessed using measurements of cell volume. It has been reported that the RVD response of a variety of cells, including UMR-106-01 osteosarcoma cells, is dependent upon the presence of extracellular Ca^{2+} (Yamaguchi *et al.* 1989). Thus the effects of removal of extracellular Ca^{2+} upon RVD were also investigated in ROS 17/2.8 cells.

6.2. Methods:

Cell volumes were measured as detailed in section 2.4. Cell diameter distribution curves were measured at 30s, 1, 2, 3, 4, 5, 10, 15, 20, 25, 30, 35, 40 and 45 min after dilution of cells into relevant incubation medium. The standard isotonic incubation medium as detailed in section 2.4 consisted of (mM): NaCl, 140; KCl, 5; $MgCl_2$, 10; $CaCl_2$, 1.5; Hepes, 10; D-glucose, 5; bovine serum albumin, 0.1% w/v; pH 7.4 with HCl (300 mosmol l^{-1}). Hypotonic incubation medium was obtained by 50 % v/v dilution with distilled H_2O and supplemented with $CaCl_2$ to maintain extracellular Ca^{2+} at 1.5 mM. The only exception to this was 'Ca^{2+} free incubation medium' which did not contain any $CaCl_2$ but was supplemented with 0.1 mM EGTA. The effects of extracellular Ba^{2+} were also studied and this was added to hypotonic incubation medium as $BaCl_2$.

Cl^- channel blockers were used at 200 μM as this was approximately twice the calculated IC_{50} values for NPPB and DIDS (see chapter 3). DPC was used at a similar concentration so that results from the three blockers would be directly comparable.

Where the effects of the polyunsaturated fatty acids, arachidonic, oleic and elaidic acids upon volume regulation were investigated, the cells were pre-incubated with the relevant fatty acid at 40 μM under isotonic conditions for 5 min prior to dilution into hypotonic incubation medium supplemented with 40 μM fatty acid. This ensured that any inhibitory effects would have time to occur prior to the hypotonic challenge, as it was found that the block by arachidonate developed over a period of approximately 4

min (see chapter 5). The value of 40 μM was chosen as it far exceeds the calculated IC_{50} value of 10 μM for arachidonate (see chapter 5), and thus would hopefully ensure that if any fatty acid was metabolised or degraded by enzymes over the 45 min period of the experiment there would still be an effective inhibitory concentration throughout.

6.3. Results:

6.3.1. Effects of hypotonic shock upon ROS 17/2.8 cell volume:

As shown in figure 6.1 under isotonic conditions ROS 17/2.8 cells maintained a constant cell volume over the 45 min duration of the experiment that was close to their basal starting volume. However, dilution into hypotonic medium produced rapid (faster than the 30 s required to load the cells into the mastersizer sample cell) cell swelling such that the cells were swollen to over twice their basal volume. This preceded a period of volume regulation where the cells attempted to return to their normal size. The majority of this process occurred during the first 10 min subsequent to the hypotonic challenge. Even at the end of the 45 min duration of the experiment the cells had not been able to return to their basal volume but the mean relative cell volume had fallen from 2.30 ± 0.21 (n = 6) to 1.29 ± 0.07.

6.3.2. Effects of Cl^- channel blockers:

The effects of the Cl^- channel blockers DIDS and NPPB upon the regulatory volume decrease response of ROS 17/2.8 cells to hypotonic shock is shown in figure 6.2. Upon dilution into hypotonic incubation medium cells still rapidly increased their volume to in excess of twice control values. The period of volume regulation that followed this effect under control conditions was however dramatically impaired such that at the end of the experiment cells were still swollen to approximately twice their basal volume (mean relative cell volumes at 45 min: NPPB, 1.77 ± 0.02, n = 4; DIDS, 1.98 ± 0.13, n = 4). DPC at 200 μM was a totally ineffective inhibitor of the volume regulatory response of these cells (Fig. 6.3; non-significant compared to hypotonicity alone at 45 min, Student's unpaired t-test).

6.3.3. Effects of removal of extracellular Ca^{2+} or inclusion of Ba^{2+}:

Incubation of ROS 17/2.8 cells with Ca^{2+}-free hypotonic medium still produced rapid cell swelling that preceded a period of volume regulation (Fig. 6.4). There was however some impairment of this process compared to control hypotonic medium (mean relative cell volume at 45 min; control hypotonic, 1.29 ± 0.07, n =6; Ca^{2+}-free hypotonic, 1.52 ± 0.05, n = 4). A similar profile was observed if 5 mM Ba^{2+} was included in control hypotonic incubation medium (Fig. 6.4; mean relative cell volume at 45 min; 5 mM Ba^{2+} hypotonic medium, 1.44 ± 0.03, n = 4).

6.3.4. Effects of arachidonic, oleic or elaidic acids:

As shown in figure 6.5 dilution of ROS 17/2.8 cells into hypotonic medium supplemented with 40 μM arachidonic acid (subsequent to a 5 min pre-incubation period with arachidonate under isotonic conditions) resulted in rapid cell swelling to levels comparable to those under control hypotonic conditions (mean relative cell volume at 30 s; control, 2.30 ± 0.21, n = 6; 40 μM arachidonate, 2.25 ± 0.09, n 4). There was however very little change in relative cell volume over the 45 min duration of the experiment such that at the conclusion of the sample period cells were still swollen to 2.30 ± 0.07 (n = 4) times basal volume; in the absence of arachidonate cells regulated their volume back to 1.29 ± 0.07 (n = 6) times basal volume over 45 min.

Experiments in which the volume regulatory response to hypotonic shock was investigated in the presence of two other polyunsaturated fatty acids, oleic and its *trans* isomer elaidic acids, showed similar profiles. Neither fatty acid appeared to exert any inhibitory effect upon the reduction in cell volume that occurred subsequent to cell swelling (fig. 6.5). At the end of the experiment (45 min) the mean relative cell volumes were 1.28 ± 0.03 (n = 4) for 40 μM oleic acid and 1.26 ± 0.04 (n = 4) for 40 μM elaidic acid; these values are non-significant (Student's unpaired t-test with bonferroni correction) compared to the control value of 1.29 ± 0.07 under normal hypotonic conditions.

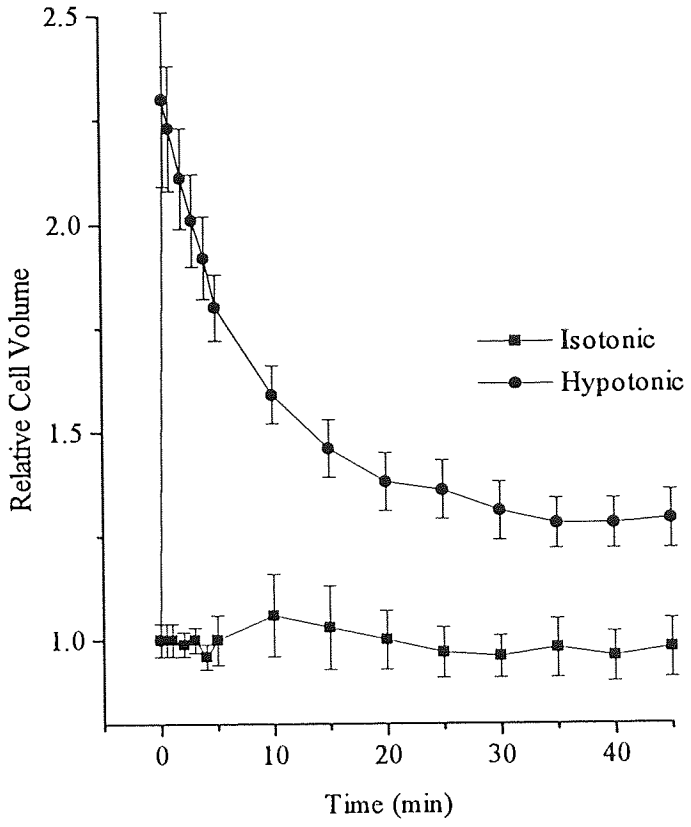

Figure 6.1. Effects of hypotonicity upon cell volume of ROS 17/2.8 cells. *Cells diluted into 50 % (150 mosmol l^{-1}) hypotonic incubation medium (●) at time zero. Cell volumes were measured at indicated intervals and expressed relative to control value as detailed in methods. Symbols represent the mean of 4 - 6 observations with S.E.M. (vertical bars). The effects of isotonicity (300 mosmol l^{-1}) are shown for comparison (■).*

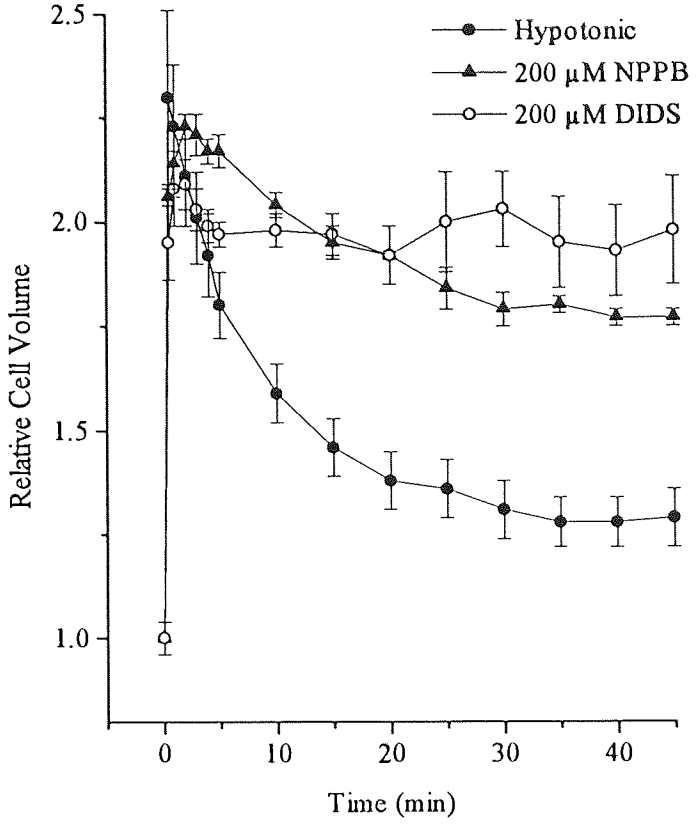

Figure 6.2. Effects of NPPB (▲) and DIDS (○) upon the regulatory volume decrease (RVD) of ROS 17/2.8 cells in response to hypotonic shock. *Effects of hypotonicity alone are shown for comparison (●). Cells were diluted into either control hypotonic solution or hypotonic solution containing 200 μM DIDS or NPPB at time zero. Cell volumes were measured at times indicated; symbols represent the mean of 4 - 6 observations with S.E.M. (vertical bars).*

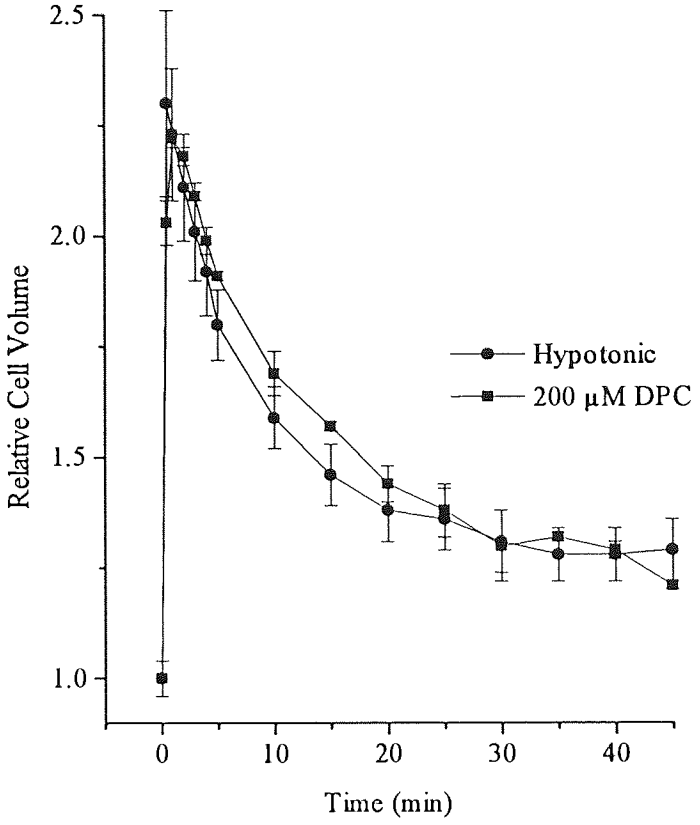

Figure 6.3. Effects of DPC (■) upon the regulatory volume decrease (RVD) of ROS 17/2.8 cells in response to hypotonic shock. *Effects of hypotonicity alone are shown for comparison (●). Cells were diluted into either control hypotonic solution or hypotonic solution containing 200 µM DPC at time zero. Cell volumes were measured at times indicated; symbols represent the mean of 4 - 6 observations with S.E.M. (vertical bars).*

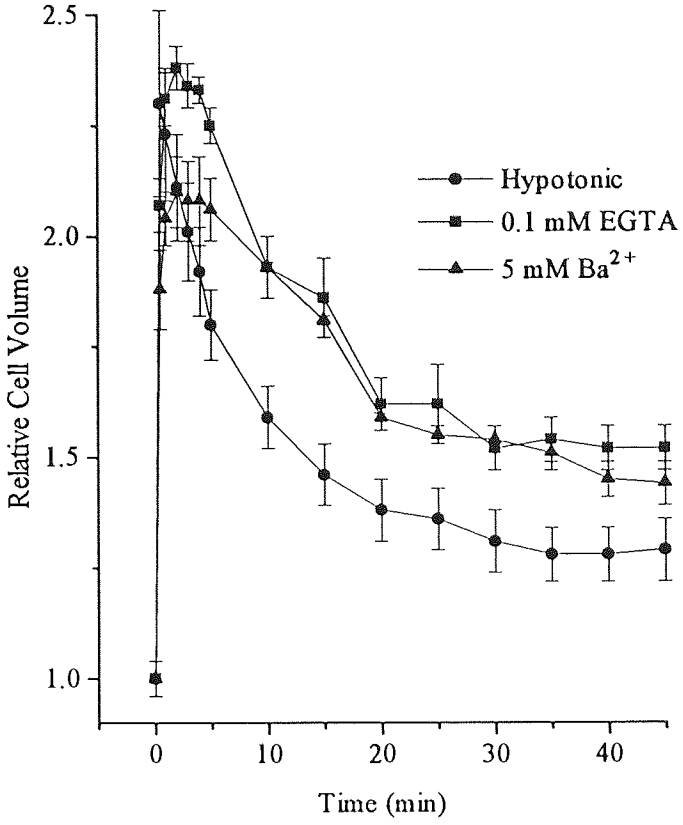

Figure 6.4. Effects of removal of extracellular Ca^{2+} (■) or inclusion of 5 mM Ba^{2+} (▲) in the incubation medium upon the regulatory volume decrease (RVD) response of ROS 17/2.8 cells. *For removal of extracellular Ca^{2+}, $CaCl_2$ was absent from the hypotonic incubation medium and replaced with 0.1 mM EGTA. Ba^{2+} was added as $BaCl_2$ to otherwise standard hypotonic incubation medium. Symbols represent the mean with S.E.M. (vertical bars) of 4 - 6 observations.*

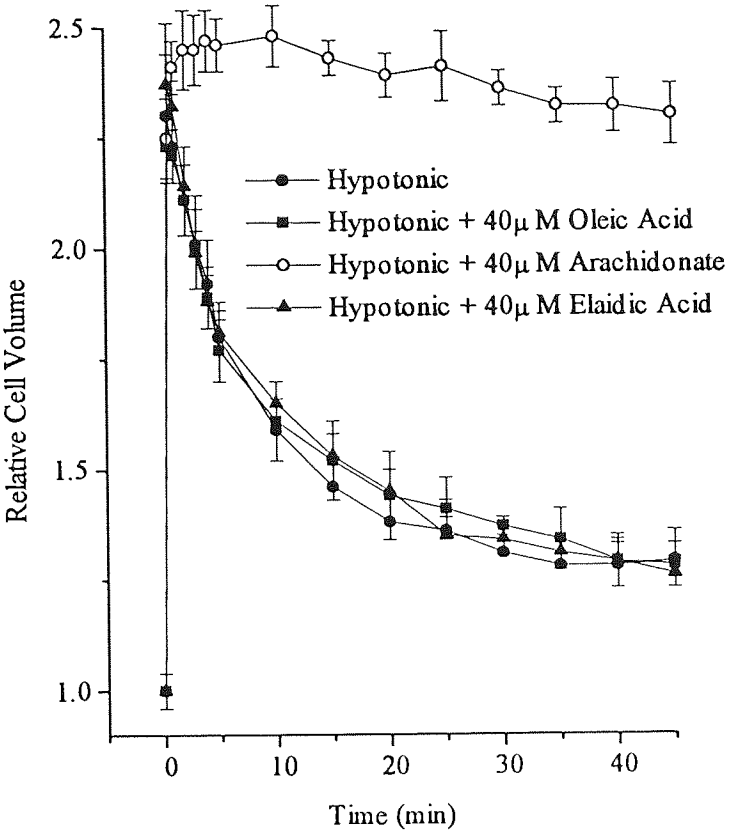

Figure 6.5. Effects of the polyunsaturated fatty acids, arachidonic (○), oleic (■) and elaidic (▲) acids upon the regulatory volume decrease of ROS 17/2.8 cells in response to a reduction in external osmolarity. *Cell were pre-incubated with the fatty acid under isotonic conditions for 5 min prior to dilution into hypotonic incubation medium supplemented with the relevant fatty acid at 40 μM. Cell volumes were measured at the time intervals indicated. Effects of hypotonicity alone (●) are shown for comparison. Symbols represent the mean with S.E.M. (vertical bars) of 4 - 6 experiments.*

6.4. Discussion:

6.4.1. Effects of hypotonicity:

As shown in figure 6.1 ROS 17/2.8 cells responded to hypotonic shock with cell swelling that was followed by a period of volume regulation; the majority of this regulatory volume decrease (RVD) occurred in the first 10 min subsequent to the reduction in extracellular osmolarity. A similar effect and profile has been demonstrated by the clonal osteosarcoma cell line UMR 106-01 (Yamaguchi *et al.* 1989). It is interesting to note that ROS 17/2.8 cells swelled to 2.30 ± 0.21 times their basal cell volume in response to a 50 % (300 mosmol l^{-1} to 150 mosmol l^{-1}) reduction in the osmolarity of the incubation medium, close to the expected value for a perfect osmometer of exactly 2.

6.4.2. Effects of Cl^- channel blockers:

The Cl^- channel blockers NPPB and DIDS are effective inhibitors of the volume-sensitive Cl^- conductance in ROS 17/2.8 cells (see chapter 3); DPC, another blocker, was however ineffectual even at 500 μM. As shown by figures 6.2 and 6.3, NPPB and DIDS substantially impaired the RVD response of ROS 17/2.8 cells to hypotonic shock, whereas DPC was totally ineffective. This suggests that the volume-regulated Cl^- current in ROS 17/2.8 cells may have an important role in the RVD process. This conclusion assumes that the blockers exhibit selectivity for the ion channel. Particularly with the stilbene-derivative blockers such as DIDS, it has been shown that at high

concentrations they will block other Cl^--transporting proteins (Greger, 1990). Indeed it has been shown that DIDS inhibits the Cl^-/HCO_3^- exchanger in mouse and rat bone organ culture systems leading to inhibition of bone resorption (Klein-Nulend & Raisz, 1989; Hall & Chambers, 1989). However, this type of non-specific effect has not been reported for NPPB and other carboxylate analogues, thus it seems unlikely that the effects of these blockers upon RVD is reliant upon inhibition of non-ion channel Cl^--transporting proteins.

6.4.3. Effects of removal of extracellular Ca^{2+} or inclusion of Ba^{2+}:

The effects of removal of extracellular Ca^{2+} (and replacement with 0.1 mM EGTA) or inclusion of 5 mM BaCl in the incubation medium produced RVD profiles that were almost identical (Fig. 6.4). Impairment of the RVD response is clearly evident but not as pronounced as that produced by DIDS and NPPB. This suggests that there is some dependence of the RVD process in ROS 17/2.8 cells upon extracellular Ca^{2+}, a finding that agrees with that documented in UMR 106-01 cells where volume-sensitive Ca^{2+}-permeating pathways have been clearly demonstrated (Yamaguchi *et al.* 1989). Though increased Cl^- permeability is known to be a requisite for volume regulation (Grinstein & Foskett, 1990) it must be accompanied by a parallel K^+-conductive pathway, leading to KCl efflux and associated osmotically obligated water. As the volume-sensitive Cl^- current in these cells is independent of intracellular Ca^{2+} (see chapter 3) this may suggest that the K^+ efflux pathway is Ca^{2+}-dependent. This hypothesis is supported by the similarity in the inhibitory effect of Ba^{2+}, an inorganic cation which is known to block a variety of K^+ conductances, including Ca^{2+}-sensitive

K^+ channels (Hille, 1992). As removal of extracellular Ca^{2+} or inclusion of Ba^{2+} does not produce inhibition of RVD to the same extent as the effective Cl^- channel blockers this may suggest that there is incomplete blockade by Ba^{2+}, or that K^+ efflux is still occurring via a Ba^{2+}-insensitive or Ca^{2+}-independent pathway.

6.4.4. Effects of polyunsaturated fatty acids:

As shown in figure 6.5, arachidonate effectively inhibits the RVD exhibited by ROS 17/2.8 cells in response to a reduction in extracellular osmolarity. Oleic and elaidic acids, which were ineffective inhibitors of the volume-sensitive Cl^- conductance (see chapter 5), were without effect upon RVD. Thus inhibition of RVD by arachidonate may occur as a consequence of its inhibitory effects upon the volume-sensitive Cl^- current. However as K^+ efflux is also required to effect an RVD response it is not possible to exclude any as yet unknown inhibitory effects of arachidonate upon the K^+ conductances that facilitate this K^+ efflux in ROS 17/2.8 cells. A stretch and volume-sensitive K^+ current that is suggested to fulfil this role has been characterised in G292 osteoblast-like cells, however the effects of fatty acids were not investigated (Davison, 1993). Inhibitory effects of arachidonic and other fatty acids upon RVD have previously been reported in Ehrlich ascites tumour cells and Intestine 407 cells (Lambert, 1987; Kubo & Okada, 1992), in both cases this effect was either supposed (Ehrlich ascites cells) or demonstrated (Intestine 407) to be due to inhibitory effects upon the volume-induced Cl^- efflux pathway.

6.5. Conclusion:

Effective inhibitors of the volume-sensitive Cl^- current in ROS 17/2.8 cells (DIDS, NPPB and arachidonate) are also effective inhibitors of the RVD response of these cells to hypotonic shock. These results strongly intimate that this conductance has a vital role in the RVD process of ROS 17/2.8 cells. As the degree of RVD inhibition produced by DIDS, NPPB and arachidonate was far more substantial than that exhibited upon removal of extracellular Ca^{2+} or by Ba^{2+}, this may suggest that Cl^- efflux is the rate-determining factor in the RVD response. In light of the complete correlation in the pharmacologies of the volume-sensitive Cl^- current and the RVD response of ROS 17/2.8 cells, measurements of cell volume may provide a useful method to investigate possible modulatory effects of drugs upon the volume-regulated Cl^- current present in these cells.

Chapter 7.

BIOCHEMICAL AND ELECTROPHYSIOLOGICAL EFFECTS OF VASOPRESSIN UPON L6 SKELETAL MYOCYTES

7.1. Background:

The nonapeptide, vasopressin (arginine vasopressin), has been shown to elicit a variety of physiological effects acting as a potent vasoconstrictor, an antidiuretic hormone and a neurotransmitter. Cellular responses to vasopressin are mediated by two broad classes of receptor; the V_1 receptor which couples to phospholipase C (PLC) and induces breakdown of phosphoinositides to yield a variety of second messengers including inositol 1,4,5-trisphosphate ($InsP_3$) and diacylglycerol (Michell, Kirk & Billah, 1979) and the V_2 receptor which is coupled to adenylate cyclase (Orloff & Handler, 1962).

The biochemical effects of vasopressin have been widely characterised in a variety of cell types, however, only recently has any electrophysiological investigation of the peptide's effects been undertaken. In the aortic smooth muscle cell line A7r5 vasopressin has been shown to modulate the spontaneous electrical activity of these cells at nanomolar concentration (Van Renterghem, Romey & Lazdunski, 1988). This occurs as a result of the action of vasopressin upon three different ionic conductances. Vasopressin was found to activate a Ca^{2+}-sensitive K^+ conductance, inhibit the L-type Ca^{2+} current and also induce activation of a non-selective cation conductance. A similar effect has been reported in primary rat hepatocytes where vasopressin increases the cytosolic Na^+ concentration via activation of a Ca^{2+}-permeable non-selective cation conductance (Lidofsky, Xie, Sostman, Scharschmidt & Fitz, 1993). Further investigation of the effect of vasopressin upon A7r5 cells under conditions when other currents were suppressed, have also shown it activates a small amplitude Ca^{2+} entry

pathway believed to be due to receptor-operated Ca^{2+} channels (Van Renterghem & Lazdunski, 1994).

The effects of vasopressin upon skeletal muscle are largely unknown though some studies have suggested vasopressin could influence carbohydrate metabolism (Hems & Whitton, 1980; Wakelem & Pette, 1982). The L6 cell line, derived from rat thigh muscle (Yaffe, 1968), is a clonal cell line that has retained the characteristics of skeletal muscle. The cells possess a variety of receptors, such as those for calcitonin gene-related peptide (CGRP; Poyner, Andrew, Bose & Hanley, 1992), and also functional vasopressin V_1 receptors (Wakelam, Patterson & Hanley, 1987). The transduction mechanism of this receptor in L6 cells has been extensively characterised, and it has been demonstrated that vasopressin produces stimulation of inositol phosphate production and a biphasic increase in the cytosolic free Ca^{2+} concentration (Wakelam *et al.*, 1987; Teti, Naro, Molinaro & Adamo, 1993). In this chapter the electrophysiological consequences of vasopressin treatment have been investigated in L6 skeletal myocytes.

7.2. Methods:

Measurements of inositol phosphate production and intracellular membrane potential recording were performed as detailed in sections 2.2 and 2.3.1 respectively.

Patch clamp recordings were obtained using the whole-cell and cell-attached configurations as described in experimental procedures (section 2.3.3). The normal

'quasiphysiological' solutions used in these experiments consisted of (mM): extracellular (bathing) solution; NaCl 140, $CaCl_2$ 2, $MgCl_2$ 1, $KHCO_3$ 5, Hepes 10, glucose 17; intracellular (pipette) solution; KCl 145, KOH 7, Hepes 10, EGTA 0.05, Na_2ATP 2, Na_2GTP 0.5 (pH of both solutions was adjusted to pH 7.2). Any modifications to these solutions are detailed as appropriate.

7.3. Materials:

Vasopressin, heparin, inositol 1,4,5-trisphosphate ($InsP_3$), apamin and caffeine were all dissolved into either water and subsequently diluted into the test solution, or directly into the test solution. All compounds were obtained from Sigma (USA).

7.4. Results:

7.4.1. Inositol phosphate accumulation:

As shown in figure 7.1 treatment of L6 cells with 1 μM vasopressin for 30 min produced a significant increase in the incorporation of [^{3}H]-inositol into inositol phosphates. Calcitonin gene-related peptide (CGRP), a neuropeptide whose receptors have been shown to couple to adenylate cyclase in this cell line (Poyner *et al.* 1992), was without significant effect upon basal levels of inositol phosphate production.

7.4.2. Intracellular recording:

The resting membrane potential of L6 cells immediately subsequent to cell penetration was -70.8 ± 1.1 mV (n = 48). This value agrees closely with that reported by Kidokoro (1975) of -71 ± 3 mV.

The membrane potential response to 1 μM vasopressin is shown in figure 7.2A. Vasopressin induced a sharp hyperpolarisation that preceded a period of slow repolarisation back toward resting potential. In 6 cells tested, vasopressin produced a hyperpolarisation from -71.2 ± 1.3 mV to -92.8 ± 2.9 mV. In 3/6 cells the depolarising phase of the response continued past the initial resting membrane potential and was accompanied by phasic hyperpolarising 'spikes' as shown in figure 7.2B.

7.4.3. Whole-cell patch-clamp recording:

7.4.3.1. Effects of vasopressin:

To study the effects of vasopressin upon membrane currents in L6 skeletal myocytes, cells were equilibrated with 'quasiphysiological' solutions (detailed in section 7.2) and voltage-clamped at 0 mV. This potential was chosen as the membrane potential response to vasopressin, as measured by intracellular recording, was a hyperpolarisation to approximately -90 mV (~ potassium reversal potential, E_K). This suggested that the current induced by vasopressin would be carried mainly by K^+ ions. Voltage-clamping at 0 mV provides a substantial outward electrochemical gradient for

K^+ (E_K = -86 mV under these conditions) and avoids any possible contamination from Cl^- currents as E_{Cl} = 0 mV. Under these conditions there was normally a small outward holding current, in 45 cells with a mean cell capacitance of 57 ± 4 pF the mean holding current was 118.0 ± 16.5 pA.

As shown in figure 7.3A, at 0 mV 1 μM vasopressin produced a rapid but transient increase in outward current. In 25 cells with a mean cell capacitance of 52 ± 4 pF the mean peak current was 3449.2 ± 496.8 pA (77.8 ± 11.5 pA pF^{-1}). This current had an onset within 5 s (mean 3.8 ± 0.4 s, n = 25) of commencing vasopressin superfusion, reached peak in 17.1 ± 3.0 s and had returned to baseline current levels after 73.5 ± 8.3 s. A small number of cells (6/25) responded to vasopressin with more than a single transient current response. In 2 cells, phasic, transient outward currents were observed that continued after cessation of vasopressin superfusion (Fig 7.4). When L6 cells were voltage-clamped at -100 mV (negative to E_K) the current reversed direction and became inward (Fig 7.3B). In 2 cells the mean inward current induced by vasopressin at -100 mV was -1361.1 pA (-28.3 pA pF^{-1}).

7.4.3.2. Assessment of the reversal potential of the current induced by vasopressin:

As the current response to vasopressin was transient (see Fig 7.1) it was difficult to assess the current reversal potential (E_{rev}) using a ramp voltage-clamp stimulus. To overcome this an alternating voltage-clamp pulse protocol was employed to assess the current response rapidly at three different potentials (shown in figure 7.5A). Cells were held at -50 mV, and stepped to -100 mV and 0 mV for 500 ms, at 5 s intervals (0.2

Hz). The current at each potential was measured at the peak of the response and the current-voltage relationship (I - V curve) was plotted. The three points were joined with a straight line fitted by linear regression and the zero current potential evaluated. Using this method the estimated E_{rev} was -78.9 ± 1.0 mV (n = 6), under the assumption that the I - V curve was linear.

7.4.3.3. Effects of changes in extracellular K^+ concentration upon the reversal potential:

Using the method for assessing E_{rev} as described in 7.4.3.2, the effect of changes in the extracellular K^+ ion concentration were investigated. This was achieved by substituting NaCl in the standard 'quasiphysiological' extracellular solution with KCl. When the extracellular K^+ concentration was raised to 40 mM and 150 mM total, E_{rev} was estimated to be -28.7 ± 3.3 mV (n = 4) and +3.4 ± 2.8 mV (n = 5) respectively. This corresponds to a 55 mV change in E_{rev} for a 10 fold change in the extracellular K^+ concentration (55 mV decade^{-1}; Fig. 7.6). This is close to the Nernstian predicted value of 58 mV decade^{-1} for a perfectly K^+-selective conductance under these conditions.

7.4.3.4. Effects of intracellular dialysis with $InsP_3$ and heparin upon cell membrane current and the vasopressin response:

In light of the well characterised production of $InsP_3$ in response to vasopressin, the membrane current effects of this second messenger molecule were investigated on the cells. To measure whole-cell currents at the instant that $InsP_3$ entered the cell, the

holding potential was set to 0 mV in the cell-attached configuration prior to establishing whole-cell recording mode. Inclusion of 10 μM $InsP_3$ into the patch pipette solution elicited an outward current in 6/14 cells. The mean peak current was 2270.1 pA (60.5 ± 8.7 pA pF^{-1}) occurring 18.6 ± 2.3 s after establishing whole-cell mode. In 5/6 responding cells the current response to intracellular $InsP_3$ consisted of more than a single 'spike', and as shown in figure 7.7A in one cell the response was phasic. Of the 8 cells that were unresponsive to $InsP_3$ dialysis, 5 cells were subjected to a subsequent vasopressin challenge. All cells so tested responded to 1 μM vasopressin with large amplitude (mean peak current, 2023.9 ± 592.9 pA), transient outward currents (Fig. 7.7B).

Heparin is a well characterised competitive antagonist of $InsP_3$ acting by binding to its receptor (Worley, Baraban, Supattapone, Wilson & Snyder, 1987). Thus, the effects of intracellular dialysis with 0.5 mg ml^{-1} and 5 mg ml^{-1} heparin upon the vasopressin current response were investigated. At both concentrations of heparin tested vasopressin still elicited large amplitude, transient increases in membrane conductance (mean peak currents: 0.5 mg ml^{-1}; 3149.6 ± 651.4 pA, n = 6; 5 mg ml^{-1}, 2102.8 ± 219.0 pA, n = 4).

7.4.3.5. Effects of removal of extracellular Ca^{2+} and increasing intracellular EGTA upon the vasopressin-induced membrane response:

When the EGTA concentration of the pipette solution was raised from 0.05 mM to 10 mM the current response to 1 μM was virtually abolished (Fig. 7.8A). In 4 cells tested

the mean peak current only amounted to 29.3 ± 22.9 pA (0.3 ± 0.2 pA pF^{-1}) compared to the control value of 3427.7 ± 496.8 pA (n = 25).

To assess the effects of removing extracellular Ca^{2+} upon the vasopressin response without significantly depleting intracellular stores, cells were bathed in normal 'quasiphysiological' extracellular solution and challenged with vasopressin and 'Ca^{2+}-free' extracellular solution simultaneously. In 8 cells tested with 1 μM vasopressin only a single cell responded with outward of only 19.6 pA. In 2 cells there was a notable reduction in the holding current (Fig. 7.8B) upon commencing superfusion with vasopressin under Ca^{2+}-free conditions. Of the 7 cells that did not exhibit any current response to vasopressin under Ca^{2+}-free conditions, 6 cells were subsequently challenged with 1 μM vasopressin under normal extracellular conditions (i.e. extracellular solution containing 2 mM $CaCl_2$). This challenge routinely occurred 20 s after commencing vasopressin superfusion under Ca^{2+}-free conditions. This time interval should have been sufficient to allow the cell to respond, as under control conditions currents reached their peak values in 17.1 ± 3.0 s (n = 25). Of the 6 cells tested in this fashion, replacing extracellular Ca^{2+} when 1 μM vasopressin was still present in the bath produced large transient outward currents in all 6 cells (see Fig. 7.8B). The mean peak current was 3494.5 ± 456.9 pA (n = 6) occurring 12.6 ± 2.4 s after commencing superfusion.

7.4.3.6. Effects of caffeine and ionomycin upon membrane currents in L6 cells:

Caffeine is known to release Ca^{2+} from intracellular stores sensitive to both ryanodine (Endo, 1985) and $InsP_3$ (Komori & Bolton, 1991; Loirand, Grégoire & Pacaud, 1994). In 7/9 cells challenged with extracellular application of 30 mM caffeine large outward currents were observed (Fig. 7.9A). The mean peak current was 3385.5 ± 824.2 pA, occurring 15.1 ± 2.7 s after onset of caffeine superfusion.

The Ca^{2+} ionophore, ionomycin, was also able to elicit large amplitude, outward currents in all of 7 cells tested (mean peak current 6073.0 ± 1213.1 pA). As shown in figure 7.9B the current response to 5 μM ionomycin was rapid and stayed relatively constant for the duration of ionomycin superfusion. The reversal potential of the ionomycin-induced current at steady state assessed using a ramp voltage-clamp stimulus was -77.0 ± 1.7 mV (n = 6; Fig. 7.9C).

7.4.3.7. Effects of apamin upon membrane currents elicited by 1 μM vasopressin:

The honeybee venom, apamin, is a potent and selective inhibitor of the small conductance (SK) class of Ca^{2+}-dependent K^+ channels (Hughes, Romey, Duval, Vincent & Lazdunski, 1982). To assess if this channel was responsible for the current responses elicited by vasopressin, L6 cells were challenged with 1 μM vasopressin in the presence of 500 nM apamin. Of 6 cells tested, all responded with large outward currents (Fig. 7.10; mean peak current 3385.5 ± 824.2, n = 6) that reached peak rapidly after onset of vasopressin superfusion (mean time to peak 10.5 ± 1.1 s).

7.4.4. Single channel recording:

To isolate the channel underlying the currents induced by vasopressin in L6 cells, cell-attached recordings were made with patch pipettes filled with normal extracellular bathing solution. As shown in figure 7.11, there was substantial single channel activity that commenced rapidly following the onset of vasopressin superfusion. These single channel openings are more clearly visible in figure 7.12. In all cells subjected to a vasopressin challenge (9/9) this increased activity was transient and had subsided after around 60 s even though vasopressin was still present in the superfusing solution. In some patches there were clear, slow fluctuations in the background holding current that occurred subsequent to the vasopressin challenge. These fluctuations, which probably represented changes in the membrane potential of the attached cell, made accurate determination of the single channel amplitude difficult. However, when the pipette potential was changed from a depolarising potential (-60 mV; patch potential = cell resting membrane potential - pipette potential) to a hyperpolarising one (+60 mV) the current did change direction (from outward to inward). The single channel amplitude estimates from these recordings are shown in figure 7.13, and correspond to an estimated single channel conductance (γ) of approximately 20 pS.

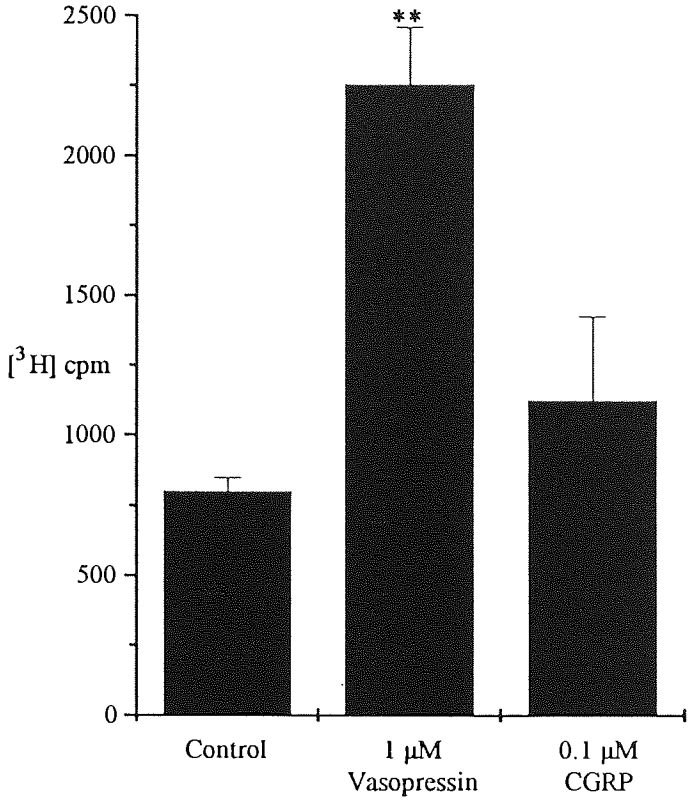

Figure 7.1. Effects of 1 μM vasopressin and 0.1 μM calcitonin gene-related peptide (CGRP) upon inositol phosphate production in L6 skeletal myocytes. *Cells were loaded with [^{3}H]-inositol for 24 hr and pre-incubated with 10 mM LiCl prior to 30 min drug challenge. Cells were assayed as detailed in 'experimental procedures'. Column represent the means of 4 experiments, each performed in triplicate, with S.E.M. shown by vertical bars. ** denotes $p < 0.005$ compared to control (Student's unpaired t-test).*

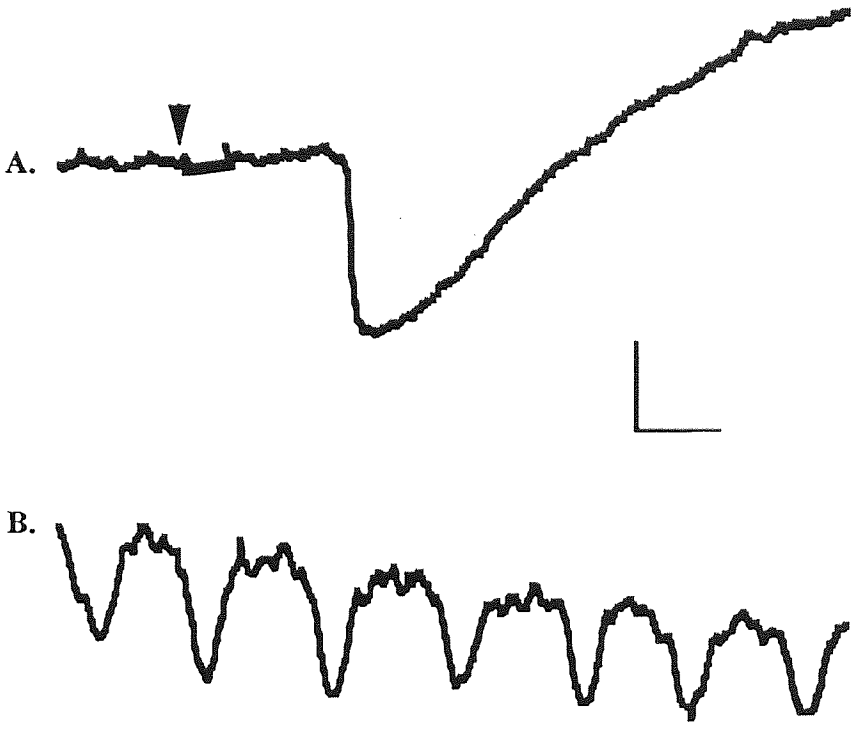

Figure 7.2. Effects of 1 μM vasopressin upon membrane potential of L6 skeletal myocytes. *A, biphasic response to vasopressin (added at arrow) consisting of a rapid hyperpolarisation followed by a depolarising phase (data from a single cell representative of 5 other experiments). B, transient hyperpolarising bursts that accompanied the depolarising phase of the vasopressin response (observed in 3/6 cells; vasopressin added 10 min prior to start of record). Resting potentials; A, -77 mV; B, -69 mV. Scale bar: vertical 10 mV (hyperpolarisation downwards), horizontal 1 min.*

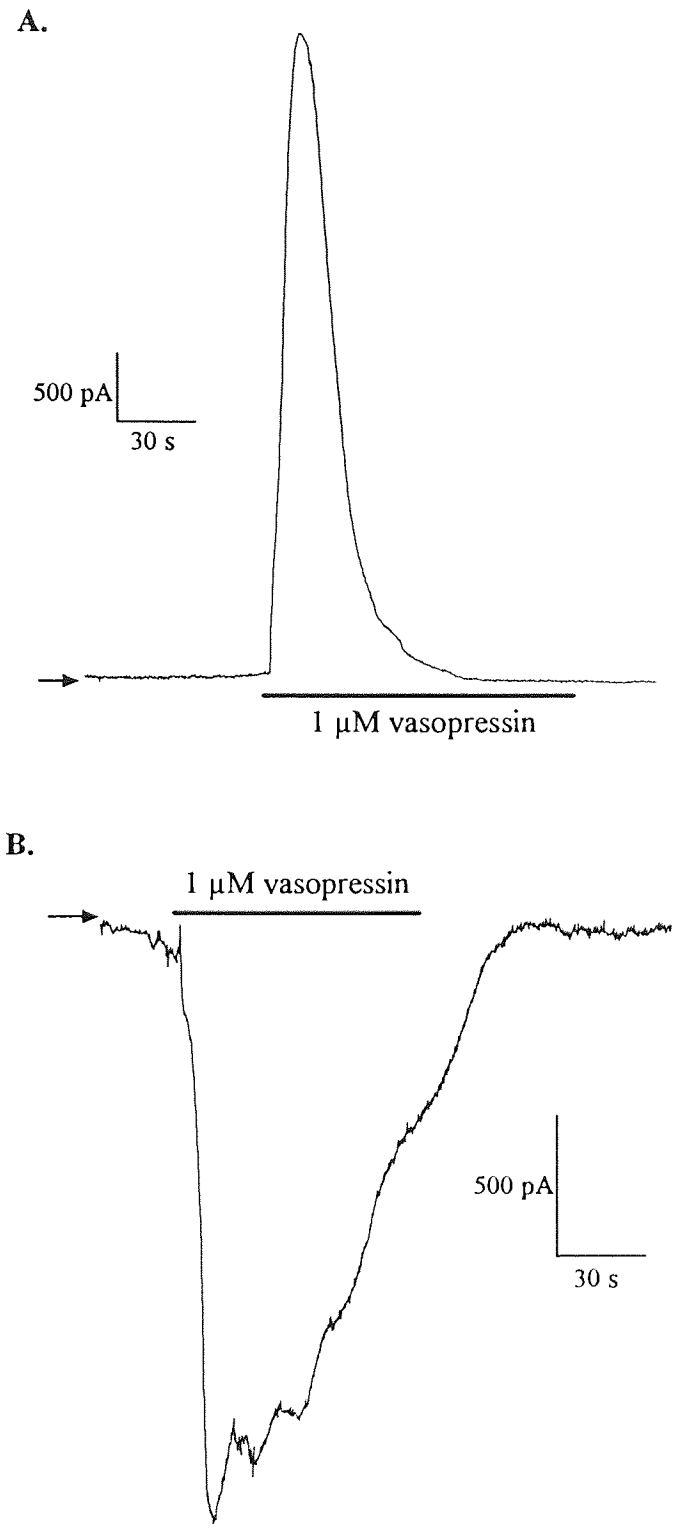

Figure 7.3. Effects of vasopressin upon membrane current in single L6 skeletal myocytes. *A, currents recorded in a single cell equilibrated with quasiphysiological*

solutions, voltage-clamped at 0 mV, prior and subsequent to addition of 1 μM vasopressin. B, current recorded in a cell voltage-clamped at -100 mV (E_K = -86 mV). Duration of vasopressin exposure indicated by solid bars, horizontal arrows denote zero current levels. Note the transient nature of the current response even though vasopressin was still present in the perfusion bath. Data representative of 25 (A) and 2 (B) similar experiments.

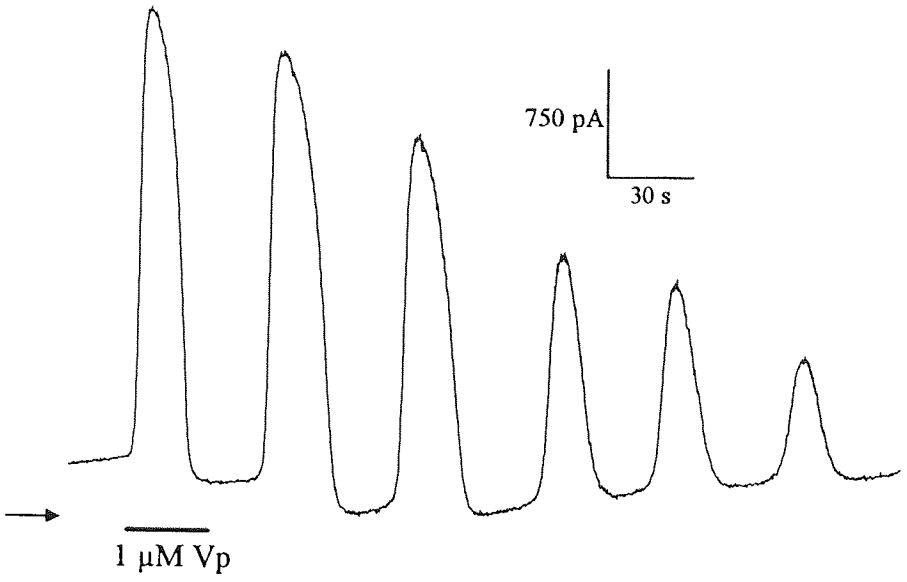

Figure 7.4. Multiple phasic current responses to 1 μM vasopressin in L6 skeletal myocyte. *Cell equilibrated with standard 'quasiphysiological' solutions was superfused with 1 μM vasopressin (Vp) as indicated by the solid bar. Note the current responses continue after cessation of vasopressin exposure. Horizontal arrow indicates zero current level; data from a single cell representative of 5 other observations.*

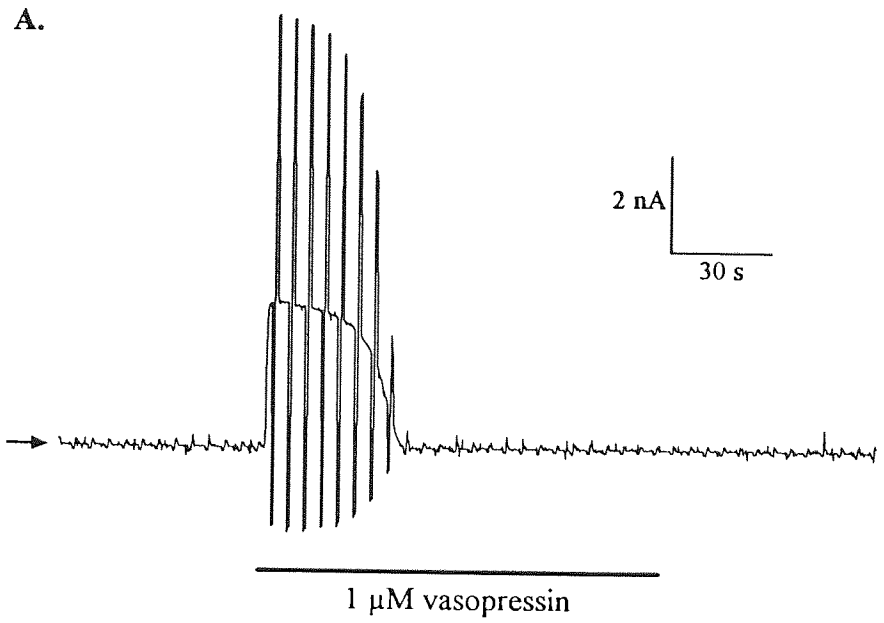

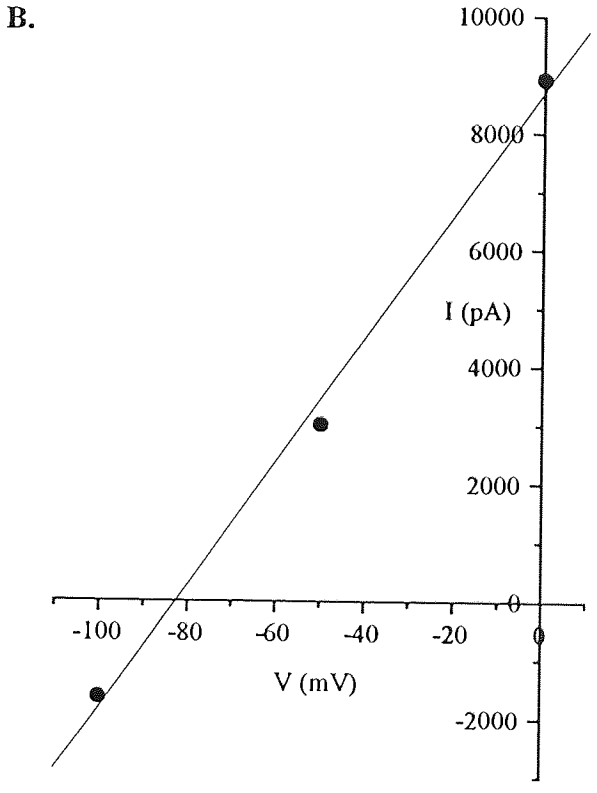

Figure 7.5. Assessment of the reversal potential (E_{rev}) of the current activated by 1 μM vasopressin in L6 skeletal myocytes. A, current responses to an alternating step

voltage-clamp protocol to 0 and -100 mV from a holding potential of -50 mV, applied at 5 s intervals to single L6 cell equilibrated with standard 'quasiphysiological' solutions. 1 μM vasopressin applied as indicated by solid bar, zero current level denoted by horizontal arrow. B, current-voltage relationship for peak currents elicited by vasopressin as shown in A. Line shown was fitted by linear regression (Equation Y = 8703.6 + (105.32 x X), R = 0.998) and gives estimated reversal potential (E_{rev}) of -82.6 mV, close to that predicted by Nernstian theory of -86 mV under these conditions. Data representative of 5 similar experiments.

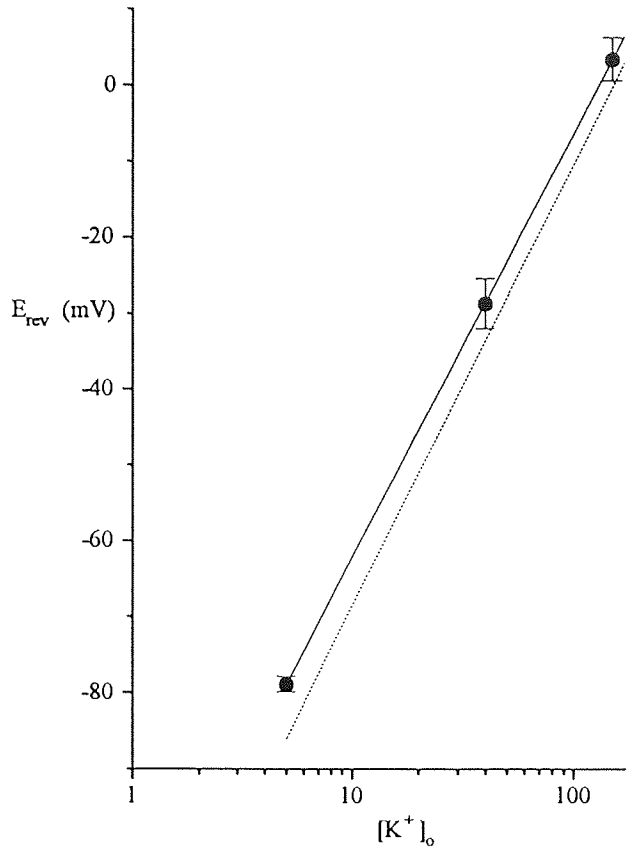

Figure 7.6. Effects of extracellular K^+ concentration changes upon the vasopressin-induced current reversal potential (E_{rev}) in L6 skeletal myocytes. *Reversal potentials determined as shown in Fig. 7.5 with extracellular bathing solutions containing 5, 40 and 150 mM K^+. This was achieved by replacing NaCl with KCl in normal 'quasiphysiological' bathing solution. Each symbol represents the mean of 4 - 6 observations with the S.E.M. (vertical bars). The line is a linear fit with a 55 mV decade^{-1} slope. The theoretical Nernstian prediction is shown by the dotted line for comparison and has a slope of 58 mV decade^{-1}.*

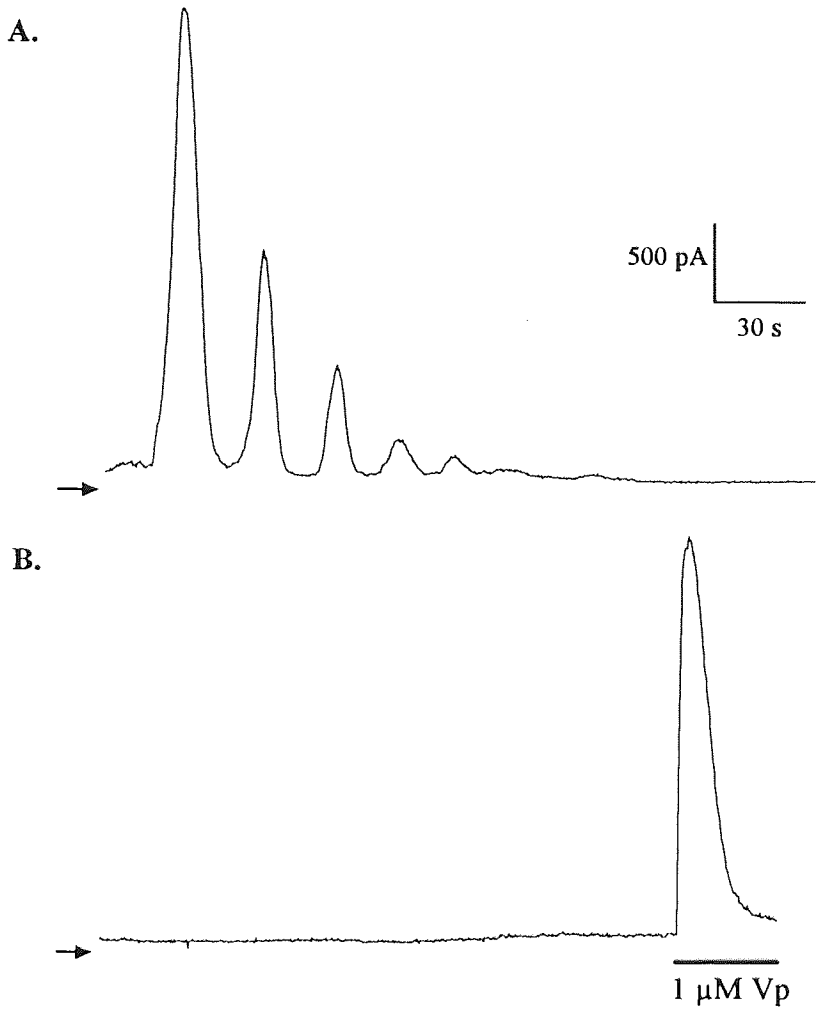

Figure 7.7. Effects of intracellular dialysis with $InsP_3$ upon membrane current responses of L6 skeletal myocytes. *A, multiple phasic current response to standard intracellular solution supplemented with 10 μM $InsP_3$. Cell was bathed in standard 'quasiphysiological' extracellular solution and voltage-clamped at 0 mV. Record commenced on breakthrough from cell-attached to whole-cell mode. First current spike occurs 23.8 s after start of record. Data representative of 5 similar experiments. B, L6 cell in which internal dialysis with 10 μM $InsP_3$ failed to elicit a current response. This cell did however respond to extracellularly applied 1 μM vasopressin. Conditions as described for A, data from a single cell representative of 4 other observations.*

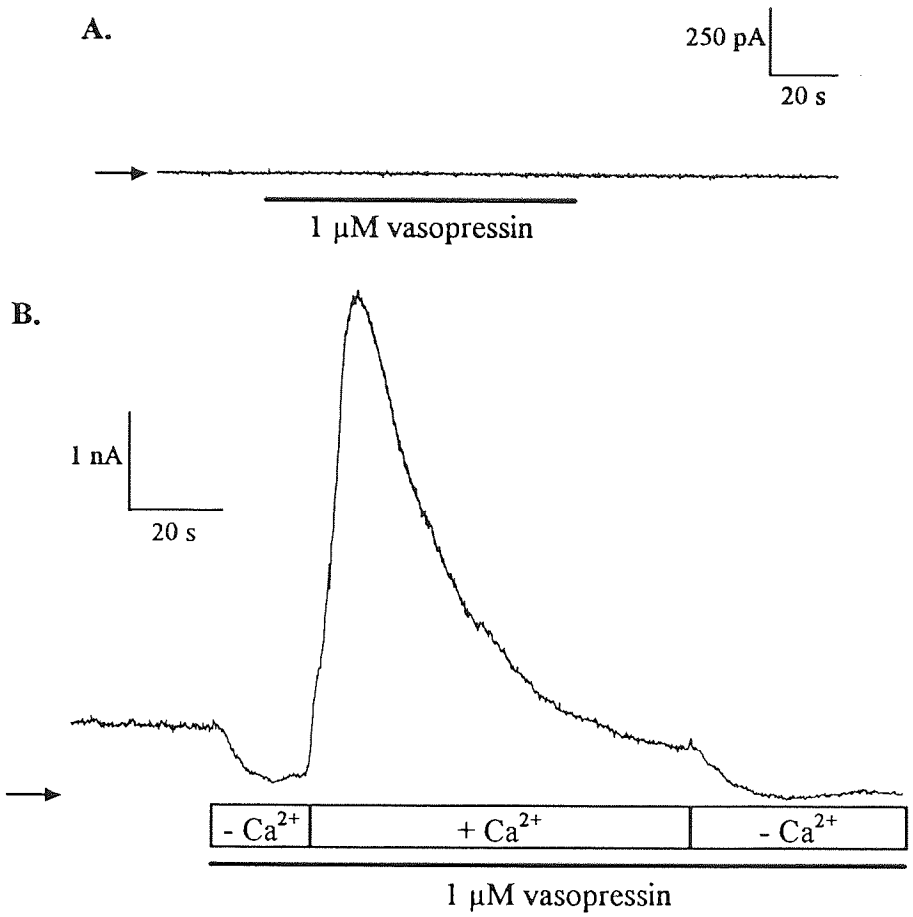

Figure 7.8. Effects of increased intracellular EGTA (A) and removal of extracellular calcium (B) upon the current response of L6 skeletal myocytes to 1 μM vasopressin. *A, a single L6 cell was internally dialysed with standard intracellular solution with EGTA concentration elevated to 10 mM for 5 min prior to 1 μM vasopressin challenge. Data representative of 3 similar experiments. B, an L6 cell was challenged with 1 μM vasopressin in the presence and absence of intracellular Ca^{2+} as indicated (achieved by removal of $CaCl_2$ from standard 'quasiphysiological' bathing medium). Note the reduction in baseline outward current upon removal of extracellular Ca^{2+} and the dependence of the current spike upon the presence of extracellular Ca^{2+}. Data from a single cell representative of 4 similar observations. In both cases cells were voltage-clamped at 0 mV.*

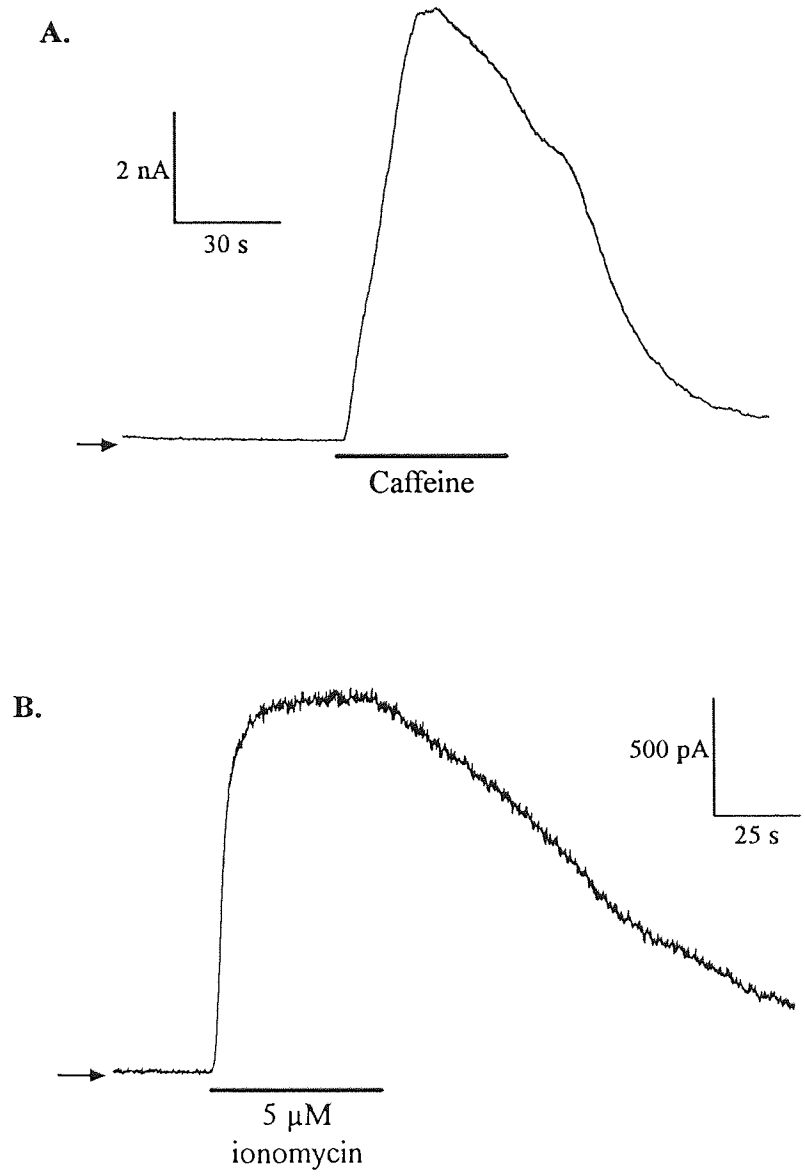
A.
2 nA
30 s
Caffeine
B.
500 pA
25 s
5 μM
ionomycin
C.
10000
8000
I (pA)
6000
4000
2000
0
-2000
-80
-40
40
80
V (mV)
5 μM ionomycin
Control

Figure 7.9. Effects of caffeine and ionomycin upon membrane conductance of L6 skeletal myocytes. *Currents induced by extracellular application of 30 mM caffeine (A) or 5 μM ionomycin (B) to single L6 skeletal myocytes voltage-clamped at 0 mV, equilibrated with standard 'quasiphysiological' solutions. C, current-voltage relationship for ionomycin elicited current as assessed by ramp voltage-clamp stimulus (-80 to +80 mV over 2 s period; mean* E_{rev} *= -77.0 ± 1.7 mV, n = 6). Data from single cells representative of 7 (A) and 8 (B) observations. Duration of drug challenge indicated by solid bars, zero current levels denoted by horizontal arrows.*

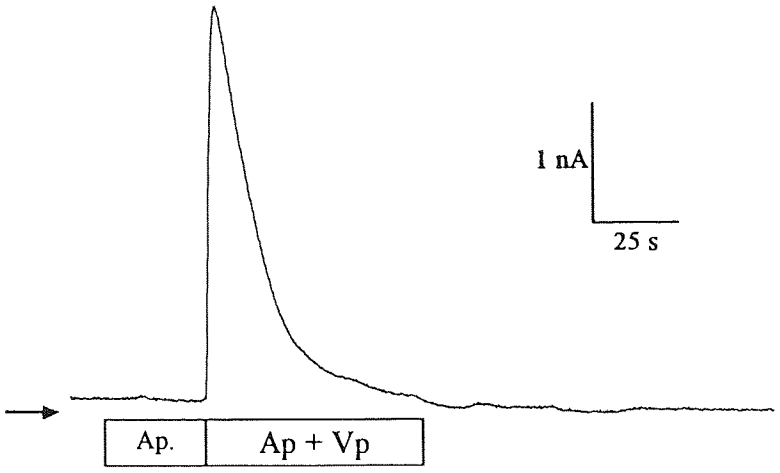

Figure 7.10. Effects of apamin upon the membrane currents elicited by 1 μM vasopressin in L6 skeletal myocyte. *Current response shown for a single L6 cell voltage-clamped at 0 mV (standard solutions) that was superfused with extracellular 500 nM apamin (Ap) for 30 s prior to superfusion with solution containing both 500 nM apamin and 1 μM vasopressin (Ap + Vp). Data from a single cell representative of 5 similar experiments.*

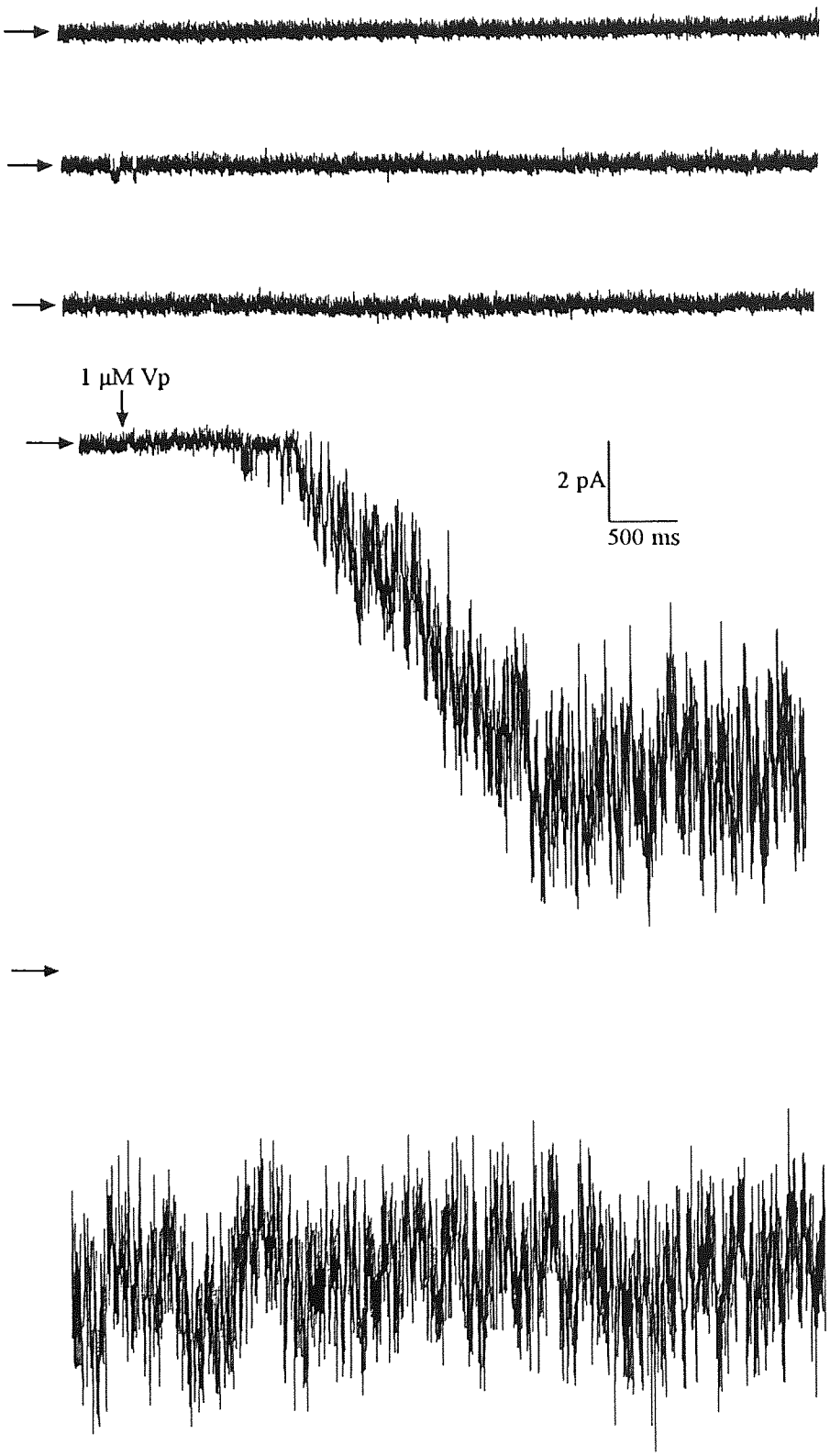
1 μM Vp
2 pA
500 ms

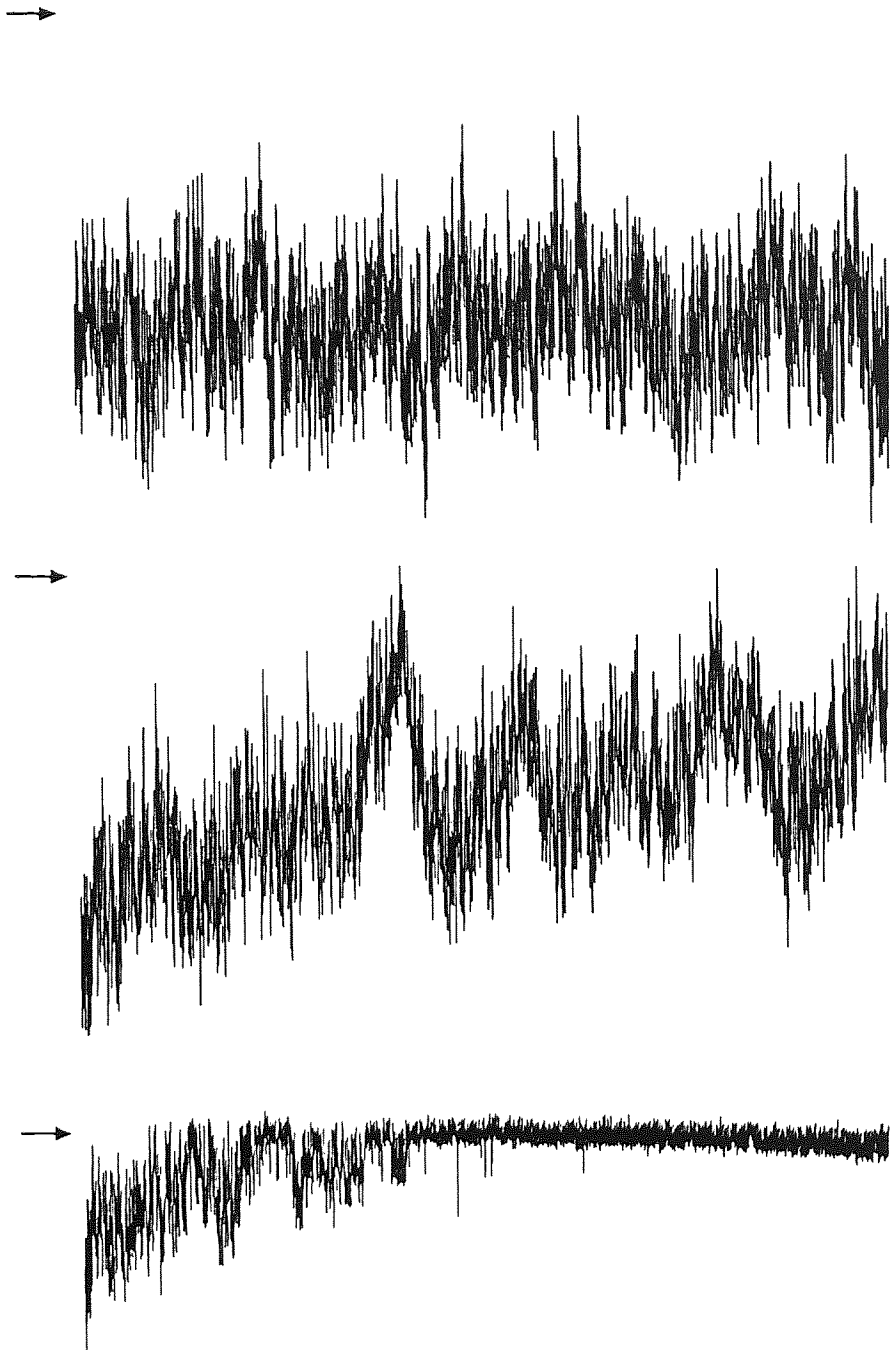

Figure 7.11. Single channel activity in response to 1 μM vasopressin in a cell-attached patch from an L6 skeletal myocyte. The cell was extracellularly superfused with 1 μM vasopressin, commencing as indicated by the vertical arrow and continuing for the remainder of the record. Note that substantial channel activity

rapidly follows onset of superfusion (openings are downwards). The number of channels in the patch is unclear but there appears to be at least 6 on the basis of single channel amplitude (-0.801 pA). Pipette had an applied potential of -60 mV, records digitised at 5 kHz and low-pass filtered at 1 kHz. Data from a single cell representative of 2 other experiments.

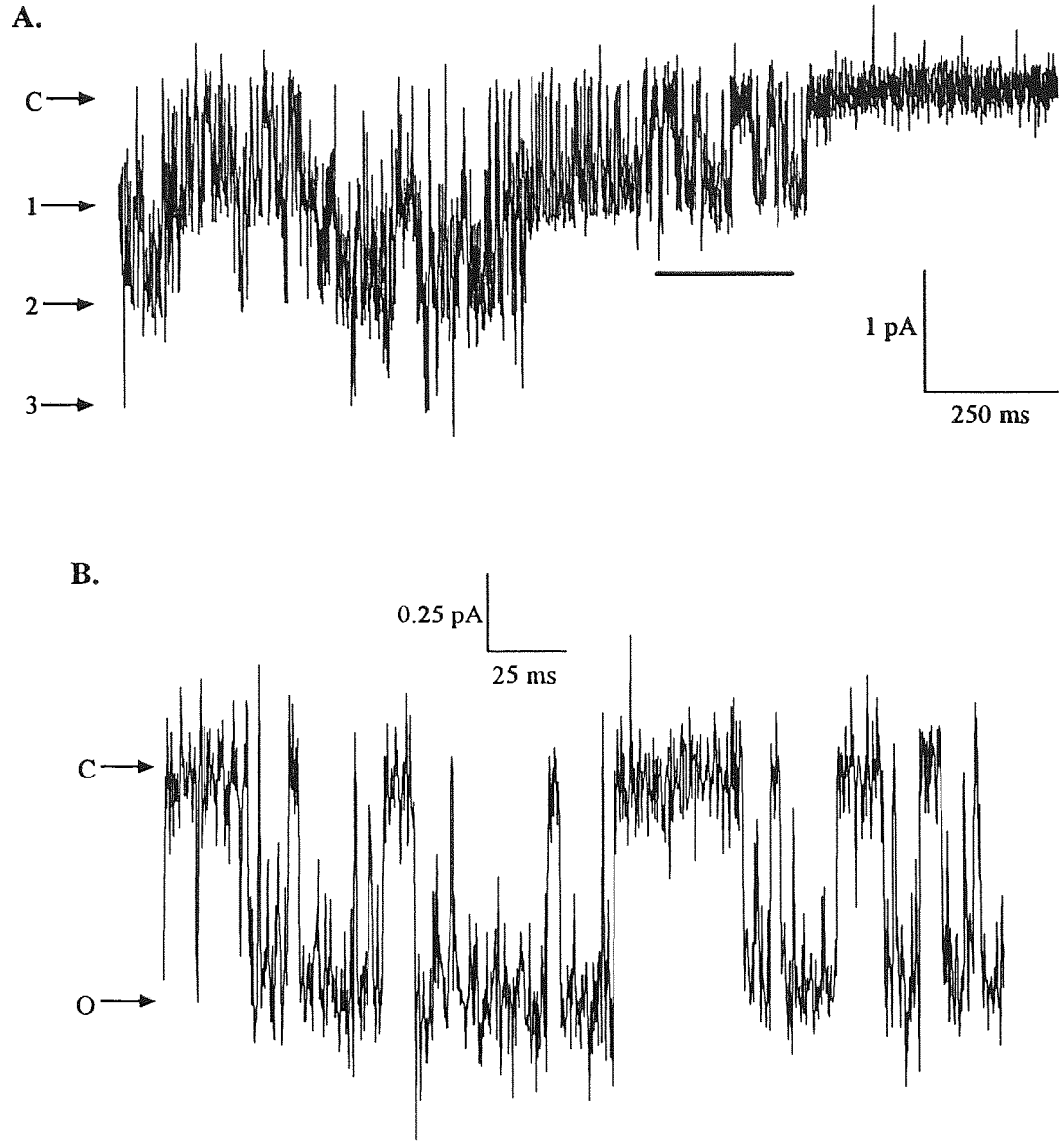

Figure 7.12. Single channel activity elicited by 1 μM vasopressin in a cell-attached patch from a single L6 cell. *A, trace showing vasopressin-induced single channel activity (openings downwards; closed level indicated by C) in a patch containing 3 channels. Open levels are clearly visible and indicated by horizontal arrows. Pipette had an applied potential of -60 mV, and contained normal 'quasiphysiological' extracellular solution. Vasopressin superfusion commenced 5 s prior to the start of*

the record. B, section of trace in A indicated by solid bar on an expanded scale. Records were digitised at 5 kHz and low pass filtered at 1 kHz; data from a single L6 cell representative of 2 other experiments.

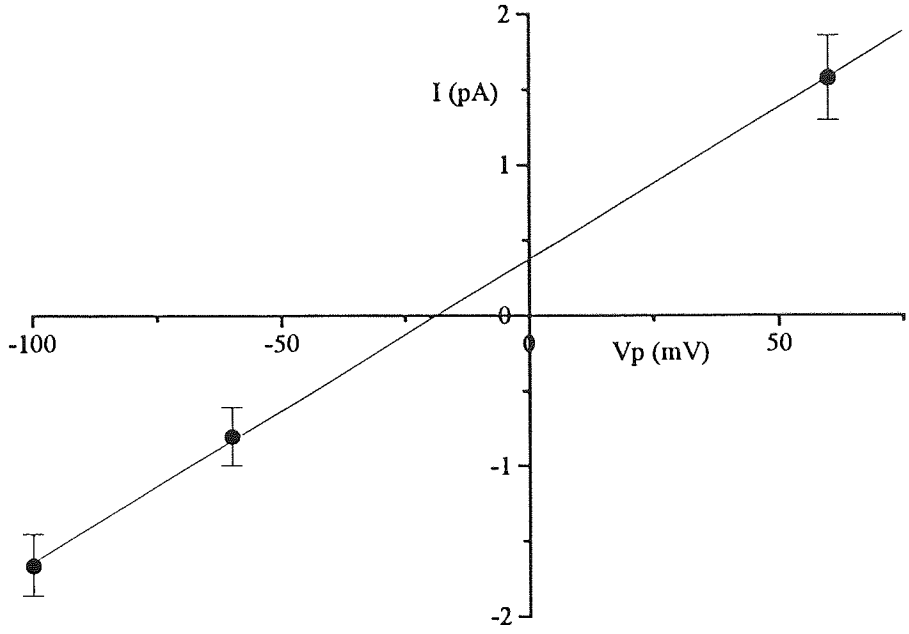

Figure 7.13. Current-voltage relationship for the single channel activated by vasopressin in L6 cells. *Single channel amplitudes measured in cell-attached patches of L6 cells under 'quasiphysiological' conditions. Cell-attached patches were subjected to indicated pipette potential prior to superfusion with 1 μM vasopressin. Single channel amplitudes were measured from sections of records where the number of channels open simultaneously was low, and clear open levels could be determined (as in Fig. 7.12). Symbols represent the mean single channel amplitude determined in 3 separate cell-attached patches at each potential, with S.D. represented by the vertical bars. The line is a linear regression fit to the points and gives a single channel conductance of approximately 20 pS;* E_{rev} *= -19 mV.*

7.5. Discussion:

7.5.1. Membrane effects of vasopressin:

The results detailed above show that electrophysiologically L6 skeletal myocytes respond to vasopressin with a rapid hyperpolarisation that precedes a slow depolarising phase (Fig. 7.2). Whole-cell voltage clamp experiments using 'quasiphysiological' intracellular and extracellular solutions suggest that this hyperpolarisation is mediated by a rapidly activating, transient current (Fig. 7.3), that on the basis of reversal potentials and dependence upon the extracellular K^+ ion concentration, is carried by K^+ ions (Figs 7.5 & 7.6). The membrane current response to vasopressin was abolished by raising the concentration of EGTA in the intracellular solution from 0.05 to 10 mM (Fig. 7.8), suggesting that Ca^{2+} has a vital role in the mechanism of current activation. Further evidence for the role of Ca^{2+} in the vasopressin current response was provided by the effects of the calcium ionophore, ionomycin, and also caffeine which displaces Ca^{2+} from intracellular stores. Both compounds rapidly elicited large amplitude, outward currents at 0 mV (Fig. 7.9), suggesting the current is likely to be a Ca^{2+}-sensitive K^+-conductance. The reason for the depolarising phase subsequent to L6 cell hyperpolarisation is as yet unexplained (Fig. 7.2). In A7r5 cells which show a similar membrane potential response, the depolarising phase was attributed to activation of a non-selective cation channel permeable to Ca^{2+}, Na^+ and K^+ (Van Renterghem *et al.* 1988). This is however, unlikely to be the case in L6 cells as there was no evidence of inward current subsequent to the rapid initial outward current at 0 mV (Fig. 7.3A)

elicited by vasopressin, and no measurable inward current when the intracellular EGTA concentration was elevated (Fig. 7.8A).

7.5.2. Identity of the channel responsible for the vasopressin-induced current:

Ca^{2+}-activated K^+ channels are found in most cell types and have been putatively classified according to their conductance and pharmacology (reviewed by Blatz & Magleby, 1987; Latorre, Oberhauser, Labarca & Alvareaz, 1989). Large conductance (BK or maxi-K) Ca^{2+}-activated K^+-channels have a single channel conductance (γ) in the region of 100 - 300 pS and are sensitive to the scorpion venoms charybdotoxin and iberiotoxin at nanomolar concentration. In contrast small conductance (SK) channels have a conductance typically between 5 and 15 pS and are resistant to charybdotoxin but are effectively inhibited by the honeybee venom, apamin. Both types of channel have been shown to be present in cultured rat skeletal muscle (Romey & Lazdunski, 1984; Blatz & Magleby, 1986). As shown in figure 7.10 the outward current elicited by vasopressin in L6 cells was resistant to inhibition by 500 nM apamin. Single channel records from cell-attached patches of L6 cells challenged with vasopressin (Figs. 7.11 & 7.12) suggest that the current is due to activation of a low conductance channel (estimated single channel conductance of approximately 20 pS; Fig. 7.13). Apamin resistance and a single channel conductance of 20 pS suggest that this channel is most likely to belong to an intermediate conductance (IK) class of Ca^{2+}-sensitive K^+ channels. Further single channel and pharmacological analysis is however required to confirm this putative identification.

7.5.3. Mechanism of vasopressin-induced current activation:

It has been clearly demonstrated that vasopressin produces a 10 - 15 fold increase in production of inositol phosphates in L6 skeletal myocytes (Wakelam *et al.* 1987; Teti *et al.* 1993). This finding is confirmed by the present study, though the observed increase was more modest (Fig. 7.1) being only 3 fold compared to basal levels. It is thus expected that the resulting increase in levels of inositol phosphates, particularly $InsP_3$, may produce an elevation of intracellular Ca^{2+} levels in L6 cells (Teti *et al.* 1993). This would occur as the result of Ca^{2+} release from $InsP_3$ sensitive intracellular stores. Such an elevation of intracellular Ca^{2+} levels would lead to activation of Ca^{2+}-sensitive K^+ channels and explain the vasopressin-induced current. This hypothesis is particularly attractive as agonists that couple to phospholipase C (PLC) have been shown to induce oscillations in the levels of intracellular Ca^{2+} (for reviews see Berridge & Irvine, 1993; Berridge, 1993) which would explain the phasic hyperpolarising bursts (Fig. 7.2) and currents (Fig. 7.4) observed in these cells in response to vasopressin. The results from the patch-clamp experiments performed, however suggest that this is not the mechanism by which vasopressin activates the Ca^{2+}-sensitive K^+ conductance. Dialysis with $InsP_3$ directly elicited currents in only 6/14 cells whereas vasopressin induced currents in all cells tested, and of the $InsP_3$ unresponsive cells, a subsequent vasopressin challenge produced currents in 5/5 cells tested (Fig. 7.7). This is supported by experiments with the $InsP_3$ receptor antagonist, heparin, which when included in the patch pipette solution at 5 mg ml^{-1} was unable to substantially inhibit the vasopressin current response. This concentration of heparin has been previously shown to totally abolish currents produced by caged $InsP_3$ in intestinal smooth muscle cells (Komori &

Bolton, 1991). Inositol 1,3,4,5-tetrakisphosphate ($InsP_4$) has been shown to modulate the actions of $InsP_3$, and under certain circumstances, $InsP_4$ must be present for $InsP_3$ to effectively produce an elevation of intracellular Ca^{2+} levels (Berridge & Irvine, 1989). As $InsP_4$ was not included in the pipette solution with $InsP_3$ this may account for the lack of a consistent current response to dialysis with $InsP_3$. Experiments in which extracellular Ca^{2+} was removed, however suggest that this is unlikely to be the case and do shed some light on the likely mechanism by which vasopressin elicits the currents in L6 cells. As shown in figure 7.8 removal of extracellular Ca^{2+} for a period too short to produce depletion of intracellular Ca^{2+} stores totally removed the membrane current effects of vasopressin. When extracellular Ca^{2+} is returned so is the vasopressin response. Indeed in some cases the holding current fell on removal of extracellular Ca^{2+} (in the presence of vasopressin) suggesting that under basal conditions there may some tonic current activation. These results indicate that the activation of Ca^{2+}-sensitive K^+ channels by vasopressin occurs as the result of calcium entry from the extracellular milieu. The pathway by which this occurs is yet to be clarified, but it is tempting to speculate that receptor-operated calcium channels (ROCCs) are involved as is the case with vasopressin's actions upon vascular smooth muscle cells (Van Renterghem & Lazdunski, 1994). Measurements of intracellular Ca^{2+} levels in L6 cells bathed in Ca^{2+}-free extracellular solution have shown that vasopressin can still elicited a substantial transient elevation, however the stable plateau phase that normally follows the transient rise was absent and cells promptly returned to near basal levels (Teti *et al.* 1993). As vasopressin can produce an elevation of intracellular Ca^{2+} levels in the absence of extracellular Ca^{2+} it would be expected that under these conditions a current response would still be observed. The reason for the absence of an

effect is presently unexplained, but there may however exist spatial consequences of both intracellular Ca^{2+} release and extracellular Ca^{2+} entry that play an important role in current activation. Ca^{2+} waves and oscillations in single cells are a well documented phenomena showing that intracellular Ca^{2+} levels can be raised in specific localised regions of the cell (Berridge, 1993). In L6 cells Ca^{2+} entry via ROCCs may elevate Ca^{2+} levels close to the plasma membrane where the ion channels are located, whereas release from intracellular stores (e.g. in response to $InsP_3$) may only elevate the Ca^{2+} levels deeper into the cell cytosol.

7.6. Conclusions:

Vasopressin produces a sharp and rapid hyperpolarisation of L6 cells that results from the activation of Ca^{2+}-sensitive K^+ channels. These channels have a single channel conductance (γ) of approximately 20 pS and may belong to the intermediate conductance (IK) class of Ca^{2+}-sensitive K^+ channels. The mechanism by which vasopressin activates these channels is unclear but is dependent upon the presence of extracellular Ca^{2+}, and unlikely to involve Ca^{2+} release from intracellular stores via $InsP_3$ formation.

Chapter 8.

GENERAL DISCUSSION

The results presented in Chapters 3 and 4 of this thesis show that the ROS 17/2.8 osteosarcoma cell line and mouse primary cultured calvarial osteoblasts express a volume-regulated Cl^- conductance. This conductance appears to be similar in its characteristics to those widely described in a variety of other cell types (see Table 1.1) in that it is outwardly rectifying, exhibits an anion permeability sequence of $SCN^- > I^- > Br^- > Cl^- > F^- >$ gluconate$^-$ and is effectively inhibited by NPPB and DIDS. Its lack of dependence upon intracellular nucleotides and resistance to block by verapamil suggest the current is unlikely to be that associated with P-gp expression (Valverde *et al.* 1992; Dìaz *et al.* 1993; Higgins, 1995). The mechanism by which current activation occurs is undetermined but does not appear to involve cyclic AMP, Ca^{2+}, tyrosine kinases, actin filament disruption or arachidonic acid production. A direct link between the underlying channel and membrane tension is a tempting explanation. However, whole-cell experiments using dipyridamole to generate membrane tension were ineffective, as were single channel experiments using negative pressure applied to the patch pipette, in activating the volume-regulated Cl^- current. In the absence of any measurable single channel activity in experiments from cell-attached patches of hypotonically swollen cells it seems that the underlying channel may be of very low conductance.

As shown in Chapter 5 the volume-sensitive Cl^- current is effectively inhibited by arachidonate. The mechanism of blockade by arachidonate appears to be direct as inhibitors of the enzymes responsible for processing arachidonate to bioactive metabolites were ineffective. Acceleration of the time-dependent inactivation at depolarised potentials may reflect open channel block by arachidonate. This effect of polyunsaturated fatty acids has been reported previously (e.g. McEvoy *et al.* 1995;

Garratt & Owen, 1995) but usually upon voltage-gated K^+ channels. As the volume-sensitive Cl^- current is active over the entire range of potentials and shows voltage-dependence only at strong depolarisations, this hypothesis may not be valid.

Measurements of cell volume (Chapter 6) have shown that like most other cells, osteoblastic cells can regulate their volume when hypotonically challenged. Effective inhibitors of the volume-sensitive Cl^- current (NPPB, DIDS and arachidonate) drastically compromise this ability. This effect suggests that the current possesses a vital role in the RVD response of osteoblasts and may be its physiological function. Providing a Cl^- efflux pathway to achieve effective reduction in cell volume is a function that has been widely attributed to this type of Cl^- conductance (e.g. Hoffman & Simonsen, 1989; Grinstein & Foskett, 1990; Kubo & Okada, 1992). Modulation of volume-sensitve Cl^- currents and RVD by arachidonic acid have been reported previously (Lambert, 1987; Kubo & Okada, 1992) though the significance of the effect is as yet unknown. It is possible that ion channel modulation by fatty acids may represent a physiological mechanism by which RVD can be controlled and possibly suppressed. In osteoblasts this may have substantial physiological implications as changes in osteoblast shape are a critical step in the bone resorbtion process by facilitating the resorbing action of osteoclasts (Lindskog *et al.* 1987). These morphological changes are suggested to occur as a result of a reduction in cell volume and may involve a volume-sensitive Cl^- conductance. Thus inhibition of this current may interfere in this process and result in decreased bone resorbtion and increased ossification. Two studies have shown that stilbene-derivative Cl^- channel inhibitors, such as DIDS, inhibit bone resorbtion in bone organ culture systems (Hall &

Chambers, 1989; Klein-Nulend & Raisz, 1989). This effect was explained by inhibition of Cl^-/bicarbonate exchangers in the osteoclast membrane which led to acidification and ineffecient bone resorbtion by these cells. In light of the effects of the Cl^- channel inhibitors upon osteoblastic volume regulation, their effects upon bone resorbtion may merit further investigation.

As detailed in Chapter 7 vasopressin produced hyperpolarisation of L6 skeletal myocytes, an effect that appeared to be due to activation of Ca^{2+}-sensitive K^+ channels. Activation of these channels was found to depend upon extracellular Ca^{2+} suggesting that vasopressin activated a Ca^{2+} influx pathway, possibly ROCCs. This finding was unexpected as vasopressin has been shown by this study, and others (Wakelam *et al.* 1987; Teti *et al.* 1993), to produce a significant increase in inositol phosphate production and elevation of intracellular Ca^{2+}. The inability of heparin to antagonise the K^+ current induced by vasopressin further suggests that Ca^{2+} release from $InsP_3$ sensitive stores is not the underlying mechanism. As the effects of vasopressin upon skeletal muscle are not known, it is difficult to comment upon the possible physiological significance of it's electrophysiological effects.

Overall the results from this study emphasize the complexity of ion channel regulation. In both cell types the 'expected' activation mechanisms (e.g. in ROS 17/2.8 cells the volume-sensitive Cl^- channel was activated by a simple link to the cytoskeleton, or in L6 cells the Ca^{2+} required to activate the K^+ channels was released from $InsP_3$ sensitive internal stores) were unable to explain current activation. Thus more work is required to fully characterise how these ion channels are regulated in these model systems.

REFERENCES

ACKERMAN, M.J., WICKMAN, K.D. & CLAPHAM, D.E. (1994) Hypotonicity activates a chloride current in *Xenopus* oocytes. *Journal of General Physiology* **103**, 153 - 179.

ALTON, E.W.F.W. & WILLIAMS, A.J. (1992) Modification of gating of an airway epithelial chloride channel by 5-nitro-2-(3-phenylpropylamino)benzoic acid (NPPB). *Journal of Membrane Biology* **128**, 141 - 151.

ANDERSON, J.W., JIRSCH, J.D. & FEDIDA, D. (1995) Cation regulation of anion current activated by cell swelling in two types of human epithelial cancer cells. *Journal of Physiology* **483**, 549 - 557.

ANDERSON, M.P., GREGORY, R.J, THOMPSON, S., SOUZA, D.W., PAUL, S., MULLIGAN, R.C., SMITH, A.E. & WELSH, M.J. (1991) Demonstration that CFTR is a chloride channel by alteration of its anion selectivity. *Science* **253**, 202 - 205.

ANDERSON, M.P. & WELSH, M.J. (1990) Fatty acids inhibit apical membrane chloride channels in airway epithelia. *Proceedings of the National Academy of Sciences of the USA* **87**, 7334 - 7338.

ANDERSON, M.P. & WELSH, M.J. (1991) Calcium and cAMP activate different chloride channels in the apical membrane of normal and cystic fibrosis epithelia. *Proceedings of the National Academy of Sciences of the USA* **88**, 6003 - 6007.

ARREOLA, J., MELVIN, J.E. & BEGENISICH, T. (1995) Volume-activated chloride channels in rat parotid acinar cells. *Journal of Physiology* **484**, 677 - 687.

BANDERALI, U. & ROY, G. (1992) Activation of K^+ and Cl^- channels in MDCK cells during volume regulation in hypotonic media. *Journal of Membrane Biology* **126**, 219 - 234.

BAQUET, A., MIEJER, A.J. & HUE, L. (1991) Hepatocyte swelling increases inositol 1,4,5-trisphosphate, calcium and cyclic AMP but antagonizes phosphorylase activation by Ca^{2+}-dependent hormones. *FEBS Letters* **278**, 103 - 106.

BERRIDGE, M.J. (1993) Inositol trisphosphate and calcium signalling. *Nature* **361**, 315 - 325.

BERRIDGE, M.J. & IRVINE, R.F. (1989) Inositol phosphates and cell signalling. *Nature* **341**, 197 - 204.

BETTENDORF, L., KOLB, H.-A. & SCHOFFENIELS, E. (1993) Thiamine triphosphate activates an anion channel of large conductance in neuroblastoma cells. *Journal of Membrane Biology* **136**, 281 - 288.

BINDERMAN, I., ZOR, U., KAYE, A.M., SHIMSHONI, Z., HARELL, A. & SÖMJEN, D. (1988) The transduction of mechanical force into biochemical events in

bone cells may involve activation of phospholipase A_2. *Calcified Tissue International* **42**, 261 - 266.

BJURHOLM, A. (1991) Neuroendocrine peptides in bone. *International Orthopaedics* **15**, 325 - 329.

BLATZ, A.L. & MAGLEBY, K.L. (1983) Single voltage-dependent chloride selective channels of large conductance in cultured rat muscle. *Biophysical Journal* **43**, 237 - 241.

BLATZ, A.L. & MAGLEBY, K.L. (1986) Single apamin-blocked Ca-activated K^+ channels of small conductance in cultured rat skeletal muscle. *Nature* **323**, 718 - 720.

BLATZ, A.L. & MAGLEBY, K.L. (1987) Calcium-activated potassium channels. *Trends in Neuroscience* **10**, 463 - 467.

BOTHCKIN, L.M. & MATTHEWS, G. (1993) Chloride current activated by swelling in retinal pigment epithelium cells. *American Journal of Physiology* **265**, C1037 - C1045.

BROWN, A.M. & BIRNBAUMER, L. (1990) Ionic channels and their regulation by G protein subunits. *Annual Review of Physiology* **52**, 197 - 213.

BUI, A.H. & WILEY, J.S. (1981) Cation fluxes and volume regulation by human lymphocytes. *Journal of Cell Physiology* **108**, 47 - 54

CATTERALL, W.A. (1993) Structure and function of voltage-gated ion channels. *Trends in Pharmacological Sciences* **16**, 500 - 506.

CHAN, H.C., GOLDSTEIN, J. & NELSON (1992) Alternate pathways for chloride conductance activation in normal and cystic fibrosis airway epithelial cells. *American Journal of Physiology* **262**, C1273 - C1283.

CHAN, H.C., FU, W.O., CHUNG, Y.W., HUANG, S.J., ZHOU, T.S. & WONG, P.Y.D. (1993) Characterization of a swelling-induced chloride conductance in cultured rat epididymal cells. *American Journal of Physiology* **265**, C997 - C1005.

CHAN, H.C., FU, W.O., CHUNG, Y.W., HUANG, S.J., CHAN, P.S.F. & WONG, P.Y.D. (1994) Swelling-induced anion and cation conductances in human epididymal cells. *Journal of Physiology* **478**, 449 - 460.

CHESNOY-MARCHAIS, D. & FRITSCH, J. (1988) Voltage-gated sodium and calcium currents in rat osteoblasts. *Journal of Physiology* **398**, 291 - 311.

CHESNOY-MARCHAIS, D. & FRITSCH, J. (1989) Chloride current activated by cyclic AMP and parathyroid hormone in rat osteoblasts, *Pflügers Archiv* **415**, 104 - 114.

CHESNOY-MARCHAIS, D. & FRITSCH, J. (1994a) Concentration-dependent modulations of potassium and calcium currents of rat osteoblastic cells by arachidonic acid. *Journal of Membrane Biology* **138**, 159 - 170.

CHESNOY-MARCHAIS, D. & FRITSCH, J. (1994b) Activation by hyperpolarization and atypical osmosensitivity of a Cl^- current in rat osteoblastic cells. *Journal of Membrane Biology* **140**, 173 - 188.

CHRISTENSEN, O. (1987) Mediation of cell volume regulation by Ca^{2+} influx through stretch-activated channels. *Nature* **330**, 66 - 68.

CLIFF, W.H. & FRIZZELL, R.A. (1990) Separate Cl^- conductances activated by cAMP and Ca^{2+} in Cl^--secreting epithelia. *Proceedings of the National Academy of Sciences of the USA* **87**, 4956 - 4960.

CORNET, M., UBL, J. & KOLB, H-A (1993) Cytoskeleton and ion movements during volume regulation in cultured PC12 cells. *Journal of Membrane Biology* **133**, 161 - 170.

DAVIDSON, R.M. (1993) Membrane stretch activates a high-conductance K^+ channel in G292 osteoblastic-like cells. *Journal of Membrane Biology* **131**, 81 - 92.

DI STEFANO, A., WITTNER, M., SCHLATTER, E., LANG, H.J., ENGKERT, H. & GREGER, R. (1985) Diphenylamine-2-carboxylate, a blocker of the Cl^--conductive pathway in Cl^--transprting epithelia. *Pflügers Archiv* **405**, S95 - S100.

DÍAZ, M., VALVERDE, M.A., HIGGINS, C.F., RUCÂREANU, C. & SEPÚLVEDA, F.V. (1993) Volume-activated chloride channels in HeLa cells are blocked by verapamil and dideoxyforskolin. *Pflügers Archiv* **422**, 347 - 353.

DIXON, S.J., AUBIN, J.E. & DAINTY, J. (1984) Electrophysiology of a clonal osteoblast-like cell line: evidence for the existence of a Ca^{2+}-activated K^+ conductance. *Journal of Membrane Biology* **80**, 49 - 58.

DOWNES, C.P., HAWKINS, P.T. & IRVINE, R.F. (1986) Inositol 1,3,4,5-tetrakisphosphate and not phosphatidylinositol 3,4-bisphosphate is the probable precursor of 1,3,4-trisphosphate in agonist-stimulated parotid gland. *Biochemical Journal* **238**, 501 - 506.

DOIGE, C.A. & AMES, G.F.L. (1993) ATP-dependent transport systems in bacteria and humans: relevance to cystic fibrosis and multidrug resistance. *Annual Review of Microbiology* **47**, 291 - 319.

DUNCAN, R. & MISLER, S. (1989) Voltage-activated and stretch-activated Ba^{2+} conducting channels in an osteoblast-like cell line (UMR 106). *FEBS Letters* **251**, 17 - 21.

ENDO, M. (1977) Calcium release from the sarcoplasmic reticulum. *Physiological Reviews* **57**, 71 - 108.

ENDO, M. (1985) Calcium release from sarcoplasmic reticulum. *Current Topics in Membranes and Transport* **25**, 181 - 230.

EVANS, M.G. & MARTY, A. (1986) Calcium-dependent chloride currents in isolated cells from rat lacrimal glands. *Journal of Physiology* **378**, 437 - 460.

FASOLATO, C., INNOCENTI, B. & POZZAN, T. (1994) Receptor-activated Ca^{2+} influx: how many mechanisms for how many channels. *Trends in Pharmacological Sciences* **15**, 77 - 83.

FENWICK, E.M., MARTY, A. & NEHER, E. (1982) A patch-clamp study of bovine chromaffin cells and of their sensitivity to acetylcholine. *Journal of Physiology* **331**, 577 - 597.

FERRIER, J., WARD-KESTHELY, A., HOMBLE, F. & ROSS, S. (1987) Further analysis of the spontaneous membrane potential activity and the hyperpolarising response to parathyroid hormone in osteoblast-like cells. *Journal of Cell Physiology* **130**, 344 - 351.

FRANCIOLINI, F. & PETRIS, A. (1990) Chloride channels of biological membranes. *Biochimica et Biophysica Acta* **1031**, 247 - 259.

GABRIEL, S.E., CLARKE, L.L., BOUCHER, R.C. & STUTTS, M.J. (1993) CFTR and outward rectifying chloride channels are distinct proteins with a regulatory relationship. *Nature* **363**, 263 - 266.

GALCHEVA-GARGOVA, Z., DÉRIJARD, B., WU, I-H. & DAVIS, R.J. (1994) An osmosensing signal transduction pathway in mammalian cells. *Science* **265**, 806 - 811.

GALIONE, A., MCDOUGALL, A., BUSA, W.A., WILLMOTT, N., GILLOT, I. & WHITAKER, M. (1993) Redundant mechanisms of calcium-induced calcium release underlying calcium waves during fertilization of sea urchin eggs. *Science* **261**, 348 - 351.

GARCIA-PEREZ, A. & BURG, M.B. (1991) Renal medullary organic osmolytes. *Physiological Reviews* **71**, 1081 - 1115.

GARRATT, J.C. & OWEN, D.G. (1995) External blockade of a single cloned potassium channel, mKv1.1, by docosahexaenoic acid. *Journal of Physiology* (in the press).

GÖGELEIN, H. (1988) Chloride channels in epithelia. *Biochimica et Biophysica Acta* **947**, 521 - 547.

GRAY, P.T.A. & RITCHIE, J.M. (1986) A voltage-gated chloride conductance in rat cultured astrocytes. *Proceedings of the Royal Society (London B)* **228**, 267 - 288.

GREGER, R. (1990) Chloride channel blockers. *Methods in Enzymology* **191**, 793 - 810.

GRINSTEIN, S. & FOSKETT, J.K. (1990) Ionic mechanisms of cell volume reguation in leukocytes. *Annual Review of Physiology* **52**, 399 - 414.

GRÜNDER, S., THIEMANN, A., PUSCH, M. & JENTSCH, T.J. (1992) Regions involved in the opening of ClC-2 chloride channel by voltage and cell volume. *Nature* **360**, 759 - 762.

GUBITOSI-KLUG, R.A., YU, S.P., CHOI, D.W. & GROSS, R.W. (1995) Concomitant acceleration of the activation and inactivation kinetics of the human dealyed rectifier K^+ channel (Kv1.1) by Ca^{2+}-independent phospholipase A_2. *Journal of Biological Chemistry* **270**, 2885 - 2888.

GUHARAY, F. & SACHS, F. (1984) Stretch-activated single ion channel currents in tissue-cultured embryonic chick skeletal muscle. *Journal of Physiology* **352**, 685 - 701.

HALL, T.J. & CHAMBERS, T.J. (1989) Optimal bone resorption by isolated osteoclasts requires chloride-bicarbonate exchange. *Calcified Tissue International* **45**, 378 - 380.

HALM, D.R., RECHKEMMER, G.R., SCHOUMACHER, R.A. & FRIZZELL, R.A. (1988) Apical membrane chloride channels in a colonic cell line activated by secretory agonists. *American Journal of Physiology* **254**, C505 - C511.

HAMILL, O.P., MARTY, A., NEHER, E., SAKMANN, B. & SIGWORTH, F. (1981) Improved patch-clamp techniques for high resolution current recordings from cells and cell-free membrane patches. *Pflügers Archiv* **391**, 85 - 100.

HAMILL, O.P. & MCBRIDE, D.W. (1994) The cloning of a mechano-gated membrane ion channel. *Trends in Neuroscience* **17**, 439 - 443.

HARDY, S.P., VALVERDE, M.A., GOODFELLOW, H.R., HIGGINS, C.F. & SEPÚLVEDA, F.V. (1994) Regulation of volume-activated chloride channels by protein kinase C mediated phosphorylation of P-glycoprotein. *Japanese Journal of Physiology* **44**, S9 - S15.

HAZAMA, A. & OKADA, Y. (1988) Ca^{2+} sensitivity of volume-regulatory K^+ and Cl^- channels in cultured human epithelial cells. *Journal of Physiology* **402**, 687 - 702.

HAZAM, A. & OKADA, Y. (1990) Biphasic rises in cytosolic free Ca^{2+} in association with activation of K^+ and Cl^- conductances during the regulatory volume decrease in cultured human epithelial cells. *Pflügers Archiv* **416**, 710 - 714.

HECKER, M., BARA, A.T., BAUERSACHS, J. & BUSSE, R. (1994) Charatcerization of endothelium-derived hyperpolarizing factor as a cytochrome P450-

derived arachidonic acid metabolite in mammals. *Journal of Physiology* **481**, 407 - 414.

HEMS, D.A. & WHITTON, P.D. (1980) Control of hepatic glycogenolysis. *Physiological Reviews* **60**, 1 - 50.

HIGGINS, C.F. (1995) Volume-activated chloride currents associated with the multidrug resistance P-glycoprotein. *Journal of Physiology* **482P**, 31S - 35S.

HILLE, B. (1992) Ionic channels of excitable membranes (2nd edition). pp 607, USA: Sinauer Associates Inc..

HO, M.W.Y., DUSZYK, M. & FRENCH, A.S. (1994) Evidence that channels below 1 pS cause the volume-sensitive chloride conductance in T84 cells. *Biochimica et Biophysica Acta* **1191**, 151 - 156.

HODGKIN, A.L. & HUXLEY, A.F. (1952) The components of membrane conductance in the giant axon of *Loligo*. *Journal of Physiology* **116**, 473 - 496.

HOFFMAN, E.K. & LAMBERT, I.H. (1983) Amino acid transport and cell volume regulation in Ehrlich ascites tumor cells. *Journal of Physiology* **338**, 613 - 625.

HOFFMAN, E.K. & SIMONSEN, L.O. (1989) Membrane mechanisms in volume and pH regulation in vertebrate cells. *Physiological Reviews* **69**, 315 - 382.

HONORÉ, E., BARHANIN, J., ATTALI, B., LESAGE, F. & LAZDUNSKI, M. (1994) External blockade of the major cardiac delayed-rectifier K^+ channel (Kv1.5) by polyunsaturated fatty acids. *Proceedings of the National Academy of Sciences of the USA* **91**, 1937 - 1944.

HUGHES, M., ROMEY, G., DUVAL, D., VINCENT, J.P. & LAZDUNSKI, M. (1982) Apamin is a selective blocker of calcium-dependent potassium channels in neuroblastoma cells: voltage-clamp and biochemical characterization of the toxin receptor. *Proceedings of the National Academy of Sciences of the USA* **79**, 1308 - 1312.

HURNÁK, O. & ZACHAR, J. (1992) Maxi chloride channels in L6 myoblasts. *General Physiology and Biophysics* **11**, 389 - 400.

HURNÁK, O. & ZACHAR, J. (1993) High-conductance chloride channels in BC_3H_1 myoblasts. *General Physiology and Biophysics* **12**, 171 - 182.

HWANG, T.C., GUGGINO, S.E. & GUGGINO, W.B. (1990) Direct modulation of secretory chloride channels by arachidonic and other *cis* unsaturated fatty acids. *Proceedings of the National Academy of Sciences of the USA* **87**, 5706 - 5709.

IRVINE, R.F. (1982) How is the level of free arachidonic acid controlled in mammalian cells ? *Biochemical Journal* **204**, 3 - 16.

JACKSON, T.R. & HANLEY, M.R. (1989) Tumour promoter 12-O-tetradecanoylphorbol 12-acetate inhibits mas/angiotensin receptor stimulated inositol phosphate production and intracellular Ca^{2+} elevation in the 401L-C3 neuronal cell line. *FEBS Letters* **251**, 27 - 30.

JENNINGS, M.L. & SCHULTZ, R.K. (1990) Swelling-activated KCl cotransport in rabbit red cells: flux is determined mainly by cell volume rather than shape. *American Journal of Physiology* **259**, C960 - C967.

JENTSCH, T.J. (1993) Chloride channels. *Current Opinion in Neurobiology* **3**, 316 - 321.

JENTSCH, T.J., GÜNTHER, W., PUSCH, M. & SCHWAPPACH, B. (1995) Properties of voltage-gated chloride channels of the ClC gene family. *Journal of Physiology* **482**, 19S - 25S.

JIRSCH, J.D., DEELEY, R.G., COLE, S.P.C., STEWART, A.J. & FEDIDA, D. (1993) Inwardly rectifying K^+ channels and volume-regulated anion channels in multidrug-resistant small cell lung carcinoma cells. *Cancer Research* **53**, 4156 - 4160.

JIRSCH, J.D., LOE, D.W., COLE, S.P.C., DEELEY, R.G. & FEDIDA, (1994) ATP is not required for anion current activated by cell swelling in multidrug-resistant lung cancer cells. *American Journal of Physiology* **267**, C688 - C699.

KAMP, F. & HAMILTON, J.A. (1992) pH gradients across phospholipid membranes caused by fast flip-flop of un-ionized fatty acids. *Proceedings of the National Academy of Sciences of the USA* **89**, 11367 - 11370.

KELLY, M.E.M., DIXON, S.J. & SIMS, S.M. (1994) Outwardly rectifying chloride current in rabbit osteoclasts is activated by hyposmotic stimulation. *Journal of Physiology* **475**, 377 - 389.

KEMP, P.J., MACGREGOR, G.G. & OLVER, R.E. (1993) G protein-regulated large-conductance chloride channels in freshly isolated type II alveolar epithelial cells. *American Journal of Physiology* **265**, L323 - L329.

KIDOKORO, Y. (1975) Developmental changes of membrane electrical properties in a rat skeletal muscle cell line. *Journal of Physiology* **244**, 129 - 143.

KLAUSNER, R.D., KLEINFELD, A.M., HOOVER, R.L. & KARNOVSKY, M.J. (1980) Lipid domains in membranes. Evidence derived from structural peturbations induced by free fatty acids and lifetime heterogeneity analysis. *Journal of Biological Chemistry* **255**, 1286 - 1295.

KLEIN-NULEND, J. & RAISZ, L.G. (1989) Effects of two inhibitors of anion transport on bone resorption in organ culture. *Endocrinology* **125**, 1019 - 1024.

KOMORI, S. & BOLTON, T.B. (1991) Calcium release induced by inositol 1,4,5-trisphosphate in single rabbit intestinal smooth muscle cells. *Journal of Physiology* **433**, 495 - 517.

KRAPIVINSKY, G.B., ACKERMAN, M.J., GOERDON, E.A., KRAPIVINSKY, L.D. & CLAPHAM, D.E. (1994) Molecular characterization of a swelling-induced chloride conductance regulatory protein, pI_{Cln}. *Cell* **76**, 439 - 448.

KRICK, W., DISSER, J., HAZAMA, A., BURCKHARDT, G. & FRÖMTER, E. (1991) Evidence for a cytosolic inhibitor of epithelial chloride channels. *Pflügers Archiv* **418**, 491 - 499.

KROUSE, M.E., HAWS, C.M., XIA, Y., FANG, R.H. & WINE, J.J. (1994) Dissociation of depolarization-activated and swelling-activated Cl^- channels. *American Journal of Physiology* **267**, C642 - C649.

KUBO & OKADA (1992) Volume-regulatory Cl^- channel currents in cultured human epithelial cells. *Journal of Physiology* **456**, 351 - 371.

KURACHI, Y., ITO, H., SUGIMOTO, T., SHIMIZU, T., MIKI, I. & UI, M. (1989) Arachidonic acid metabolites as intracellular modulators of the G protein-gated cardiac K^+ channel. *Nature* **337**, 555 - 557.

LAMBERT, I.H. (1987) Effect of arachidonic acid, fatty acids, prostaglandins, and leukotrienes on volume regulation in Ehrlich ascites tumor cells. *Journal of Membrane Biology* **98**, 207 - 221.

LANGTON, P.D. (1993) A versatile superfusion system suitable for whole-cell and excised patch-clamp experiments. *Journal of Physiology* **467**, 244P.

LATORRE, R., OBERHAUSER, A., LABARCA, P. & ALVAREZ, O. (1989) Varieties of calcium-activated potassium channels. *Annual Review of Physiology* **51**, 385 - 399.

LEWIS, R.S., ROSS, P.E. & CALAHAN, M.D. (1993) Chloride channels activated by osmotic stress in T lymphocytes. *Journal of General Physiology* **101**, 801 - 826.

LIDOFSKY, S.D., XIE, M.-H., SOSTMAN, A., SCHARSCHMIDT, B.F. & FITZ, J.G. (1993) Vasopressin increases cytosolic sodium concentration in hepatocytes and activates calcium influx through cation-selective channels. *Journal of Biological Chemistry* **268**, 14632 - 14636.

LINDSKOG, S., BLOMLÖF, L. & HAMMARSTRÖM, L. (1987) Comparitive effects of parathyroid hormone on osteoblasts and cementoblasts. *Journal of Clinical Peridontology* **14**, 386 - 389.

LOIRAND, G., GRÉGOIRE, G. & PACAUD, P. (1994) Photoreleased inositol 1,4,5-trisphosphate-induced response in single smooth muscle cells of rat portal vein. *Journal of Physiology* **479**, 41 - 52.

MAJESKA, R.J., RODAN, S.B. & RODAN, G.A. (1980) Parathyroid hormone-responsive clonal cell lines fron rat osteosarcoma. *Endocrinology* **107**, 1494 - 1503.

McCANN, J.D., LI, M. & WELSH, M.J. (1989) Identification and regulation of whole-cell chloride currents in airway epithelium. *Journal of General Physiology* **94**, 1015 - 1036.

McCARTY, N.A. & O'NEIL, R.G. (1992) Calcium signalling in cell volume regulation. *Physiological Reviews* **72**, 1037 - 1061.

McEVOY, M.P., OWEN, D.G. & GARRATT, J.C. (1995) Effects of arachidonic acid on the cloned potassium channel mKv1.2 in CHO cells. *Journal of Physiology* (in the press).

MENNITI, F.S., BIRD, G.S.J., GLENNON, M.C., OBIE, J.F., ROSSIER, M.F. & PUTNEY, J.W. (1992) Inositol polyphosphates and calcium signalling. *Molecular and Cellular Neurosciences* **3**, 1 - 10.

MICHELL, R.H., KIRK, C.J. & BILLAH, M.M. (1989) Hormonal stimulation of phosphatidylinositol breakdown, with particular reference to the hepatic effect of vasopressin. *Biochemical Society Transactions* **7**, 861 - 865.

MILLER, B., SARANTIS, M., TRAYNELIS, S.F. & ATTWELL, D. (1992) Potentiation of NMDA receptor currents by arachidonic acid. *Nature* **355**, 722 - 725.

MILLER, C. (1986) Ion channel reconstitution. pp 577, USA: Plenum.

MILLER, S.S., WOLF, A.M. & ARNAUD, C.D. (1976) Bone cells in culture: morphologic transformation by hormones. *Science* **192**, 1340 - 1343.

MILLS, J.W., SCHWIEBERT, E.M. & STANTON, B.A. (1994) Evidence for the role of actin filaments in regulating cell swelling. *Journal of Experimental Zoology* **268**, 111 - 120.

MINTENIG, G.M., VALVERDE, M.A., SEPÚLVEDA, F.V., GILL, D.R., HYDE, S.C., KIRK, J. & HIGGINS, C.F. (1994) Specific inhibitors distinguish the chloride channel and drug transporter functions associated with the human multidrug resistance P-glycoprotein. *Receptor Channels* **1**, 305 - 313.

MURAKAMI, K. & ROUTENBURG, A. (1985) Direct activation of purified protein kinase C by unsaturated fatty acids (oleate and arachidonate) in the absence of phospholipids and Ca^{2+}. *FEBS Letters* **192**, 189 - 193.

NEEDLEMAN, P., TURK, J., JAKSCHIK, B.A., MORRISON, A.R. & LEFKOWITH, J.B. (1986) Arachidonic acid metabolism. *Annual Review of Biochemistry* 55, 69 - 102.

NEHER, E. & SAKMANN, B. (1976) Single-channel currents recorded from membrane of denervated frog muscle fibres. *Nature* **260**, 779 - 802.

NERNST, W. (1888) Zur kinetik der in lösung befindlichen körper: theorie der diffusion. *Z. Phys. Chem* 613 - 637.

NILIUS, B., SEHRER, J. & DROOGMANS, I. (1994a) Permeation properties and modulation of volume-activated Cl^--currents in human endothelial cells. *British Journal of Pharmacology* **112**, 1049 - 1056.

NILIUS, B., OIKE, M., ZAHRADNIK, I. & DROOGMANS, I. (1994b) Activation of a Cl^- current by hypotonic volume increase in human endothelial cells. *Journal of General Physiology* **103**, 787 - 805.

NILIUS, B., SEHRER, J., VIANA, F., DE GREEF, C., RAEYMAEKERS, L., EGGERMONT, J. & DROOGMANS, G. (1994c) Volume-activated Cl^- currents in different mammalian non-excitable cell types. *Pflügers Archiv* **428**, 364 - 371.

NISHIMOTO, I., WAGNER, J.A., SCHULMAN, H. & GARDNER, P. (1991) Regulation of chloride channels by multifunctional CaM kinase. *Neuron* **6**, 547 - 555.

OBERLEITHNER, H., RITTER, M., LANG, G. & GUGGINO, W. (1983) Anthracene-9-carboxylic acid inhibits renal chloride reabsorption. *Pflügers Archiv* **398**, 172 - 174.

OKADA, Y. & HAZAMA, A. (1989) Volume-regulatory ion channels in epithelia. *News in Physiological Sciences* **4**, 238 - 242.

ORDWAY, R.W., WALSH, J.V. & SINGER. J.J. (1989) Arachidonic acid and other fatty acids directly activate potassium channels in smooth muscle cells. *Science* **244**, 1176 - 1179.

ORDWAY, R.W., SINGER, J.J. & WALSH J.V. (1991) Direct regulation of ion channels by fatty acids. *Trends in Neuroscience* **14**, 96 - 100.

ORLOFF, J. & HANDLER, J.S. (1962) The similarity of effects of vasopressin, adenosine-3',5'-phosphate (cyclic AMP) and theophylline on the toad bladder. *Journal of Clinical Investigation* **41**, 702 - 709.

PAHAPILL, P.A. & SCHLICHTER, L.C. (1992) Cl^--channels in intact human lymphocytes-T. *Journal of Membrane Biology* **125**, 171 - 183.

PARKER, J.C. (1983) Hemolytic action of potassium salts on dog red blood cells. *American Journal of Physiology* **244**, C313 - C317.

PAULMICHL, M., LI, Y., WICKMAN, K., ACKERMAN, M., PERALTA, E. & CLAPHAM, D. (1992) New mammalian chloride channel identified by expression cloning. *Nature* **356**, 238 - 241.

PETROU, S., ORDWAY, R.W., SINGER, J.J. & WALSH, J.V. (1993) A putative fatty acid-binding domain of the NMDA receptor. *Trends in Biochemical Sciences* **18**, 41 - 42.

PIERCE, S.K. & POLITIS, A.D. (1990) Ca^{2+}-activated cell volume recovery mechanisms. *Annual Review of Physiology* **52**, 27 - 42.

POLING, J.S., KARANIAN, J.W., SALEM, N. & VICINI, S. (1995) Time- and voltage-dependent block of the delayed rectifier potassium channels by docosahexaenoic acid. *Molecular Pharmacology* **47**, 381 - 390.

POLLARD, C.E. (1993) A volume-sensitive Cl^- conductance in a mouse neuroblastoma x rat dorsal root ganglion cell line (F11). *Brain Research* **614**, 178 - 184.

POYNER, D.R., ANDREW, D.P., BROWN, D., BOSE, C. & HANLEY, M.R. (1992) Pharmacological characterization of a receptor for calcitonin gene-related peptide on rat, L6 myocytes. *British Journal of Pharmacology* **105**, 441 - 447.

PURVES, R.D. (1981) Circuitry for recording. In: Microelectrode methods for intacellular recording and ionophoresis. pp 39 - 75. Great Britain: Academic Press Inc..

PUSCH, M. & JENTSCH, T.J. (1994) Molecular physiology of voltage-gated chloride channels. *Physiological Reviews* **74**, 813 - 827.

RAVESLOOT, J.H., VAN HOUTEN, R.J., YPEY, D.L. & NIJWEIDE, P.J. (1991) High-conductance anion channels in embryonic chick osteogenic cells. *Journal of Bone and Mineral Research* **6**, 355 - 363.

RINGER, S. (1883) A further contribution regarding the influence of the different constituents of the blood on the contraction of the heart. *Journal of Physiology* **4**, 29 - 42.

RIORDAN, J.R., ROMMENS, J.M., KEREM, B.S., ALON, N., ROZMAHEL, R., GRZELCZAK, Z., ZIELENSKI, J., LOK, S., PLAVSIK, N., CHOU, J.L., DRUMM, M.L., IANNUZZI, M.C., COLLINS, F.S. & TSUI, L.C. (1989) Identification of the cystic fibrosis gene: cloning and characterization of complementary DNA. *Science* **245**, 1066 - 1073.

ROBSON, L. & HUNTER, M. (1994) Role of cell volume and protein kinase C in regulation of Cl^- conductance in single proximal tubule cells of *Rana temporaria*. *Journal of Physiology* **480**, 1 - 7.

RODAN, G.A. & RODAN, G.B. (1984) Expression of the osteoblastic phenotype. In: Bone and Mineral Research. pp 244 - 285. ed: Peck, W.A. Elsevier, Amsterdam.

ROMEY, G. & LAZDUNSKI, M. (1984) The coexistence in rat muscle cells of two distinct classes of Ca^{2+}-dependent K^+ channels with different pharmacological

properties and different physiological functions. *Biochemical and Biophysical Research Communications* **118**, 669 - 674.

ROUZAIRE-DUBOIS, B., GÉRARD, V. & DUBOIS, J.M. (1991) Modification of K^+ channel properties induced by fatty acids in neuroblastoma cells. *Pflügers Archiv* **419**, 467 - 471.

RUDY, B. (1998) Diversity and ubiquity of K^+ channels. *Neuroscience* **25**, 729 - 749.

SACKIN, H. (1989) A stretch-activated K^+ channel sensitive to cell volume. *Proceedings of the National Academy of Sciences of the USA* **86**, 1731 - 1735.

SAKAI, H., OKADA, Y., MORRII, M. & TAKEGUCHI, N. (1992) Arachidonic acid and prostaglandin E_2 activate small conductance Cl^- channels in the basolateral membrane of rabbit parietal cells. *Journal of Physiology* **448**, 293 - 306.

SAKMANN, B. & NEHER, E. (1983) Single-channel recording. pp 503, USA: Plenum.

SANDY, J.R., MEGHJI, S., FARNDALE, R.W. & MEIKLE, M.C. (1989) Dual elevation of cyclic AMP and inositol phosphates in response to mechanical deformation of murine osteoblasts. *Biochimica et Biophysica Acta* **1010**, 265 - 269.

SARKADI, B., CHEUNG, R., MACK, E., GRINSTEIN, S., GELFAND, E.W. & ROTHSTEIN, A. (1985) Cation and anion transport pathways in volume regulatory response of human lymphocytes to hyposmotic media. *American Journal of Physiology* **248**, C480 - C487.

SCHWIEBERT, E.M., MILLS, J.W. & STANTON, B.A. (1994) Actin-based cytoskeleton regulates a chloride channel and cell volume in a renal cortical collecting duct cell line. *Journal of Biological Chemistry* **259**, 7081 - 7089.

SCHWIEBERT, E.M., EGAN, M.E., HWANG, T.H., FULMER, S.B., ALLEN, S.S. CUTTING, G.R. & GUGGINO, W.B. (1995) CFTR regulates outwardly rectifying chloride channels through an autocrine mechanism involving ATP. *Cell* **81**, 1063 - 1073.

SEPULVEDA, F.V., FARGON, F. & MCNAUGHTON, P.A. (1991) K^+ and Cl^- currents in enterocytes isolated from guinea-pig small intestinal villi. *Journal of Physiology* **434**, 351 - 367.

SHIP, S., SHAMI, Y., BREUER, W. & ROTHSTEIN, A. (1977) Synthesis of tritiated 4,4'-diisothiocyano-2,2'-stilbene disulfonic acid ([^{3}H]DIDS) and its covalent reaction with sites related to anion transport in red blood cells. *Journal of Membrane Biology* **33**, 311 - 324.

SOLC, C.K. & WINE, J.J. (1991) Swelling-induced and depolarization-induced Cl^- channels in normal and cystic fibrosis epithelial cells. *American Journal of Physiology* **261**, C658 - C674.

STODDARD, J.S., STEINBACH, J.H. & SIMCHOWITZ, L. (1993) Whole-cell Cl^- currents in human neutrophils induced by cell swelling. *American Journal of Physiology* **265**, C156 - C165.

SUZUKI, M., MIYAZAKI, K., IKEDA, M., KAWAGUCHI, Y. & SAKAI, O. (1993) F-actin network may regulate a Cl^- channel in renal proximal tubule cells. *Journal of Membrane Biology* **134**, 31 - 39.

TABCHARANI, J.A., ROMMENS, J.M., HOU, Y.X., CHANG, X.B., TSUI, L.C., RIORDAN, J.R. & HANRAHAN, J.W. (1993) Multi-ion pore behaviour in the CFTR chloride channel. *Nature* **366**, 79 - 82.

TALEB, O., FELTZ, P., BOSSU, J.L. & FELTZ, A. (1988) Small-conductance chloride channels activated by calcium on cultured endocrine cells from mammalian pars intermedia. *Pflügers Archiv* **412**, 641 - 646.

TETI, A., NARO, F., MOLINARO, M. & ADAMO, S. (1993) Transduction of arginine vasopressin signal in skeletal myogenic cells. *American Journal of Physiology* **265**, C113 - C121.

THIEMANN, A., GRÜNDER, S., PUSCH, M. & JENTSCH, T.J. (1992) A chloride channel widely expressed in epithelial and non-epithelial cells. *Nature* **356**, 57 - 60.

TILLY, B.C., VAN DEN BERGHE, N., TERTOOLEN, L.G.J., EDIXHOVEN, M.J. & DE JONGHE, H.R. (1993) Protein tyrosine phosphorylation is involved in osmoregualtion of ionic conductances. *Journal of Biological Chemistry* **268**, 19919 - 19922.

TILMANN, M., KUNZELMANN, K., FRÖBE, U., CABANTCHIK, I., LANG, H.J., ENGLERT, H.C. & GREGER, R. (1991) Different types of blockers of the intermediate-conductance outwardly rectifying chloride channel in epithelia. *Pflügers Archiv* **418**, 556 - 563.

TSENG, G. (1992) Cell swelling increases membrane conductance of canine cardiac cells: evidence for a volume-sensitive Cl channel. *American Journal of Physiology* **262**, C1056 - C1068.

TSIEN, R.W. (1983) Calcium channels in excitable cell membranes. *Annual Review of Physiology* **45**, 341 - 358.

TSIEN, R.Y., POZZAN, T. & RINK, T.J. (1982) T-cell mitogens cause early changes in cytoplasmic free Ca^{2+} and membrane potential in lymphocytes. *Nature* **295**, 68 - 71.

TSIEN, R.W. & TSIEN, R.Y. (1990) Calcium channels, stores and oscillations. *Annual Review of Cell Biology* **6**, 715 - 760.

UBL, J., MURER, H. & KOLB, H.-A. (1988) Hypotonic shock evoked opening of Ca^{2+}-activated K^+ channels in opossum kidney cells. . *Pflügers Archiv* **412**, 551 - 553.

VALVERDE, M.A., DÌAZ, M., SEPÚLVEDA, F.V., GILL, D.H., HYDE, S.C. & HIGGINS, C.F. (1992) Volume-regulated chloride channels associated with the multidrug resistance P-glycoprotein. *Nature* **355**, 830 - 833.

VAN RENTERGHEM, C., ROMEY, G. & LAZDUNSKI, M. (1988) Vasopressin modulates the spontaneous activity in aortic cells (line A7r5) by acting on three different types of ionic channels. *Proceedings of the National Academy of Sciences of the USA* **85**, 9365 - 9369.

VAN RENTERGHEM, C. & LAZDUNSKI, M. (1994) Identification of the Ca^{2+} current activated by vasopressin in vascular smooth muscle cells. *Pflügers Archiv* **429**, 1 - 6.

VANDENBERG, C.A. (1987) Inward rectification of a potassium channel in cardiac ventricular cells depends on internal magnesium ions. *Proceedings of the National Academy of Sciences of the USA* **84**, 2560 - 2564.

VATISH, M. & BOTD, C.A.R. (1993) Regulation of chloride conductances of human placental brush-border membrane vesicles by arachidonic acid. *Journal of Physiology* **459**, 172P.

WAKELAM, M.J.O. & PETTE, D. (1982) The control of glucose 1,6-bisphosphate by developmental state and hormonal stimulation in cultured muscle tissue. *Biochemical Journal* **204**, 765 - 769.

WAKELAM, M.J.O., PATTERSON, S. & HANLEY, M.R. (1987) L6 skeletal muscle cells have functional V_1-vasopressin receptors coupled to stimulated inositol phospholipid metabolism. *FEBS Letters* **210**, 181 - 184.

WANGEMANN, P., WITTNER, M., DI STEFANO, A., ENGLERT, H.C., LANG, H.J., SCHLATTER, E. & GREGER, R. (1986) Cl^--channel blockers of the thick ascending limb of the loop of Henle. Structure activity relationship. *Pflügers Archiv* **407**, S128 - S141.

WATSON, P.A. (1990) Direct stimulation of adenylate cyclase by mechanical forces in S49 mouse lymphoma cells during hyposmotic swelling. *Journal of Biological Chemistry* **265**, 6569 - 6575.

WORLEY, P.F., BARABAN, J.M, SUPATTAPONE, J.M., WILSON, V.S. & SNYDER, S.H. (1987) Characterization of inositol trisphosphate receptor binding in brain: regulation by pH and calcium. *Journal of Biological Chemistry* **262**, 12132 - 12136.

WORRELL, R.T. & FRIZZELL, R.A. (1991) CaMKII mediates stimulation of chloride conductance by calcium in T84 cells. *American Journal of Physiology* **260**, C877 - C882.

WORRELL, R.T., BUTT, A.G., CLIFF, W.H. & FRIZZELL, R.A. (1989) A volume-sensitive chloride conductance in human colonic cell line T84. *American Journal of Physiology* **256**, C1111 - C1119.

WRIGHT, E.M. & DIAMOND, J.M. (1977) Anion selectivity in biological systems. *Physiological Reviews* 57, 109 - 186.

YAFFE, D. (1968) Retention of differentiation potentialities during prolonged cultivation of myogenic cells. *Proceedings of the National Academy of Sciences of the USA* **61**, 477 - 483.

YAMAGUCHI, D.T., GREEN, J., KLEEMAN, C.R. & MUALLEM S. (1989) Characterization of volume-sensitive, calcium-permeating pathways in the osteosarcoma cell line UMR-106-01. *Journal of Biological Chemistry* **264**, 4383 - 4390.

YANTORNO, R.E., CARRÉ, D.A., COCA-PRADOS, M., KRUPIN, T. & CIVAN, M.M. (1992) Whole cell patch clamping of ciliary epithelial cells during anisosmotic swelling. *American Journal of Physiology* **262**, C501 - C509.

ZACHAR, J. & HURNÁK, O. (1994) Arachidonic acid blocks large-conductance chloride channels in L6 myoblasts. *General Physiology and Biophysics* **13**, 193 - 213.